DEVELOPMENT OF NICKEL-SELECTIVE MOLECULARLY IMPRINTED POLYMERS

THESIS

Submitted in fulfilment of the requirements for the Degree of

MASTER OF SCIENCE

of Rhodes University

by

TSHINYADZO ROBERT TSHIKHUDO

BSc (Unin), BSc. Hons (Rhodes)

Department of Chemistry

Rhodes University

Grahamstown

January, 2002

ABSTRACT

A series of eight novel bidentate ligands, designed for use in the construction of nickel-selective molecularly imprinted polymers (MIP's), have been prepared. The synthetic pathway was established by retrosynthetic analysis of the target molecules to the readily available precursors, pyridine-2-carbaldehyde (or 6-methylpyridine-2-carbaldehyde) and ethyl bromoacetate. The ligands were designed to contain an allyl group for co-polymerisation and amine and pyridyl nitrogen donors, located to permit the formation of 5-membered nickel chelates. The eight novel ligands and their respective precursors were characterized by elemental (high-resolution MS) and spectroscopic (IR and ^{1}H and ^{13}C NMR) analysis. High resolution electron-impact mass spectrometry has also been used, together with B/E linked scan data, to explore the fragmentation patterns of selected ligands. The various nickel(II) complexes were analyzed using spectroscopic techniques and, in some cases, elemental analysis; computer modelling has also been used to explore conformational effects and complex stability.

Numerous MIP's, containing nickel(II) complexes of the bidentate ligands, have been prepared, using ethylene glycol dimethylacrylate (EGDMA) as the cross-linker, azobis(isobutyronitrile) (AIBN) as the polymerization initiator and MeOH as the porogenic solvent. The template nickel(II) ions were leached out with conc. HCl, and the nickel(II) selectivity [in the presence of Fe(III)]of the nickel-imprinted polymers was examined by ICP-MS analysis. The ICP-MS data indicate that the MIP's examined exhibit extremely high selectivity for nickel over iron.

ACKNOWLEDGEMENTS

Firstly, I would like to thank the Almighty God who granted me life and loving-kindness, and who continually proved to be my light and my salvation. "I can do all things through Christ who strengthens me." Philippians 4:13.

I am extremely grateful to Professor Perry Kaye, for allowing me to conduct this research work under his supervision. Thank you for your tremendous support, guidance and teaching. Your love for chemistry, extensive chemical knowledge coupled with your dynamic working style have been a source of inspiration to me.

Special thanks go to MINTEK, the financial sponsor of this project, particularly Mr. Bob Tait and Dr. Brian Green at MINTEK for all your assistance. Thank you to Mr. Edward and Mrs. Gloria Nengovhela, for all your sacrifices and efforts you have made in laying down the foundation of this work, by permitting me to obtain a university education. I would also like to thank Mr. Milton and Mrs. Sandra Mangenge, and my family at large for the support and encouragement throughout.

Thanks to Dr. P. Boshoff of the Cape Technikon for high resolution MS analyses, and to Mr.Aubrey Sonemann for your help in obtaining low resolution mass spectra. Thank you immensely Dr. Eric Hoston of the University of Port Elizabeth for your great help in obtaining the ICP-MS data. Useful discussions with Dr. Kevin Wellington concerning nickel complexation, during his post-doctoral appointment at Rhodes University is greatly appreciated. Thanks to Mr. Robin Cross for your help in obtaining Scanning Electron Micrographs.

Lastly, I would like to acknowledge the friendship and support of Dr. X. Noxanda and my fellow post-graduate students who have made my working and stay at Rhodes a pleasant one. Also to the Department of Chemistry at Rhodes University, thank you for the loan of the computer.

TABLE OF CONTENTS

LIST OF SELECTED ABBREVIATIONS

AIBN	azobis(isobutyronitrile)
DDDPA	1,12-dodecanediol-*O*,*O*'-diphenylphosphonic acid
EGDMA	ethylene glycol dimethylacrylate
HPLC	high-performance liquid chromatography
MIA's	molecularly-imprinted sorbent assays
MIP's	molecularly imprinted polymers
MM	molecular mechanics
PAL	pressure sulfuric acid leach
PVP	poly(4-vinylpyridine)
ROM	run of mine
SAL	salicylaldimine
SDS	sodium dodecyl sulfate
TACN	*N*-(4-vinylbenzyl)-1,4,7-triazacyclononane
THF	tetrahydrofuran
TSA's	transition state analogues
TRIM	trimethylolpropane trimethacrylate
W/O	water in oil
W/O/W	water in oil in water

INTRODUCTION

1.1 The chemistry of nickel

1.1.1 Historical background

The name, "nickel," was proposed by Cronstead,[1] from "kupfernickel" (old Nick's copper). Kupfernickel became known in Germany, during the late seventeenth century, as a heavy reddish-brown ore. The material was believed by the Saxon miners to be a copper ore, but after attempts to isolate copper from it proved unsuccessful, the ore was named, kupfernickel, and was used to color glass green. Cronstead, in his investigations conducted in the cobalt mines in Helsingland, Sweden, obtained from kupfernickel a white, brittle metal which has no resemblance to copper and for which he proposed the name nickel.

1.1.2 The distribution and formation of nickel ores

Nickel is the seventh most abundant transition metal and, at 99 ppm, the twenty-second most abundant element in the earth's crust.[2] The total amount of nickel is believed to be greater than that of copper, zinc and lead combined, although there are relatively few known nickel deposits that are capable of being worked economically.

Of the rocks that can be seen on the earth's surface, those containing the largest amount of nickel have been shown to have risen as a melt or mush from depths well below the crust.[3] These rocks are dark and heavy, high in iron and magnesium content, and are called basic or mafic rocks in contrast with the light-coloured rocks, such as granite, that are high in silicon and contain relatively small amounts of iron or magnesium. Peridotite and gabbro rocks are classed as mafic, and constitute a major source of nickel **(Table 1)**.

Table 1. Composition of various nickel containing igneous rocks.[3]

Rock	Nickel/ %	Iron oxide and magnesium/ %	Silica and aluminium/ %
Peridotite	0.20	43.3	45.9
Gabbro	0.016	16.7	66.1
Diorite	0.004	11.7	73.4
Granite	0.0002	4.4	78.7

It is taken as a rule for igneous rocks that the more iron and magnesium and the less silicon and aluminium they contain, the higher the nickel content. Despite the greater nickel content of mafic rocks, the concentration is still too low for the economically viable recovery of nickel.[4] Fortunately, however, natural processes have concentrated nickel in mineral deposits below the earth's surface and the ores provide a source of this important metal.

1.1.2.1 Classes of nickel ores

Nickel ores fall into three main classes:- sulfides; oxides and silicates (laterites); and arsenides, although only the sulfides and laterites are commercially important (**Table 2**).[2, 3]

Table 2. Chemical composition of the principal nickel-bearing minerals found in nickel deposits.[3]

Mineral	Ideal formula	Nickel content/ %
Sulfides		
Pentlandite	$(Ni, Fe)_9S_8$	32.22
Millerite	NiS	64.67
Heazlewoodite	Ni_3S_2	73.30
Linaerite series	$(Fe, Co, Ni)_3S_4$	variable
Polydymite series	Ni_3S_4	57.86
Violarite	Ni_2FeS_4	38.94
Silicates and oxides (laterites)		
Garnerite	$(Ni, Mg)_6Si_4O_{10}(OH)_8$	variable up to 47 %
Nickeliferous/Limonite	$(Fe, Ni)O(OH).nH_2O$	low and variable
Arsenides		
Nicolite	NiAs	43.92
Maucherite	$Ni_{11}As_8$	51.85

In the sulfide-type ores, nickel-bearing minerals were apparently concentrated when the rocks in which they occur were at depths of thousands of feet below the earth's surface. Pentlandite is the commonest of the sulfide minerals and accounts for about three-quarters of the nickel mined in the world. It occurs together with iron sulfide, copper minerals (such as chalcopyrite) and minerals of platinum group metals. These deposits are commonly found in Canada, Russia and South Africa.[5] Millerite **(Table 2)** has a nickel content twice that of pentlandite, but is a minor constituent of nickel-containing minerals. Heazlewoodite has the highest nickel content of any naturally occurring nickel sulfide or arsenide, but only a few known deposits contain more than trace amounts of this mineral.

Laterites are nickel-containing oxides or silicates. In New Caledonian and Oregon ores, the nickel occurs mainly as magnesium silicate, *e.g.* garnerite (Ni, $Mg)_6Si_4O_{10}(OH)_8$. while Cuban oxide ores have a high iron content, *e.g.* limonite (Ni, Fe)O(OH).nH_2O. Since more attention has been given to the lateritic ores, the production of nickel from lateritic ores is discussed in the next section.

1.1.2.2 Formation of nickel ores

The production of lateritic nickel ores is quite complicated. Lateric weathering involves the decomposition of nickel-containing rocks exposed at the earth's surface, dissolution of the nickel in the ground water and re-deposition at greater depth to afford zones in which the nickel content is extremely high. Such zones contain two different ore types, *viz.*, Limonite (upper horizon) and Saprolite (lower horizon), and there is normally a transition zone between the two ore-types.

The limonite zone is dominated by Goethite (FeOOH), the main nickel carrier in a "cryptocrystalline form".[3,6] The transition zone consists, largely, of soft "smectite clays", usually nontronite and hard crystalline quartz, while the Saprolite zone consists of a mixture of bedrock fragments, saprolitic rims and veins of precipitated nickel-bearing serpentine, nickelferrous quartz and manganese wad with serpentine being the major nickel-bearing phase.

1.1.3 Production of nickel

1.1.3.1 Upgrading laterite nickel ores

Several approaches have been explored to enrich nickel laterite. These include upgrading by size-fraction classification (used in the Ravensthorpe nickel project in Australia)[7] and screening and classification processes to separate the fine higher-grade fraction from the course sub-grade fraction of the run of mine (ROM) ore. About 75 % of nickel recovery is achieved by the latter process, with two-thirds of the ROM material being rejected as uneconomic material with nickel grades lower than 0.45%. However, while the size classification method is considered to be the

cheapest and easiest technique, it is not generally applicable due to the fact that laterite ore bodies vary considerably in composition. Limonitic ores, for example, are not beneficiated appreciably by screening.[8] Results obtained from other strategies, including hand-picking, sink-floatation and float-separation, dry magnetic separation, electrostatic separation and froth floatation [3, 7] were also found to be poor.

1.1.3.2 Ore treatment processes

Treatment of the lower saprolite ore has tended to be preferred because of its higher nickel content and suitability for pyrometallurgical processing. Limonite on the other hand, is unsuitable for pyrometallurgical processing. Almost all saprolite mined in the world is processed pyrometallurgically to produce either ferronickel or nickel sulfide matte. The smelting process is reported to be quite simple and although there is limited potential for major advances in the chemistry, it has been recognized that "upgrading of saprolite prior to smelting could reduce energy consumption and enhance profitability as well as productivity".[7] Two commercial hydrometallurgical processes have been developed, *viz.*,

i) reduction roast-ammonia-ammonium carbonate leach, and
ii) pressure sulfuric acid leach (PAL).

Hydrometallurgical processes are in fact, essential when nickel and cobalt are in solution together.

1.1.3.3 Isolation and purification of nickel metal

The industrial production of nickel is achieved efficiently by concentrating the nickel sulfide ore by floatation and magnetic separation. The Mond process, [9, 10] outlined below, has been widely used since 1899 for the production of high purity nickel. In summary, the nickel sulfide is converted to NiO by roasting in air and the resulting NiO is treated with water gas (H_2 and CO) at atmospheric pressure, such that, the H_2 reduces NiO to Ni which is reacted, in turn, with CO to form highly toxic nickel tetracarbonyl [$Ni(CO)_4$]. The $Ni(CO)_4$ gas is then heated to 230°C to

afford the pure metal, and the CO is recycled. Thompson[11] has reviewed the hydrometallurgical processes applied to nickel sulfide ores including:- the Outokumpu process, the Sherrit Gordon process, the Falconbridge process and the INCO Matte electrolytic process, which are employed in different countries.

Mond process

$$2NiS + 3O_2 \longrightarrow 2NiO + 2SO_2$$
$$NiO + H_2 \longrightarrow Ni + H_2O$$
$$Ni + 4CO \longrightarrow Ni(CO)_4(g)$$
$$Ni(CO)_4(g) \longrightarrow Ni + 4CO$$

1.1.4 Properties and uses of nickel

1.1.4.1 Physical properties

Some of the important physical properties of nickel are detailed in **Table 3**.[1,2] Nickel is a non-toxic, silvery-white metal, capable of taking a high polish. It can be rolled into sheets in its commercially pure form (99.5 %). Nickel is moderately strong and has excellent corrosion resistant properties in many media including marine and industrial atmospheres. Its strength is retained at both high temperatures and sub-zero temperatures. Fabricated nickel has mechanical properties resembling those of mild steel but, unlike steel, it is resistant to corrosion and this property, together with the fact that it is non-toxic, has encouraged its use in the manufacture of equipment for food handling and pharmaceutical processing.[2]

Table 3. Physical properties of nickel.

Atomic number	28
Electronic configuration	$1s^2,2s^2,2p^6,3s^2,3p^6,3d^8,4s^2$
Atomic weight	58.71
M.p. (^oC)	1453
B.p. (^oC)	2732
Density at 20 ^oC, (g cm^{-3})	8.908
Ionization potential (eV)	
First	7.633
Second	18.15
Third	53.16

1.1.4.2 Chemical properties

1.1.4.2.1 *Reaction with elements*

Nickel, in finely divided state, absorbs hydrogen even at elevated temperatures, but does not absorb or combine directly with nitrogen. Nickel wire burns readily in oxygen, and nickel sheet tarnishes like steel when heated in air.[1] On heating, nickel burns in chlorine and bromine, forming the yellow nickel (II) halides; nickel and iodine react similarly when heated together in a sealed tube, while nickel(II) sulfide is formed when nickel is heated with sulfur at *ca.*445 °C. Finely divided nickel may be "pyrophoric" in air under certain conditions and, in this state, is attacked by fluorine above 400 °C.

1.1.4.2.2 *Reaction with compounds*

At moderate temperatures (above 300 °C), NH_3 is decomposed by nickel. In contrast, nickel tetracarbonyl $Ni(CO)_4$ forms at relatively low temperature (50 °C). Formation of NiF_2 is observed when hydrogen fluoride reacts with nickel powder at 225 °C; the other hydrogen halides are known to react similarly although the massive metal is only attacked slowly at temperatures below 500 °C. Hydrogen sulfide corrodes nickel, forming the black sulfide (NiS), while a mixture of NiS and Ni_2S is formed when carbon disulfide is passed over nickel filings.

Nickel is quite electropositive, its electrode potential for the reaction:-

$Ni \rightleftharpoons Ni^{2+} + 2e \quad (E^{\circ} = -0.250V)$

being similar to that for the analogous cobalt reaction. Unlike iron, nickel dissolves in dilute mineral acids, particularly in dilute nitric and nitrous acids. The ability of nickel to resist attack by caustic alkalis has led to its widespread use in the production and handling of caustic soda. Nickel is, however, attacked by aqueous ammonia.

1.1.4.3 Uses of nickel

There are several uses of nickel, some of which have already been highlighted. Other uses include electroplating and applications in catalysis and the formation of alloys. Nickel can be plated by an electrochemical process on to many base metals affording excellent resistance to corrosion for many common articles, such as pins, paper clips, scissors and fasteners, as well as for equipment used in food processing. Nickel plating[12] is also used, together with chromium plating, to provide decorative finishes and impart corrosion resistance to numerous articles. Nickel electroforming, a process in which nickel is electro-deposited into a mold which is subsequently separated from the deposit, is used to form complex shapes such as printing plates, tubing nozzles, screens and grids. Nickel plays an important role as an industrial catalyst, particularly in the food industry in the hydrogenation or dehydrogenation of triglycerides to produce edible fats and oils.[10]

About 85 % of the nickel produced is used in alloys, which may be classified as ferrous and non-ferrous alloys.

Ferrous alloys include the following.

i) Stainless steel. Small amounts of nickel and chromium in steel (*e.g.* 8 % Ni, 18 % Cr) improve mechanical properties, facilitate heat treatment, and enhance the regularity of the steel. Stainless steel is well known for its resistance to corrosion, its strength and toughness.[13]

ii) Nickel cast-iron is an alloy used for engine cylinder blocks and heads.

iii) Nickel-iron alloys. These contain *ca.* 25 % nickel and, frequently, are no longer ferromagnetic. Examples of non-magnetic ferrous alloys are "Ni-resistant" (14 % Ni, 6 % Cu, 2 % Cr, 3 % C) and "nomag"(11 % Ni and 6 % Mn), which are used in electrical engineering as they combine non-magnetic properties with high electrical resistance.[13]

iv) Permalloy and Supermalloy: These alloys contain 35-80 % nickel and have high magnetic permeability. Permalloy (78.5 % Ni and 21.5 % Fe) is used in telegraph cables. When molybdenum is added to permalloy, it gives supermalloy, which has a very high magnetic permeability, and is used in the construction of magnetic screens.[13]

The non-ferrous alloys include the following.

i) ***Monel 400 alloy.*** This contains *ca.* 32 % Cu and has relatively high strength and excellent resistance to many environments.

ii) Cupro-nickels. These are alloys of nickel containing up to 80 % Cu and are used for instance, in "silver" coins in Britain and for the American "nickel".

iii) Nickel-chromium alloys. "Nichrome" wire (40 % Cr and 60 % Ni) and "iconel"(76 % Ni, 5 % Cr with the balance being mainly Fe) are used extensively as electrical resistance materials. They are known to be oxidation resistant up to 1200 °C and exhibit good mechanical properties at high temperature, which prevents heating elements from "sagging".[13]

1.1.5 Nickel complexes

While nickel complexes have been found to occur with the metal in oxidation states ranging from -1 to +4, complexes corresponding to the lowest (-1) and to the highest (+3) and (+4) oxidation states are rare. Studies of the chemistry of nickel have tended to concentrate on the (+2) oxidation state, because most of the nickel compounds in the solid state and almost all in aqueous solution contain the metal in this oxidation state. As a result, the +2 state can be considered to be the normal oxidation state for nickel. The most stable electronic configuration of the free Ni^{2+} ion is [Ar] $3d^8$, which also reflects the ground state electronic configuration in Ni(II) complexes.[14]

1.1.5.1 Stereochemistry of Ni(II) complexes

The overwhelming majority of nickel(II) complexes have coordination numbers of four, five and six; complexes with coordination numbers of 3,7 or 8 are still quite rare.[15] There is a corresponding variability in molecular geometry [*e.g.*, four coordinate (tetrahedral or square planar), five coordinate (square pyramidal or trigonal bipyramidal) and six coordinate (octahedral)]. One of the most remarkable facts about the stereochemistry of nickel complexes is that the different structural types often exist in equilibrium. These equilibria are frequently temperature dependent and often concentration dependent. As a consequence, the stereochemistry of nickel(II) complexes can be quite complicated.[15,16]

1.1.5.1.1 *Six-coordinate Ni(II) complexes*

The most common six-coordinate complex of Ni(II) is the green, octahedral aqua ion, $[Ni(H_2O)_6]^{2+}$. The water molecules are readily replaced by other neutral or anionic ligands, and the resulting complexes can be crystallized from solution. The complexes formed with ammonia $[Ni(NH_3)_6]^{2+}$, $[Ni\ (H_2O)_4\ (NH_3)]^{2+}$, and the ethylenediamine complex $[Ni(en)_3]^{2+}$, are all octahedral.[16] The octahedral complexes, which are usually blue or sometimes purple in colour, are paramagnetic due to the d^8 ion having two unpaired electrons.

1.1.5.1.2 *Five-coordinate Ni(II) complexes*

Five-coordinate Ni(II) complexes are quite uncommon and trigonal-bipyramidal or square-pyramidal arrangements only occur when these geometries are stabilized by the donor power and steric requirements of the ligand. Diamagnetic complexes are observed with donor atoms of low electronegativity, especially phosphorous and arsenic, while paramagnetic complexes are observed with electronegative nitrogen or oxygen donors[16].

1.1.5.1.3 *Four-coordinate Ni(II) complexes*

These complexes may adopt tetrahedral or square-planar geometries. The tetrahedral complexes are less common than the square-planar complexes and are strongly coloured, typically blue or green. These complexes are of the following stoichiometric types:- $[NiX_4]_2$, NiX_3L, NiL_2X_2 and $Ni(L\text{-}L)_2$; where X represents a halogen, L a neutral ligand and L-L a bidentate uninegative ligand, such as phosphine, phosphine oxide or arsine.[15] For a given ligand set, ABCD, there is a critical dihedral angle between two planes (*e.g.* A-Ni-B and C-Ni-D) which, if exceeded, renders the complex paramagnetic and, thus, tetrahedral. On the other hand, when the angle is below the critical value the complex will be diamagnetic.[15]

Square-planar geometry is, in fact, the preferred geometry for nickel(II) complexes, and this is a natural consequence of the d^8 electronic configuration.[15] Stabilization of complexes with this configuration is effected by strong nickel-ligand covalent bonding (both δ- and π-), and short nickel-ligand bond lengths can be observed.[16] Ni(II) square-planar complexes are diamagnetic, and usually red, brown or yellow in color. An example of a square-planar complex, is the yellow $Ni(CN)_4^{2-}$, which is stabilized by the strong field ligand CN^-.

The red bis(dimethylglyoximato) complex **1** is stabilized by five-membered chelate rings, which are formed when dimethylglyoxime loses a proton. This complex, which can be used for both the detection and quantitative estimation of nickel, is square-planar in solution but, in the solid state, the square-planar molecules are stacked on top of each other resulting in Ni-Ni interactions in

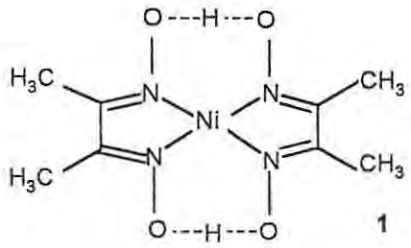

1

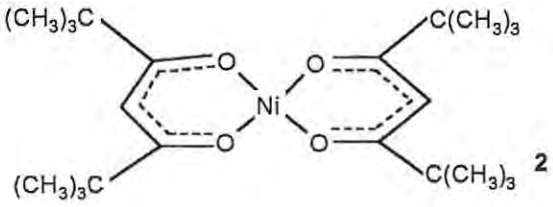

2

effective octahedral coordination. The red β-keto-enolate complex **2** is another example of a square-planar complex.[17]

1.1.5.2 Dynamic properties of nickel(II) complexes

Nickel complexes have been observed to exhibit "anomalous" behaviour by undergoing certain conformational changes; these are conveniently discussed under separate headings.

1.1.5.2.1 *Formation of five- and six-coordinate complexes from square-planar Ni(II) complexes*

The following equilibria may be established when the ligands L^1 are added to square-planar complexes NiL_4.[18]

$$ML_4 + L^1 \rightleftharpoons ML_4L^1 \qquad \text{(eq. 1)}$$

$$ML_4 + 2L^1 \rightleftharpoons ML_4L_2^1 \qquad \text{(eq. 2)}$$

In cases where $L=L^1=CN$, only five-coordinate species are formed (eq.**1**), but when L^1 is a strong donor ligand, such as pyridine, H_2O or C_2H_5OH, the equilibrium (eq. **2**) lies far to the right, favouring a *trans,* six-coordinate paramagnetic structure. The complex **2**, has been prepared in H_2O or ethanol and then isolated as a green paramagnetic dihydrate or dialcoholate. When the complex is heated, H_2O or C_2H_5OH is driven off resulting in the formation of a red, diamagnetic square-planar complex **2**.

Another of the well known Lifschitz salts, which exhibit square-octahedral ambivalence, is the Ni(II) complex **3**.[18]

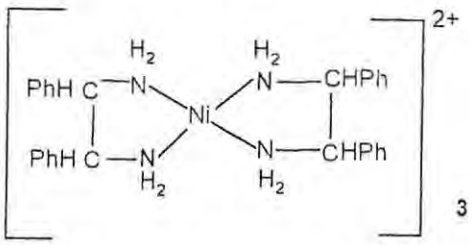

Lifschitz and co-workers [18-20] observed that such complexes were either blue and paramagnetic or yellow and diamagnetic, depending on factors, such as temperature, the nature of the counterion, the solvent in which they are dissolved or from which they are crystallized, exposure to atmospheric moisture, and the particular diamine involved. For several decades, these dynamic transformations have confused chemists, and many hypotheses have been proposed to explain some or all of them. It is now recognized that the yellow complexes are square-planar, while the blue ones are octahedral and are derived from the square-planar complexes by coordination of two additional ligands in the form of solvent molecules, H_2O molecules or anions, above and below the plane of the square-planar complex.

1.1.5.2.2 *Monomer-polymer equilibria*

Five- or six-coordinate species may result from the reversible association or polymerization of four-coordinate Ni(II) complexes. In cases where the association is particularly strong, the four-coordinate monomers are only observed at high temperatures.[21] Examples of such equilibria include the paramagnetic bis(*N*-alkylsalicylaldimine)nickel(II) complex [Ni(Me-sal)$_2$].It was observed that the magnetic moment of Ni(Me-sal)$_2$ **5** (R= Me) in chloroform and benzene increases with concentration, leading to the conclusion that the magnetic behaviour of this complex is due to an equilibrium between square-planar and associated species containing

paramagnetic nickel ions. It was also found that the $Ni(Me\text{-}sal)_2$ complex, when heated above 180 °C, converted to a polymeric paramagnetic species.[22, 23] Another example of this kind of equilibrium is provided by the nickel(II) acetylacetonate complex **4**. The structure of complex **4** (illustrated in cartoon format) has been reported to be a very stable trimer, resulting from the sharing of some of the oxygen atoms to achieve an octahedral environment around each nickel atom. Detectable quantities of the monomeric complex appear only in a non-coordinating solvent at temperatures around 200 °C. The octahedral structure of Ni-acetylacetonate is readily preserved in the presence of donor solvents such as water or pyridine.

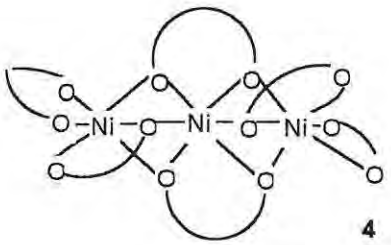

4

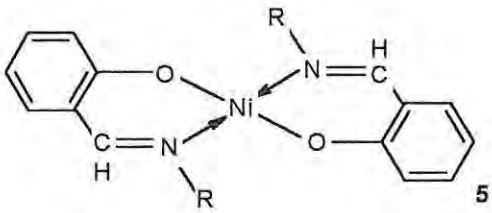

5

Another interesting feature of this structure is that substitution of the acetylacetonato methyl groups by more bulky *t*-butyl groups completely inhibits trimerization and, as a result, the planar monomer is obtained. In cases where groups sterically intermediate between methyl and *t*-butyl are employed, temperature and concentration dependent monomer-trimer equilibria are observed in non-coordinating solvents.[24, 25]

1.1.5.2.3 *Square planar-tetrahedral equilibria*

Such equilibria appear to exist in solution between complexes of the type NiL_2X_2, where L is a mixed alkyl arylphosphine. The position of the equilibrium is believed to depend, to some extent, upon steric factors, in the sense that the bis(bidentate)salicylaldimine complex **6** is *trans*-planar, while branching of the alkyl chain at the alpha carbon results in crowding in the *trans*-planar arrangement and a tetrahedral structure is favoured. Irrespective of the ring substituents, when R=Bu^t, the complex is entirely tetrahedral.[26]

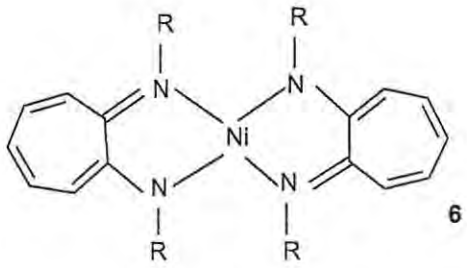

6

1.1.5.3 Macrocyclic nickel(II) complexes

The development of macrocyclic ligands capable of coordinating nickel(II) has been explored. In a recent investigation, Yaroslaw *et al.*[26] determined the crystal and molecular structures of the nickel(II) complexes of the malonamide-derived unsubstituted 14- and 13- membered tetraazamacrocyclic compounds **7** and **8** respectively. Crystallographic analysis of the nickel(II) complexes of these ligands (**7** and **8**) revealed that in both cases the nickel(II) ion possesses a square-planar coordination geometry, and is coordinated to all four of the nitrogen donors. The Ni-N bond lengths in the13-membered ring complex were found to be shorter than in the 14-membered ring, suggesting that the aperture of the 14-membered macrocycle, is too large to accommodate a low-spin nickel(II) ion in a square-planar arrangement.

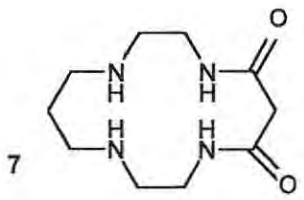

7

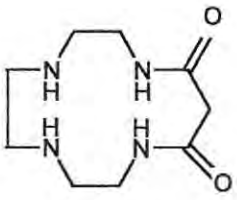

8

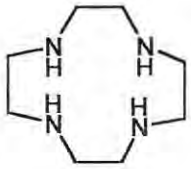

9

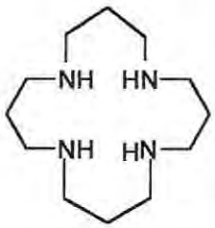

10

The stability of nickel(II) complexes of the 12- and 16-membered tetra-aza macrocyclic ligands **9** and **10**, respectively, has been determined by Viviene[27] and Mathieu [28] using potentiometric and UV-Visible spectroscopic techniques and MM calculations. As a rule the larger the metal ion, the more strongly it prefers the smaller macrocycles and *vice versa*, a trend contrary to that observed with crown ethers.[29] Viviene[27] investigated the "hole-size selectivity" of the ligands **9** and **10** using nickel(II) ion as it has both high-spin and low-spin forms. It was found that the low-spin Ni(II) ion (or other small metal ions such as Cu^{2+}) fits best in ligand **10** while, the high-spin state Ni(II) ion (or large metal ions such as Pb^{2+}) shows a preference for ligand **9**. These observations illustrate the trend that large metal ions prefer smaller macrocyclic cavities and *vice versa*. The reasons underlying this trend are that six- membered chelate rings are less flexible with respect to expansion and contraction, relative to five-membered rings, and the steric interactions with axially coordinated ligands, such as solvent molecules, are greater in ligand **9** than in ligand **10**.

Valeria *et al.*[30] have recently reported the pH-controlled translocation of Ni(II) ion within a ditopic receptor bearing an anthracene moiety exhibits "a mechanical switch-off fluorescence". They have investigated the behaviour of the sexidentate ligand **11a** having two distinct compartments, compartment *B* containing two quinoline and two amine nitrogen atoms and compartment AH_2 containing of two amide and amine nitrogen atoms.

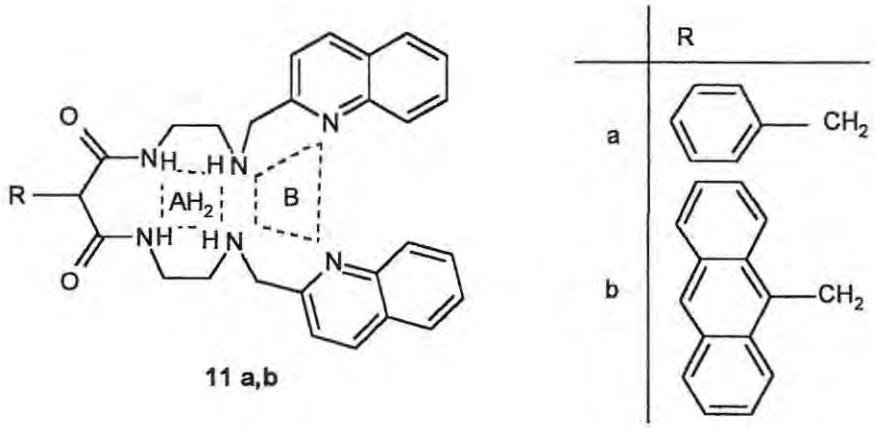

In ligand **11a**, AH_2 is a poorly coordinating compartment while the deprotonated form A^{2-} is a strongly coordinating compartment. Studies conducted by Valeria *et al.*[30] revealed that, at pH = 7.5, the Ni(II) cation stays in the *B* compartment (exhibiting high-spin, octahedral geometry) while, at pH > 9.5, the Ni(II) cation is located in the adjacent A^{2-} compartment (exhibiting low-spin, square-planar geometry). Thus, by varying the pH, the Ni(II) ion can be translocated from one compartment to the other. When an anthracene (An) fragment, was linked to the AH_2 compartment (as in ligand **11b**), the translocation of nickel switched the An fluorescent emission OFF, and *vice versa* when the nickel ion is in the *B* compartment. The quenching of fluorescent emission is ascribed to a Ni(II)-to-An* electron-transfer process.

1.1.5.4 Chelation of Ni(II) using ion exchange resins

The selective absorption of transition metal-ions, including the first triad ions, Fe(III), Ni(II) and Co(III), from sulfuric acid solutions using chelating ion exchange resins has been extensively studied by Grinstead.[31] The investigation concentrated on the use of the ion-exchange resins XFS-4195, and XFS-4308.[32] The XFS-4195 resin contains bis(picolyl)amine, attached to a polystyrene divinyl benzene co-polymer **(Figure 1a)**, while the XFS-4308 resin contains the *N*-(2-hydroxypropyl)picolylamine ligand as shown in **Figure 1b**.

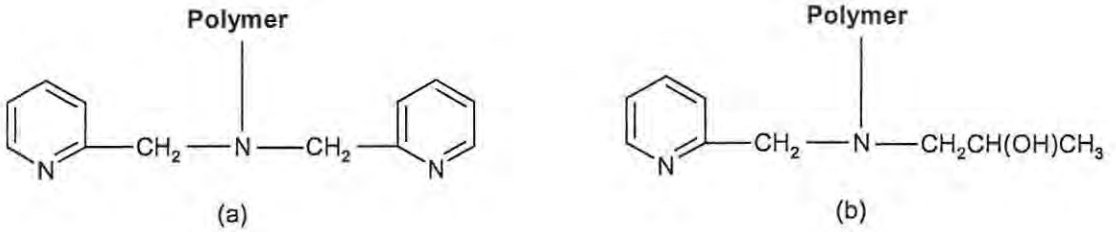

Figure 1. General structures of the resins **a**) XFS-4195 and **b**) XFS-4308.

Grinstead eluted resin XFS-4195 with 1N-sulfuric acid or 2-4N-ammonium hydroxide and the eluents were analyzed either calorimetrically or by atomic absorption spectrometry. Copper was the most strongly coordinated ion of the group examined. Uranium was also absorbed well, but difficulties were observed in eluting it with dilute sulfuric acid. The other metal ions were absorbed in the approximate order:- Ni(II) > Fe(III) > Zn(II) > Co(II) > Cd(II) > Fe(II). These chelating resins are commercially available, and Kenneth [33] has discussed the chelating properties and hydrometallurgical applications of the patented resin, XF-4196.

1.2 Molecularly Imprinted Polymers (MIP's)

Chromatographic techniques are widely employed for the "separation, identification, and determination of the chemical components in complex mixtures".[34] All of these techniques have, in common, the use of a stationary phase and a mobile phase, and the separation of the mixture of compounds is based upon the rate at which they are carried through the stationary phase by the gaseous or liquid mobile phase. Specifically, they rely on chemical or physico-chemical interactions between the stationary and mobile phases. Materials such as octyldecylsilane-derivatised silica, used in reverse-phase High Performance Liquid Chromatography (HPLC), behave in a non-specific manner, and the separation of compounds that are very similar to one another becomes problematic. However, MIP's could be the solution to this problem.

1.2.1 Definition and origin

Molecular imprinting technology, commonly described as a "way of making artificial locks" for molecular "keys", has its origin in the area of immunology.[35] Pauling's theories about the remarkable specificity of antibody-antigen complexes prompted the idea that the same concept could be used in synthetic matrices,[36] and the breakthrough in this technology was achieved in the late 1970's.This technology is currently being investigated using two basic approaches, *viz.*, self-assembled and pre-organized systems **(Figure 2)**.

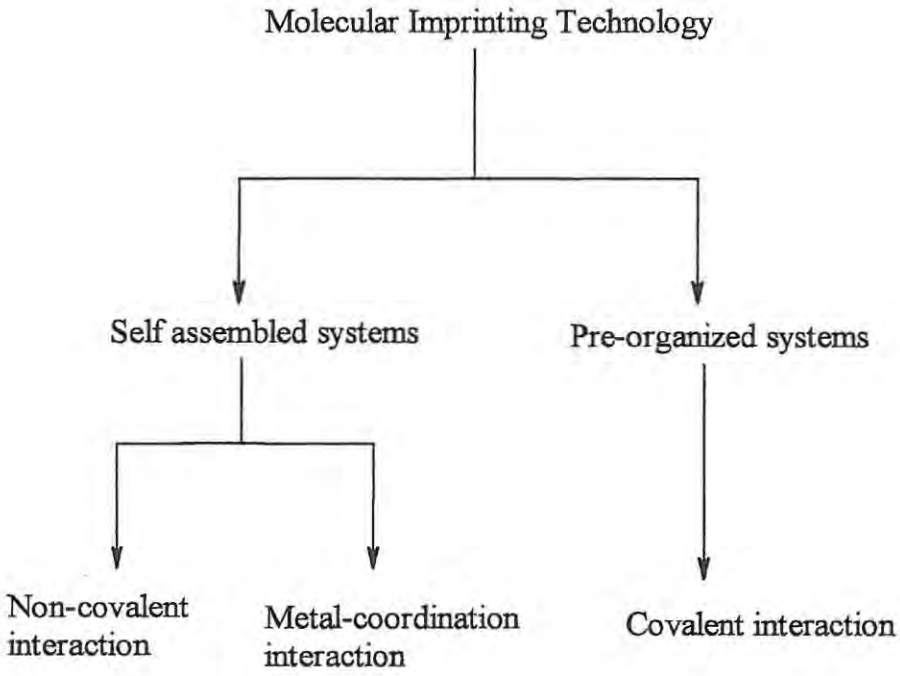

Figure 2. Two basic approaches to molecular imprinting technology.[37]

In the pre-organized systems, developed mainly by Wulf and co-workers,[38] the aggregates form in solution before polymerization is effected and are maintained by (reversible) covalent bonds. Mosbatch and co-workers,[39] on the other hand, developed self-assembled systems, in which the arrangement between the "print species" and the functional monomers involves non-covalent or metal-coordination interactions. Mosbatch defines molecular imprinting as "a methodology for the creation of selective recognition sites in synthetic polymers". This technique involves the polymerization of functional monomers in the presence of an analyte or "print species" (template). "After polymerisation, the template species is removed, leaving a glassy, rigid polymer, which contains an exact imprint of the species".[38]

1.2.2 The production of molecularly-imprinted polymers

The production of MIP's requires an appropriate "print species", a "functional" monomer and cross-linking agents, an initiator and a "porogen" as basic materials.

1.2.2.1 Print species

The "print"(imprint or template) species, is the target species of interest which is used in the imprinting procedure.[40] Examples of print species employed in imprinting protocols are listed in **Table 4.**

Table 4. Examples of print species employed in MIP syntheses.[40]

Compound class	Example
Drugs	timolol, theophylline, diazepam, ephedrine
Proteins	RNase A, urease
Carbohydrates	glucose, fucose, galactose
Amino acids	phenylalanine, tryptophan, tyrosine, aspartic acid
Nucleotide bases	adenine
Co-enzymes	pyridoxal
Hormones	cortisol
Pesticides	atrazine

1.2.2.2 Functional monomers

The functional monomers (or "lock-building monomer") are the polymerizable entities which interact with the print species. Their structures will be determined by the nature of the print species but most importantly, they must contain a polymerizable functional group.

1.6.2.3 Cross-linking agents

Cross-linkers, some of which are illustrated in **Figure 3**, are units which contain two or more polymerizable moeities permitting both attachment to the functional monomer and the formation of polymeric matrix.

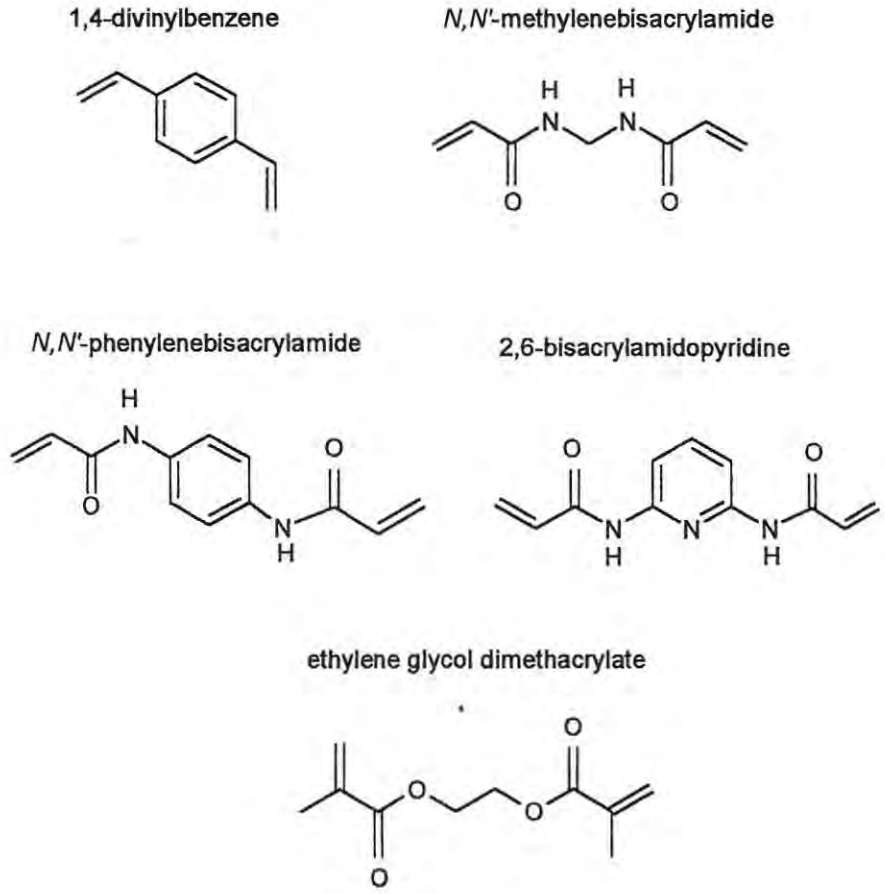

Figure 3. Examples of cross-linkers used in the production of MIP's. [41, 42]

Of the cross-linkers indicated above, many researchers choose to use ethylene glycol dimethylacrylate (EGDMA) for imprinting processes. Wulf[38] has recommended use of this cross-linker since it imparts good thermal and mechanical stability. Moreover, it has been found that chromatographic columns employing MIP's prepared with EGDMA, do not lose their selectivity (even at 80°C) during constant use over many months; in contrast, MIP's prepared using divinylbenzene as cross-linker, lose their selectivity on prolonged use at 70 °C. EGDMA is also the cheapest cross-linking agent and is easy to purify.[43]

1.2.2.4 Polymerization initiator

An initiator is a substance that starts the polymerization process. The most widely used radical initiator appears to be azobis(isobutyronitrile) (AIBN). This initiator decomposes under mild conditions (*ca.*50 ^{0}C) to afford the reactive cyanopropyl radicals which then initiate polymerization as indicated in **Figure 4**.

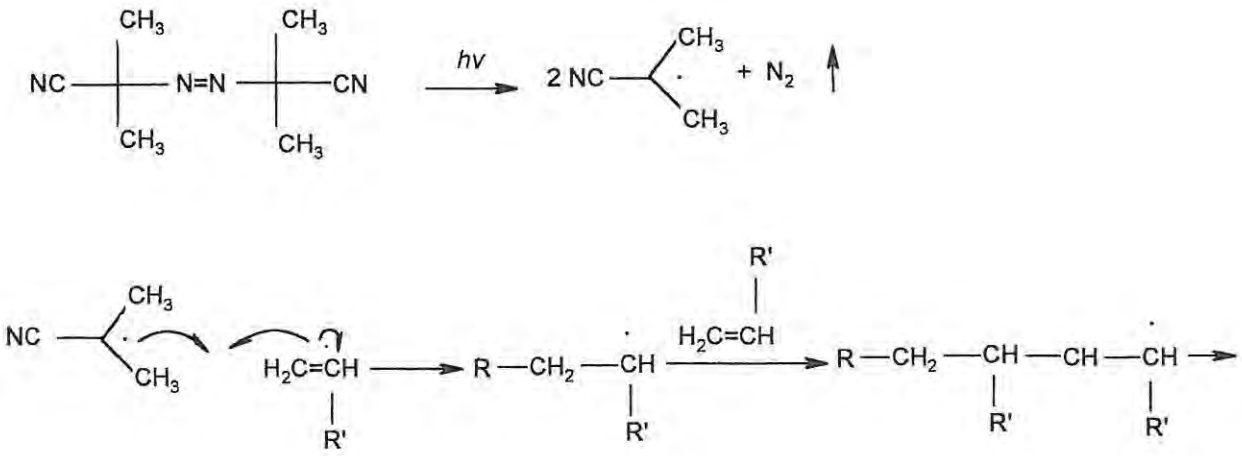

Figure 4. Schematic representation of the polymerization process using the initiator azobis(isobutyronitrile).[44]

1.2.2.5 Porogens

A porogen is a solvent that induces porosity in molecularly imprinted polymers and plays a vital role in the application outcome of MIP's.[45] It has been suggested that the more polar the porogen, the weaker the resulting recognition effect becomes. High swelling of the polymers has been observed in chlorinated solvents ($CHCl_3$, CH_2Cl_2) relative to CH_3CN and THF, and it is advisable to employ the same porogen throughout the imprinting process to avoid any problems associated with swelling.

1.2.2.6 Generating molecularly imprinted polymers

The first step in generating an MIP is to mix the print species with a functional monomer **(Figure 5)** in the presence of a porogen, thus allowing association to develop (steps **I** and **II**). The monomer assembly is then polymerized (step **III**) under conditions that lead to the formation of rigid, highly cross-linked polymers, using excess cross-linking agent. After removal of the template (step **4**), polymers with well-defined cavities are obtained. The rigid polymeric material is generally pulverized to afford fine particles, thereby increasing the surface area available for interaction with the analyte.[41,46]

1.2.3 Properties of molecularly imprinted polymers

Various physical properties influence the efficiency of MIP's.[48-51] These include the following.

i) *Stiffness of the polymer structure.* This is important for high selectivity because it allows the cavities of the polymer to retain their shape even after removal of the template.

ii) *Flexibility of the polymer structure.* This works against the above-mentioned property, but is essential for rapid equilibration with the substrate.

iii) *Accessibility.* This is a function of the porosity and ensures access to as many cavities as possible in the highly cross-linked polymer.

iv) *Mechanical stability.* This is of vital importance for many applications, for example for use in HPLC columns at high pressure or for use as a catalyst in a stirred reactor.

v) *Thermal stability of the polymers.* This permits MIP's to be used at elevated temperatures.

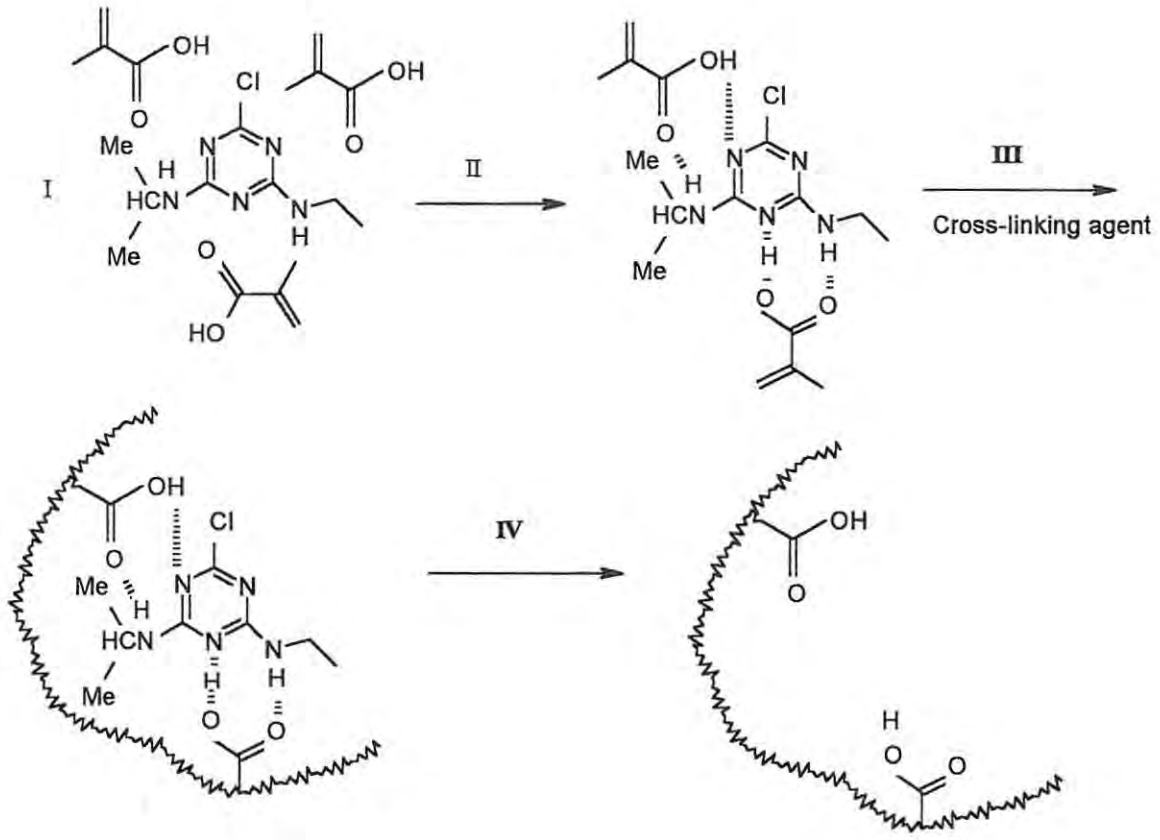

Figure 5. Illustration of MIP generation,[47] involving **I**) component mixing; **II**) H-bond formation; **III**) polymerisation; and **IV**) extraction of the template.

1.2.4 Applications of molecularly imprinted polymers

Many applications of MIP's have been developed. These include the use of MIP's in the separation and isolation of various substances, as antibody and receptor mimics in immunoassay-type analyses, in organic synthesis as enzyme mimics, and as sensors in biosensor-like devices.[52]

1.2.4.1 Separation and isolation

This is by far the most studied application and more than 20 substances have been investigated (*e.g.* therapeutic drugs, metal ions, dyes *etc.*).[41] It has been observed that remarkable stereo-and regioselective separation[38,53] may be achieved by preparing"tailor-made" supports with pre-determined selectivity. The most widely studied area in this category is the separation of enantiomers from racemic material. A high proportion of the drugs presently on the market are administered in racemic form and regulatory controls require both enantiomers to be subjected to separate "pharmacokinetic and toxicological profiling".[38] MIP's may play a vital role in this regard, being employed as a solid phase adsorbents in chromatography, especially HPLC.[54] For instance, if the *R*-enantiomer is used as the template, the *S*-form will be eluted first and *vice-versa* when the *S*-enantiomer is used as the template.[55] The use of MIP's is currently being extended to chemical applications, particularly the separation of metal ions as detailed in Section **1.2.5**.

1.2.4.2 Antibody/receptor-binding mimics

The development of MIP's as antibody mimics has been reported.[56] Mosbatch's group [39] has explored the specific recognition of therapeutic drugs such as theophylline, diazepam and morphine. Mosbatch *et al.* have described the use of theophylline and diazepam MIP's as specific adsorbents in competition binding assays called "molecularly-imprinted sorbent assays" (MIA's). MIA recognition of related systems was either non-existent or far below that of the template species. The anti-theophylline MIP's have been used for the determination of theophylline concentrations in patient serum samples demonstrating their potential as stable alternatives to antibodies in conventional immunoassays.

1.2.4.3 Catalytic and synthetic applications

The development of MIP's with catalytic activity (commonly called "plastic enzymes") has been reported.[57] In essence, this involves producing a cavity with a shape similar to that of the active enzyme. The commonest approach has been the use of "transition state analogues" (TSA's) in the imprinting procedure, thus permitting stabilization of the transition state complex and enhancing the rate of product formation. Attention has been given to the hydrolysis of esters using a phosphonate TSA as a template molecule. Reactions catalyzed by these "plastic enzymes" depend on the nature of the template employed during the MIP synthesis.[58,59]

1.2.4.4 Biosensor-like devices

MIP applications have been extended to their use as recognition elements in biosensor-like devices.[57] Ideally, the sensing element (such as an enzyme, an antibody or a receptor) is immobilized at the interface between the sensor and the analyte sample, and a chemical signal resulting from the binding of the analyte to the recognition element is transduced into an electrical signal. The MIP constitutes the "biopart" in an enzyme or antibody-based sensor,[38] and tends to be more stable than the natural counterpart, being effective even in harsh environments.

1.2.5 Metal-selective molecularly imprinted polymers

In an imprinting protocol, metal cations can also serve as templates. The resulting metal-ion selectivity of the MIP will depend on various factors, including:- cation-ligand interaction specificity; the coordination geometry and coordination number of the cations; the charge on the cation; and, to some extent, the size of the cation.[38, 60]

Various ways of preparing metal-selective imprinted polymers have been developed. In the first, mixtures of bifunctional monomers containing complexing groups are polymerized in the presence of the metal cation. The 3-oxapentanediamide derivative **12a**, for example, was employed to generate molecular imprints of Ca^{2+} and Mg^{2+} ions in divinylbenzene-based polymers.

The polymers formed were shown to bind the Ca^{2+} ion selectively over Mg^{2+}, but the selectivities were reported to be quite poor.[60]

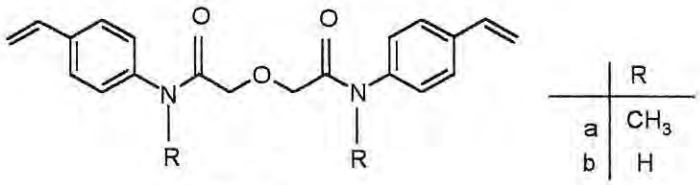

12 a,b

The second method is very similar to the first except that the polymerizable ligands interact with the print species prior to crosslinking. Very selective ion exchangers have been prepared using metallic complexes of methacrylic acid and 4-vinylpyridine.[38] **Table 5** shows the selectivity observed when Cu^{2+} imprinted resin was equilibrated with mixtures of Cu^{2+} and other cations.

Table 5. Selectivity of a Cu^{2+} imprinted resin for the separation of cationic pairs.

Metal ion pairs	α [a]	α_{blank} [b]	α^{1} [c]
Cu^{2+}/Zn^{2+}	58	42	14
Cu^{2+}/Cd^{2+}	136	3.3	41
Cu^{2+}/Pb^{2+}	28	0.46	62

α [a] = k_1/k_2 = selectivity coefficient where, k_1 is the activity for Cu^{2+} and k_2 corresponds to M^{2+}.

α_{blank} [b] = selectivity coefficient for blank resin. α^{1} [c] = α/α_{blank}

A third approach, involving the use of linear polymers, such as poly(4-vinylpyridine)(PVP) has been demonstrated by Nishide *et al.*[61] When PVP was cross-linked with 1.4-dibromobutane using a metal ion (Cu^{2+}, Co^{2+}, or Cd^{2+}) as the template, DBQP resins were obtained. The metal absorption characteristics of the resins are summarized in **Table 6**, the metal in parentheses indicating the ion used as the template.[62] Irrespective of the pH or concentrations studied, it was observed that Cu^{2+} ions are adsorbed on DBQP (Cu) much more efficiently than on DBQP (Co) and that cobalt ions are adsorbed on DBQP (Co) more efficiently than on DBQP (Cu). Selectivity for Cd^{2+} ions, however, was poor.

Table 6. Adsorption of metal ions on DBQP resins.[61]

	Adsorbed metal ions, %			
Resin	Cu^{2+}	Co^{2+}	Zn^{2+}	Cd^{2+}
DBQP (Cu)	54	6	8	9
DBQP (Co)	16	10	8	9
DBQP (Zn)	8	6	11	6
DBQP (Cd)	9	4	7	8
DBQP -1[a]	15	7	6	6

[a] Reducing the amount of copper resin.

A fourth, recently developed technique for preparing MIP's is "surface imprinting". In this approach, weak points, such as the slow re-binding kinetics associated with conventional molecular imprinting techniques are addressed. Surface imprinting is achieved *via* emulsion polymerization using a functional monomer, an imprint molecule, an emulsion stabilizer and a matrix-forming molecule, as illustrated in **Figure 6**.[62] The oil-aqueous interface is the recognition zone for the target species. Complexation of the water-soluble target species and the functional monomer occurs at the oil-aqueous interface in a regular pattern. This is followed by polymerization of the matrix-forming monomers in the organic phase with the target selective groups remaining on the polymer surface.

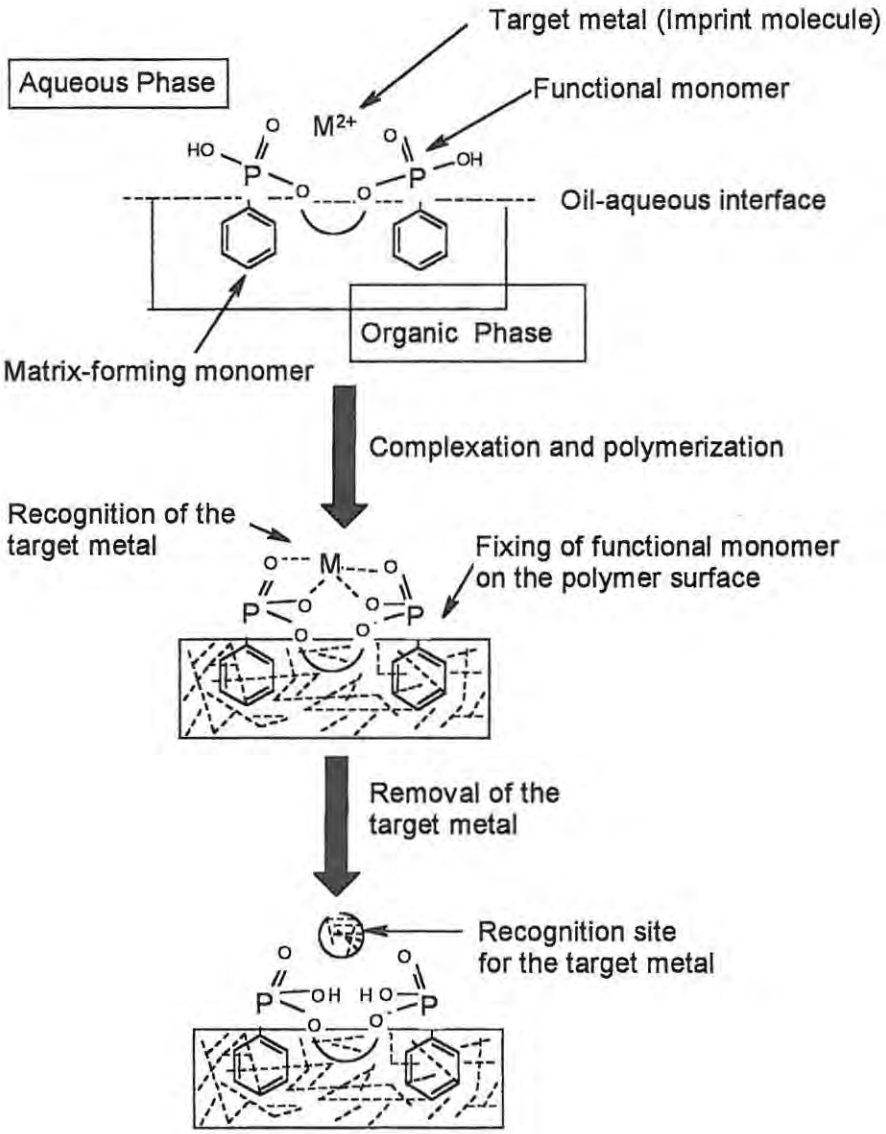

Figure 6. Schematic representation of the surface template polymerization technique.[62]

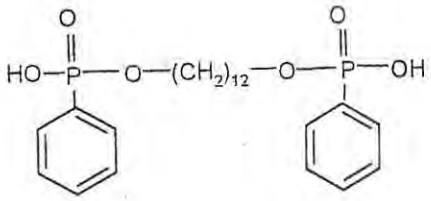

13 DDDPA

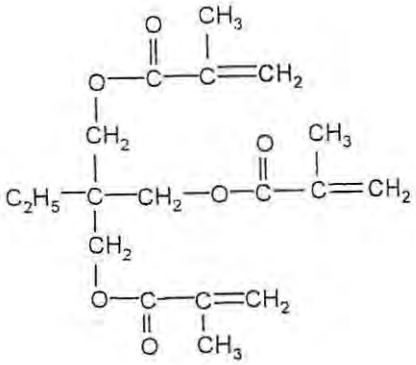

14 TRIM

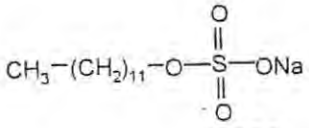

15 SDS

Three factors appear to enhance the template effect of functional monomers,[38,63] *viz.*, a long alkyl chain which leads to high interfacial activity, the presence of aromatic rings to afford enhanced rigidity in the recognition sites, and metal recognition groups which produce high binding affinities for the target metal ion. Masahiro *et al.*[64] employed the bifunctional monomer, 1,12-dodecanediol-*O,O'*-diphenylphosphonic acid (DDDPA) **13**, the matrix-forming monomer, trimethylolpropane trimethacrylate (TRIM) **14**, which has 3-polymerizable groups to enhance polymer rigidity, and sodium dodecyl sulfate (SDS) **15** as a dispersion stabilizer to prepare highly cross-linked Zn-imprinted polymer beads. The dispersion stabilizer SDS **15** is added to the aqueous phase and plays a vital role in maintaining uniformly-sized spheres. Competitive adsorption of Zn(II) and Cu(II) on Zn(II)-imprinted and unimprinted polymers using water-in-oil (W/O) or water in oil-in water (W/O/W)emulsions revealed that adsorption increased with increasing pH on all polymers, and that the Zn(II)-imprinted polymer exhibited better selectivity for zinc ions over copper ions in the pH range 1- 4. While the imprinted polymer, prepared using the W/O emulsion, exhibited

a higher template effect than the W/O/W emulsion, the latter has the advantage of promoting the formation of spherical particles which can be useful in industrial applications because they can be used directly without grinding into fine particles.[65]

Fish [66] recently reported the use of MIP's for recovering precious metals, such as gold and silver, from aqueous solution or for cleansing polluted waters of mercury and other toxic metals. To create his imprinted polymers, Fish first "sandwiched" the target metal ions between a pair of organic ligands [*e.g. N*-(4-vinylbenzyl)-1,4,7-triazacyclononane (TACN)]. The resulting "sandwich" was then cross-linked to form a polymer and, finally, the metal ion was leached out with strong acid, leaving empty sites of the right size to fit similar ions. The imprinted polymer was ground to a fine powder such that when an aqueous solution of metal ions was passed through it, the ions were trapped in the empty sites and thus removed from the solution. The metal selectivity exhibited by these systems is attributed to the fact that different metal ions have different ionic radii (the average distance at which mutual repulsion of their electric charges makes them repel one another like hard spheres). But in a situation where the ionic radii are similar [as in Cu(II) and Zn(II)], thermodynamic effects appear to be the overriding factor. Fish showed that for a solution containing equal concentrations of the ions, the TACN polymer captured 157 Cu ions for every zinc ion- an observation attributed to the greater thermodynamic stability of the Cu-TACN complex.[66]

When Cu(II) ions and Fe(III) ions were exposed to Zn-imprinted TACN polymer, the Cu(II): Fe(III) selectivity was 44 : 1. [66] In this case, the most likely explanation lies in the size of the hole in the polymer. Thus, although Fe(III) interacts more strongly with TACN than Cu(II), the ionic radius of Fe(III) is considerably smaller than that of Cu(II).[66]

1.3 Previous work done in the group

Previous work undertaken in our research group has been directed at the design, synthesis and evaluation of biomimetic and metal-specific ligands. In the development of biomimetic ligands, Wellington[67] synthesized various copper(II) complexes and cobalt(II) analogous to model the active site of the enzyme, tyrosinase. The active site is believed to resemble that in haemocyanin and to contain two copper atoms capable of coordinating dioxygen.

The development of pgm-specific ligands was investigated by Hagemann;[68] bidentate, tridentate and tetradentate sulfur-containing ligands were designed to specifically chelate platinum and palladium in the presence of base metals. Recently the programme has been extended to silver-specific ligands and Daubinet[69] has synthesized polydentate malonamide derivatives to coordinate silver(I). Extraction studies demonstrated the selectivity of these ligands for silver in the presence of base metals, and the application of computer modelling suggested the capacity of the ligands to chelate Ag(I) in a tetrahedral environment.

1.4 Aims of the present investigation

Various nickel complexing ligands have been synthesized,[70] but those containing nitrogen and oxygen donor atoms appear to complex nickel most strongly. Despite the development of numerous polydentate ligands employed to separate nickel from other metal ions, the industrial extraction of lateritic nickel oxide has not been satisfactorily achieved. This is particularly true for the extraction of nickel from acidic medium in the presence of iron. In attempting to design ligands which address these limitations, the following objectives have been identified.

1. An extensive literature survey to establish the determinants for optimal nickel selectivity, with particular emphasis on the following ligand criteria:-
   - i) stability at low pH;
   - ii) selectivity for nickel in the presence of iron; and
   - iii) high nickel stripping efficiency.

2. The design and synthesis of selected ligands, which are expected to satisfy the above criteria and offer potential for use in MIP's containing nickel-specific cavities.
3. Characterization, where possible, of the resulting ligand nickel complexes using X-ray crystallographic, spectroscopic and computer modelling methods.
4. Preparation and evaluation of nickel-selective MIP's.

2 DISCUSSION

In the discussion which follows, attention is initially given to the criteria used to design a general, nickel-selective, bidentate ligand system and its retrosynthetic analysis (Section **2.1**). This is followed by a discussion of:-the synthesis of ligand monomers containing both pyridine and amine nitrogen donors (Section **2.2**); mass spectrometric studies and the formation of metal complexes using these ligands (Section **2.3** and **2.4**, respectively); and computer modelling studies (Section **2.5**). Finally, the preparation and evaluation of molecularly imprinted polymers (MIP's) containing selected ligands are discussed in Section **2.6**.

2.1 Ligand design and retrosynthetic analysis

The design of nickel-selective ligands has focussed primarily on the ligand criteria identified in Section **1.4**. Particular emphasis has been placed on the use of nitrogen donor atoms, one of which is provided by a pyridyl moeity, selected to enhance complex stability at low pH. The preferred stereochemistry of nickel(II) complexes, *viz.*, four-coordinate tetrahedral or square-planar (see Section **1.1.5**),[71] prompted us to develop bidentate ligands capable of affording complexes with such geometries. The essential features of these systems are illustrated in **Figure 7**.

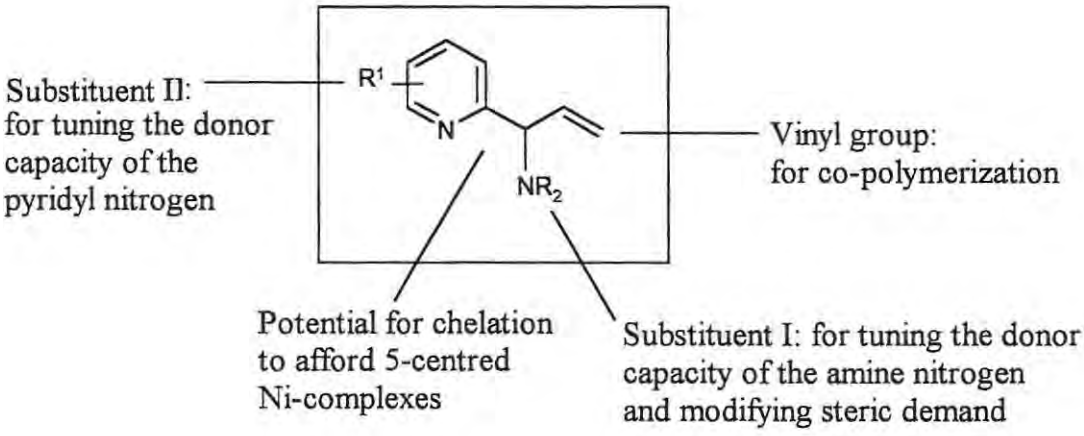

Figure 7. The proposed ligand system.

Chelation is known to contribute to coordination stability,[72,73] and the presence of five- or six-membered chelate rings appears to be vital in establishing a "*chelate effect*".[74] Chelation of the ligand system **(Figure 7)** has been designed to permit the formation of 5-centred Ni-complexes. The vinyl group was included for co-polymerization to afford MIP's containing nickel-selective cavities which can exhibit selectivity for nickel in the presence of iron. The substituent I was expected to influence the donor capacity and steric accessibility of the amine nitrogen, while substituent II was expected to influence the donor strength of the pyridyl nitrogen. The ligand was designed to satisfy the following requirements for industrial applications.

i) The use of a minimal number of reaction steps in the overall synthesis.
ii) The production of ligand systems in high yield and purity.
iii) The use of reagents that are cost effective, easy to use and environmentally friendly.

A retrosynthetic analysis was undertaken to establish a reasonable synthetic pathway to the target ligands from readily available precursors. The analysis outlined in **Figure 8** provided a basis for our synthetic efforts. Thus, a sequence of functional group interconversions (FGI's), beginning with the target molecule **(TM 1)**, led to the primary alcohol **16**, the ester **17**, and the α,β-unsaturated ester **18**. A final, Wittig disconnection afforded the pyridine-2-carbaldehyde precursor **19**. The corresponding synthesis, proposed on the basis of the retrosynthetic analysis is detailed in **Scheme 1**. In the event, a slight modification of the synthesis to afford the allyl ether system **TM 2** was necessary, and the detailed discussion about this modification is deferred to Section **2.2.2**.

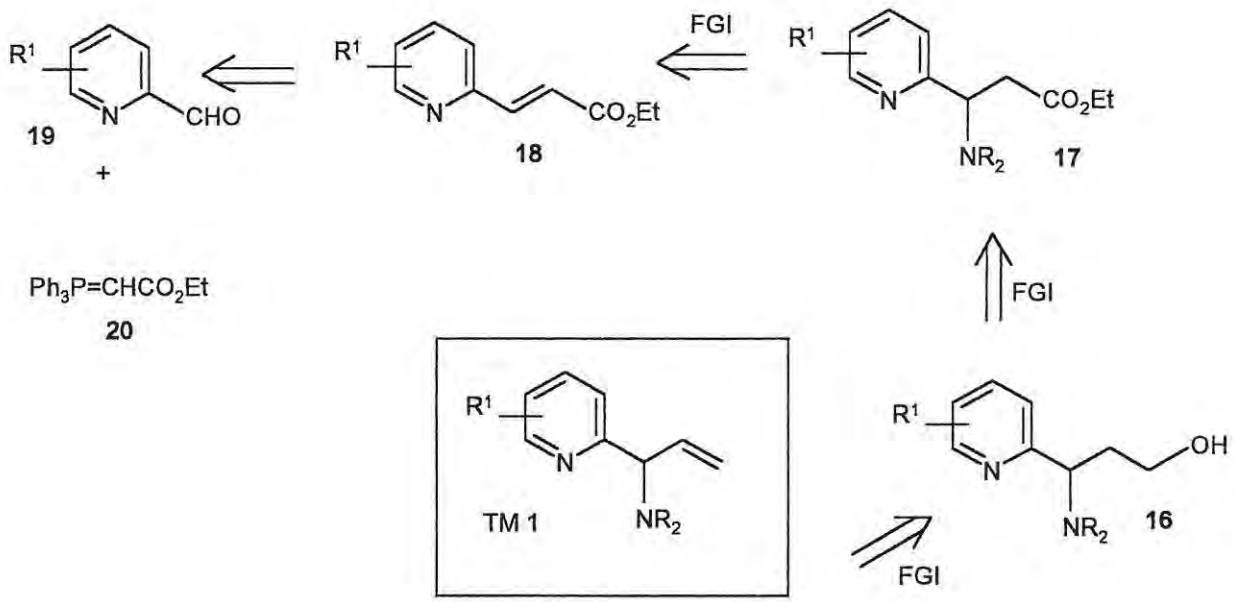

Figure 8. Retrosynthetic analysis of the desired ligand system TM 1.

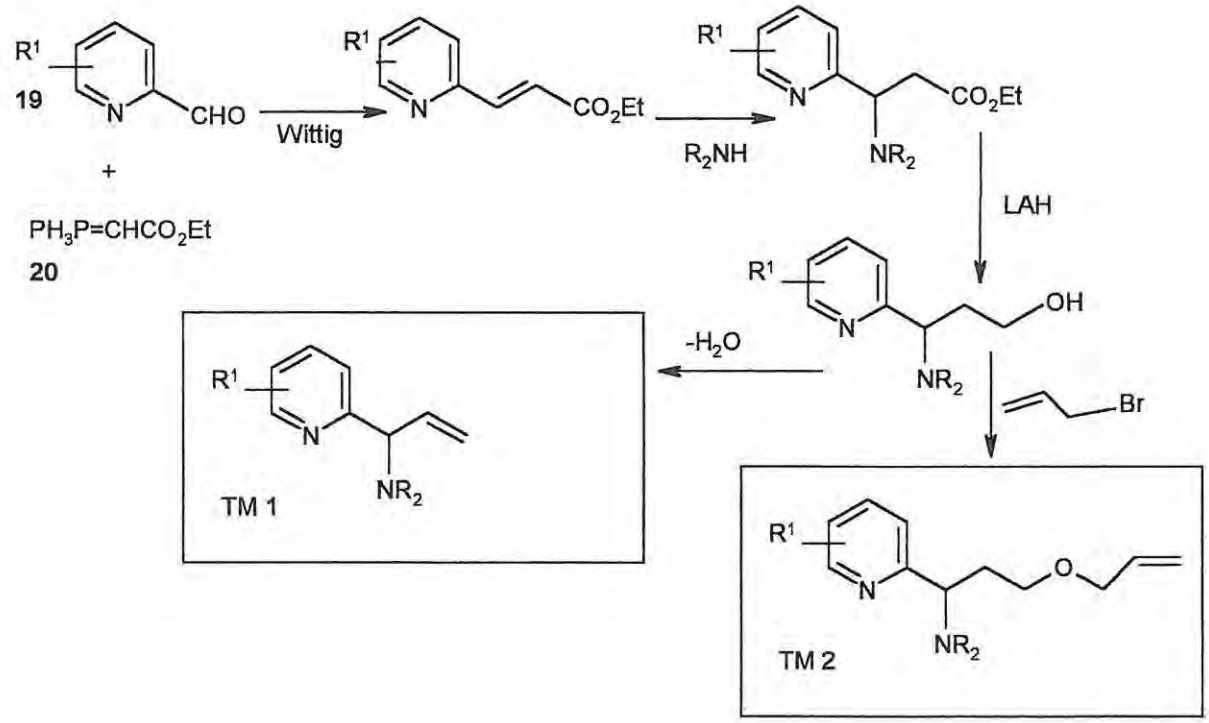

Scheme 1. General synthetic scheme.

2.2 Ligand synthesis

The first step in the proposed synthesis involved generation of the ylide **20**.[75-77] A solution of triphenylphosphine **21** in absolute EtOH, was treated with 1 equivalent of ethyl bromoacetate **22** at 0 °C under nitrogen **(Scheme 2)**. The reaction mixture was stirred for 30 min, and then allowed to stand at 5 °C for 16h, before stirring at 18 °C for 3h and re-cooling to 0 °C. The precipitate was collected, washed with cold EtOH, and dried under reduced pressure to afford, triphenylphosphonium bromide **23** in 75 % yield, as a colourless solid. Dehydrobromination of triphenylphosphonium bromide **23** with aqueous KOH to obtain ylide **20**, was not attempted, as the ylide **20** was found to be commercially available.

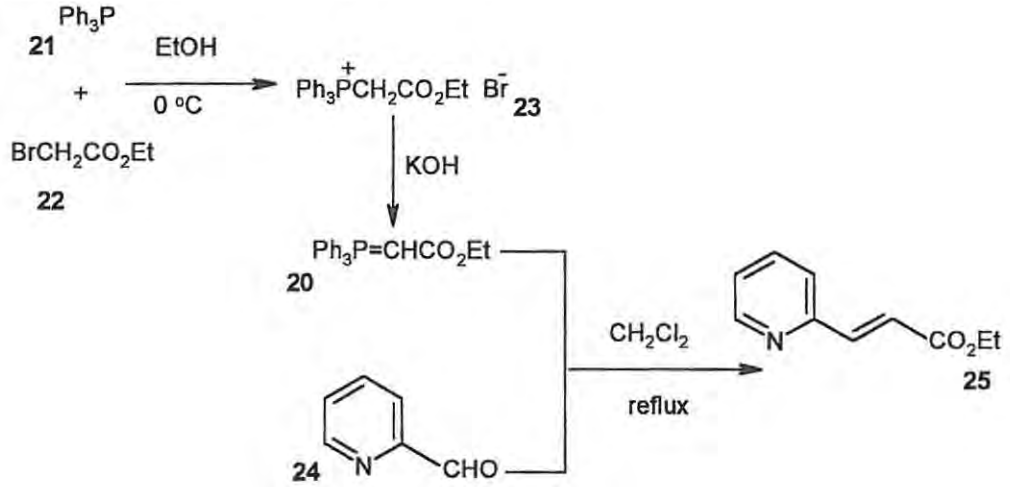

Scheme 2. Preparation of ethyl 3-(2-pyridyl)acrylate **25**.

In a Wittig reaction, the ylide **20** was treated with 1 equivalent of pyridine-2-carbaldehyde **24** in boiling CH_2Cl_2, following procedures reported by Wyne [76] and Furniss. [78] Work-up, after boiling the reaction mixture under reflux for 26h, afforded the required α,β-unsaturated ester **25** in very low yield (22 %). The reaction was repeated using the same molar ratios without CH_2Cl_2 and increasing the temperature; this resulted in an improvement in the yield of the ester **25** from 22%

to 84 % after the reaction mixture had been boiled under reflux for 24h. When the reaction time was increased to 26 h, the ester **25** was obtained in 93 % yield! The formation of ester **25** was clearly evident from the ^{1}H NMR data **(Figure 9a)**, which revealed the disappearance of the aldehyde peak at δ 9.5 ppm, the appearance of doublets at δ 6.90 ppm and at δ 7.66 ppm corresponding to the vinylic protons. A DEPT-135 NMR spectrum **(Figure 9b)** confirmed the presence of a single methylene carbon signal at δ 61.1 ppm. The *trans*-geometry of the double bond was confirmed by the large coupling (*J* 15.7 Hz) between the vinylic protons.

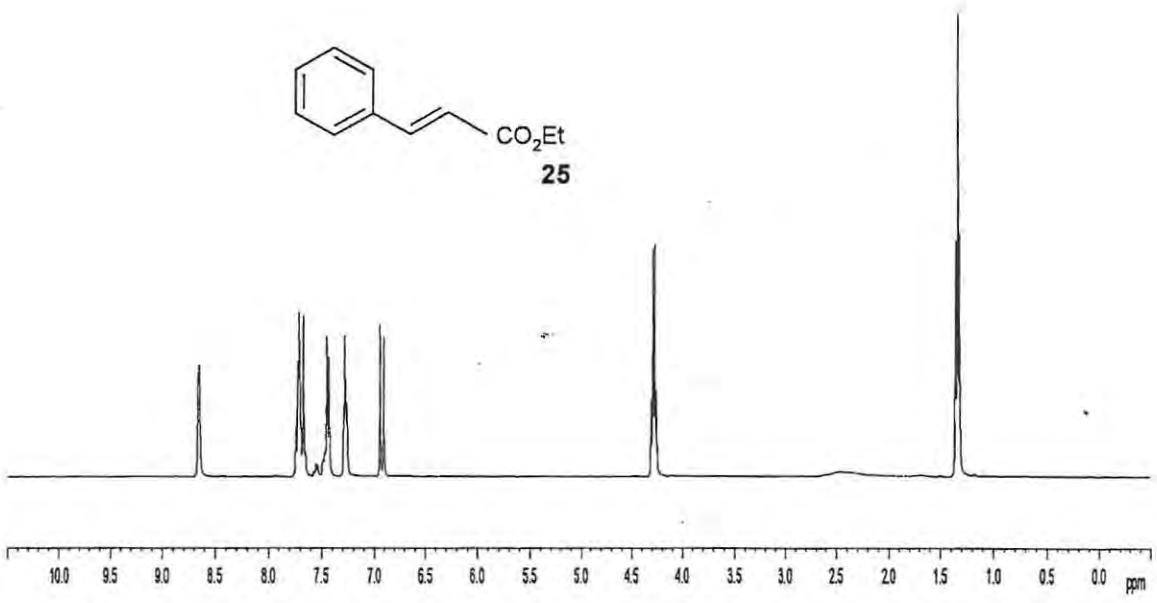

Figure 9a. 400 MHz ^{1}H NMR spectrum of the ester **25** in $CDCl_3$.

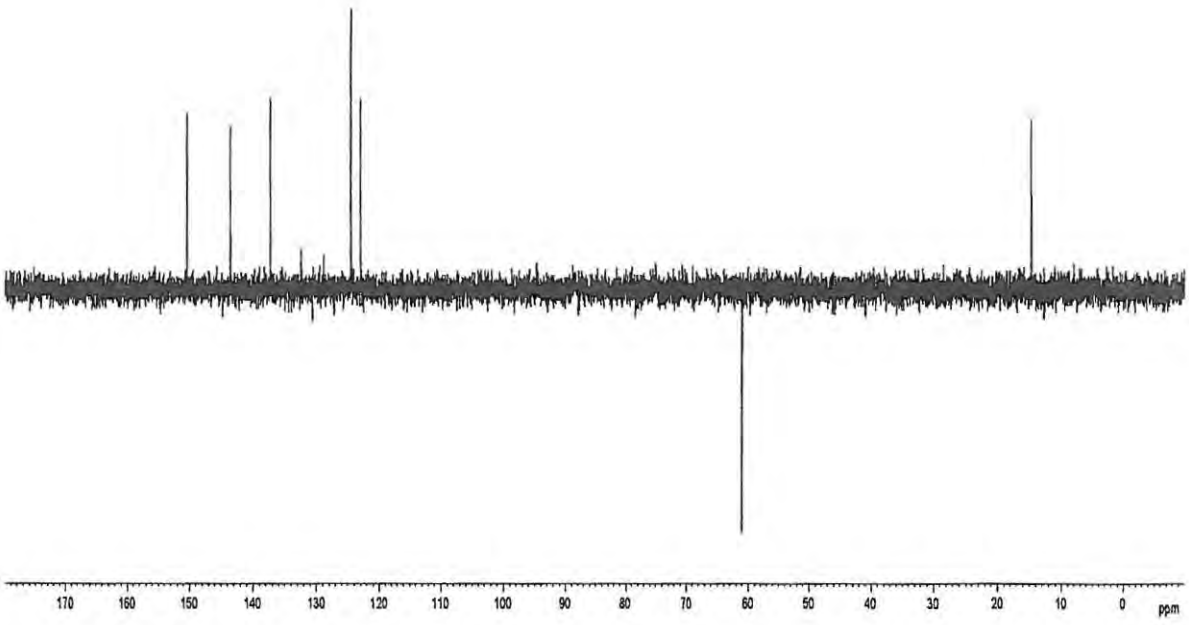

Figure 9b. DEPT-135 NMR spectrum of the ester **25** in $CDCl_3$.

The next step involved conjugate addition of an amine to the α,β-unsaturated ester **25,** and several attempts were made using piperidine **(Scheme 3)**. In the first, treatment of the ester **25** with piperidine in dry THF at room temperature for 9 days failed to afford the expected product **26**. However, when piperidine was used as both solvent and nucleophile, compound **26** was obtained in 19 % yield after stirring at room temperature for 4 days; when the reaction was repeated at reflux for 12 h, the yield increased to 34 %. The reflux period was then increased from 12h to16h, resulting in a significant improvement in the yield (from 34 to 99 %). The optimized conditions were then applied to the preparation of the pyrrolidinyl and morpholino analogues, **27** and **28**, respectively. Completion of the reaction, in each case, was confirmed by monitoring the disappearance of the vinylic protons, using ^{1}H NMR spectroscopy. The ^{1}H NMR spectrum of compound **26 (Figure 10a)** reveals a downfield multiplet at δ 4.09 ppm, corresponding to the methine proton at the chiral centre, and a multiplet at δ 2.37 ppm, due to the four piperidinyl methylene protons adjacent to nitrogen atom; significantly, there are no signals in the vinylic region (δ 4.5-6.5) confirming the absence of substrate **25**. The asymmetric methine carbon resonates at δ 67.1 ppm in the ^{13}C NMR spectrum **(Figure 10b)**.

Conjugate addition of amines to the α,β unsaturated compound **25** was then extended to the use of primary aliphatic amines, to afford the corresponding products, **29-31** and the aromatic amine, aniline, to afford the addition product **33 (Scheme 3)**. Initially, conjugate addition was attempted using butylamine as both solvent and nucleophile. The reaction mixture was stirred at room temperature for 14 days, but afforded compound **29** in only 19 % yield. However, when the reactants were boiled under reflux in THF for 24 h, compound **29** was obtained in 86 % yield, and this approach was successfully applied for the synthesis of the benzylamine and isopentylamine derivatives, **30** and **31**, respectively (see **Table 7**).

Attempts to effect conjugate addition of 3-pentylamine proved unsuccessful. At first, 3-pentylamine was used as both solvent and nucleophile, but no reaction was evident after boiling the reaction mixture under reflux for 2 weeks; when THF was used as solvent and the mixture refluxed for 6 days there was, similarly, no reaction. Attempts to effect conjugate addition using aniline as both solvent and nucleophile also failed to give the expected product **33**. The reaction

was repeated using THF as solvent but without success, suggesting that delocalisation of the nitrogen lone pair electrons into the aromatic ring decreases the nucleophilicity of the aniline nitrogen sufficiently to inhibit conjugate addition.

The ^{1}H and ^{13}C NMR spectra illustrated for compound **30** in **Figures 11a** and **11b**, respectively, are the representative of the other conjugate addition products. A broad singlet at δ 2.02 ppm **(Figure 11a)** indicates the presence of an amino proton, while the ^{13}C NMR spectrum **(Figure 11b)** reveals a methine carbon signal at δ 60.0 ppm and carbonyl carbon signal at δ 171.3 ppm.

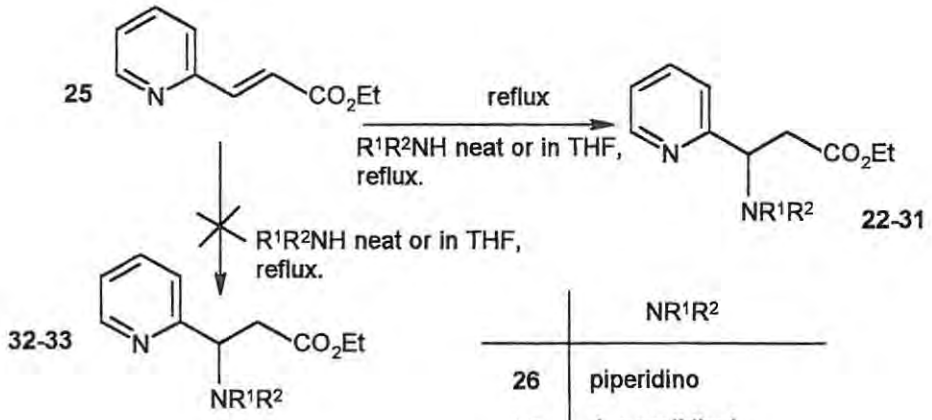

	NR^1R^2
26	piperidino
27	1-pyrrolidinyl
28	morpholino
29	BuNH
30	$PhCH_2NH$
31	$(CH_3)CHCH_2CH_2$ NH
32	$(CH_3CH_2)_2CH$ NH
33	Ph NH

Scheme 3. Formation of the conjugate addition products.

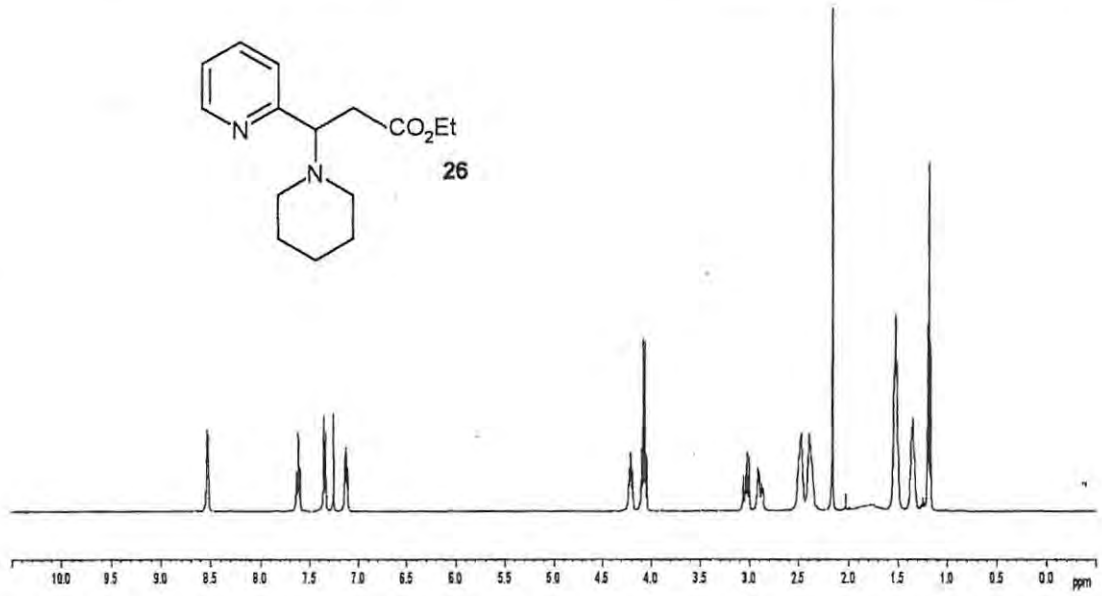

Figure 10a. 400 MHz ^{1}H NMR spectrum of the piperidine ligand **26** in $CDCl_3$.

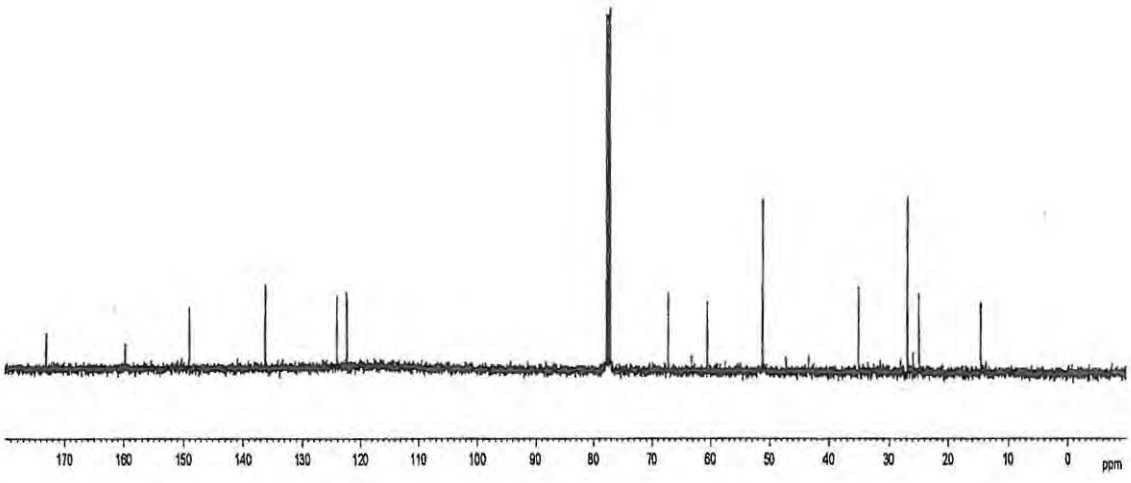

Figure 10b. 100 MHz ^{13}C NMR spectrum of the piperidine ligand **26** in $CDCl_3$.

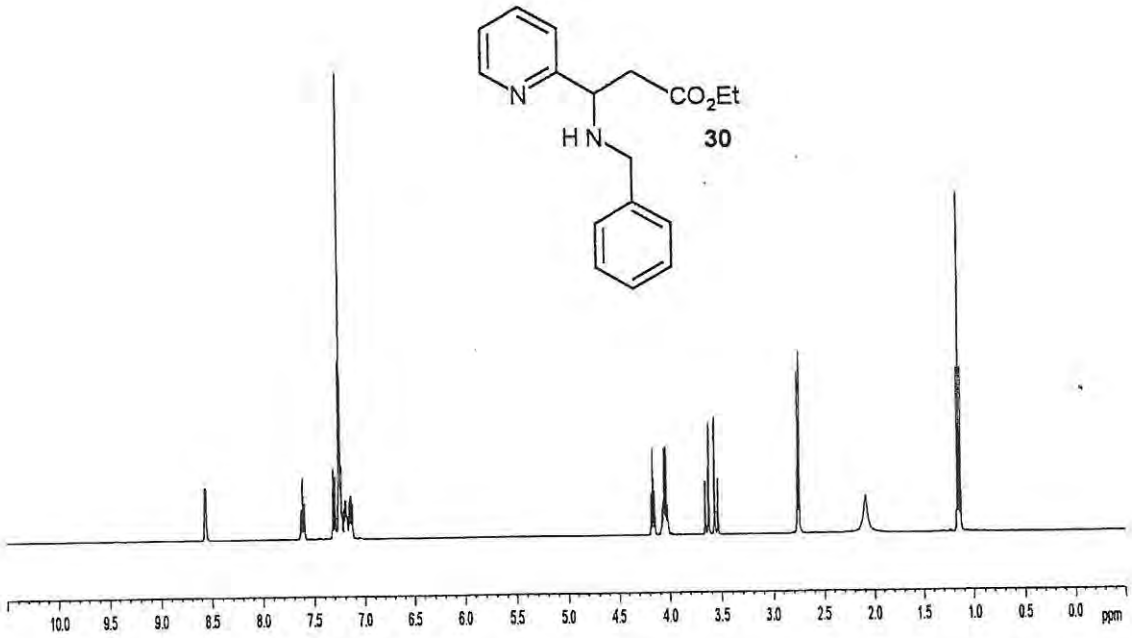

Figure 11a. 400 MHz ^{1}H NMR spectrum of the benzylamino ligand **30** in $CDCl_3$.

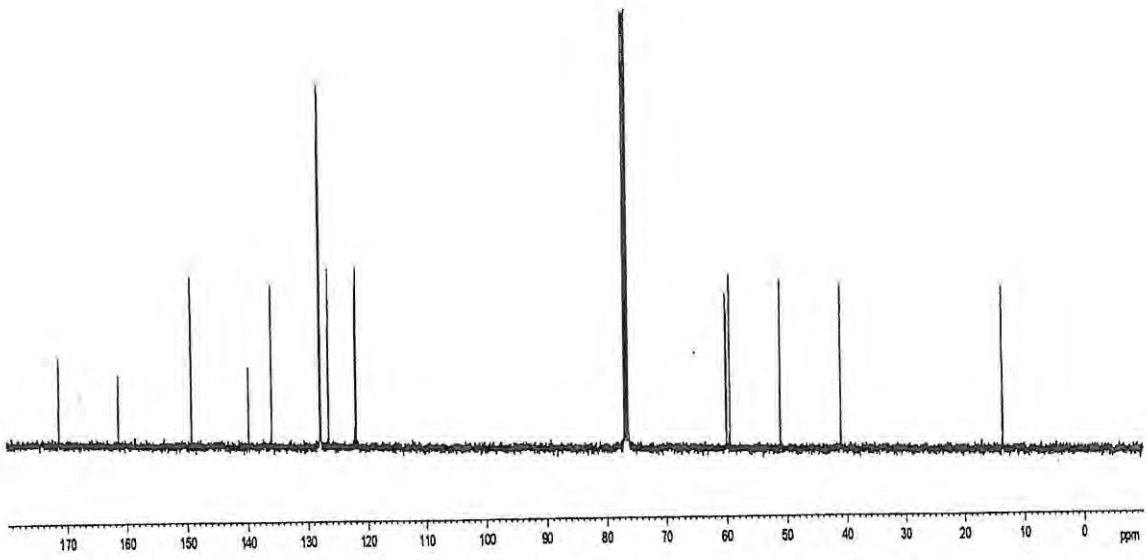

Figure 11b. 100 MHz ^{13}C NMR spectrum of the benzylamine ligand **30** in $CDCl_3$.

Table 7. Yields for the formation of the conjugate addition products **26-31**.

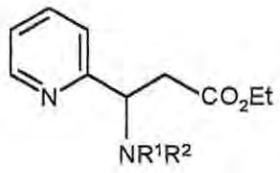

Compound	NR^1R^2	Time	Yield [a] / %
26	Piperidino	16h	99
27	1-Pyrrolidinyl	16h	92
28	Morpholino	14h	96
29	Butylamino	24h	86
30	Benzylamino	26h	32
31	Isopentylamino	24h	92
32	3-Pentylamino	6d	-[b]
33	Anilino	10d	-[b]

[a] Based on pure product obtained from flash chromatography. [b] Product not isolated from the reaction mixture.

The conjugate addition products **26-31** were all fully characterized by elemental (high-resolution electron-impact MS) and spectroscopic (IR and ^1H and ^{13}C NMR) analysis, and used in the next step of the synthetic sequence, *viz.*, reduction of the ester group **(Scheme 4)**. Lithium aluminium hydride, commonly used for this purpose, was selected as the reducing agent and the reductions were effected in refluxing THF under nitrogen.

Scheme 4. Formation of the reduction products.

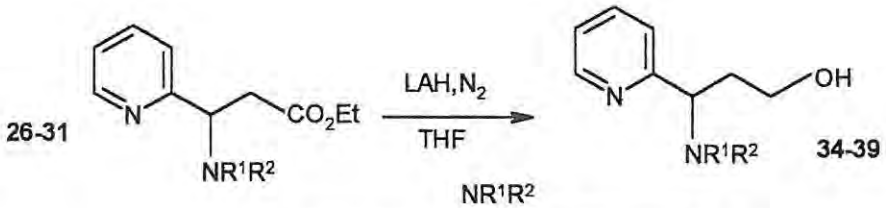

	NR¹R²	
26	Piperidino	34
27	1-Pyrrolidinyl	35
28	Morpholino	36
29	Butylamino	37
30	Benzylamino	38
31	Isopentylamino	39

Although the ester reduction proved successful it was observed that excess $LiAlH_4$ was required and that it was advisable to check $LiAlH_4$ reactivity and to ensure dryness of the solvent before use. In the first reaction attempted, a solution of compound **26** in dry Et_2O **(Scheme 4)** was treated with 2 equivalents of $LiAlH_4$ under nitrogen for 3h, to afford the alcohol **34** in 44 % yield. When the procedure was repeated using 4 equivalents of $LiAlH_4$, the alcohol **34** was obtained in 62 % yield after boiling under reflux for 3h **(Table 8)**. The morpholino analogue **36** was obtained in relatively high yield (77 %), but reduction of the pyrrolidinyl derivative proved to be less efficient, affording the alcohol **35** in only 30 % yield using 4 equivalents of fresh $LiAlH_4$ and after boiling under reflux for 3h. Excellent yields were obtained for the reduction of the butylamino and isopentylamino derivatives [**29** ⇨ **37** (88 %) and **31** ⇨ **39** (94 %)], but attempts to improve the yield of the benzylamino alcohol **38** beyond 34 % proved unsuccessful.

Table 8. Yields for the formation of reduction products **34-39.**

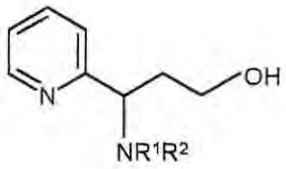

Compound	NR^1R^2	Yield [a] / %
34	Piperidino	62
35	1-Pyrrolidinyl	30
36	Morpholino	77
37	Butylamino	88
38	Benzylamino	34
39	Isopentylamino	94

[a] Based on pure product obtained from flash chromatography.

The primary alcohols **34-39** all appear to be new compounds and were fully characterized. The ^{1}H NMR spectrum of the piperidinyl derivative **34 (Figure 12a)** is typical of the series in which the disturbed baseline (*ca.*3.60-4.11 ppm) is due to the alcohol hydroxyl signal. The disappearance of the base line irregularity after the addition of D_2O **(Figure 12b)** and the absence of the typical ethyl ester signals confirm reduction to the alcohol. The COSY spectrum **(Figure 12c)** clearly illustrates the ^{1}H-^{1}H correlation of the methine proton with the two adjacent methylene protons at *ca.* 3.98 and 2.50 ppm, respectively, while the DEPT-135 spectrum (**Figure 12d**) indicates the presence of the methine carbon signal at δ 71.7 ppm and all the methylene carbons resonating in the range, δ 24.3-63.3 ppm.

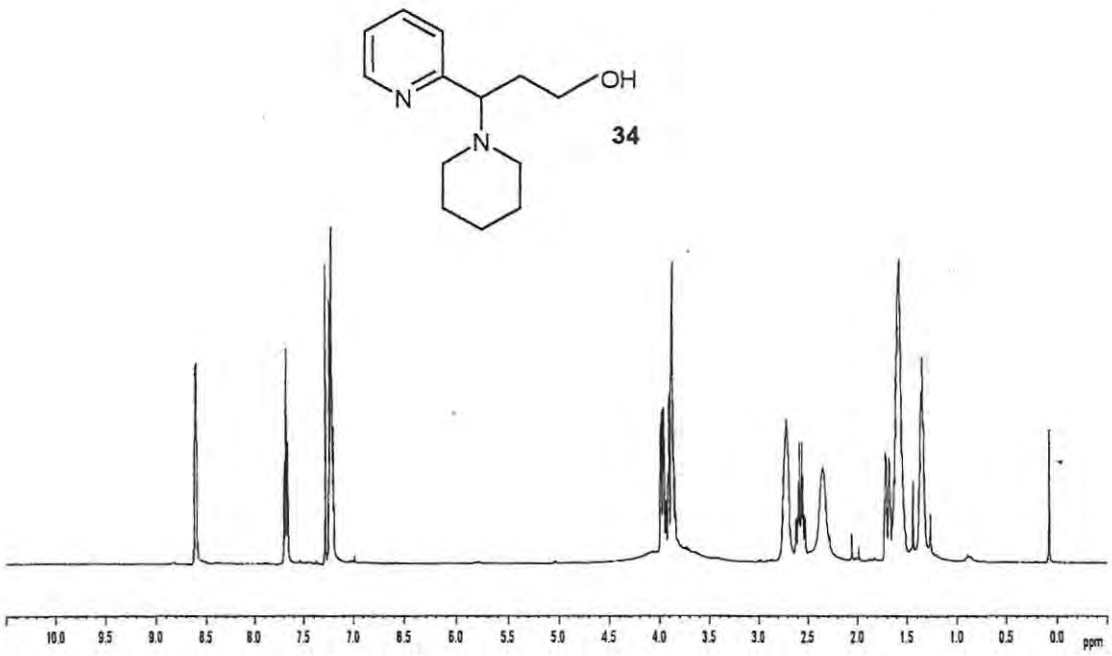

Figure 12a. 400 MHz ^{1}H NMR spectrum of the alcohol **34** in $CDCl_3$.

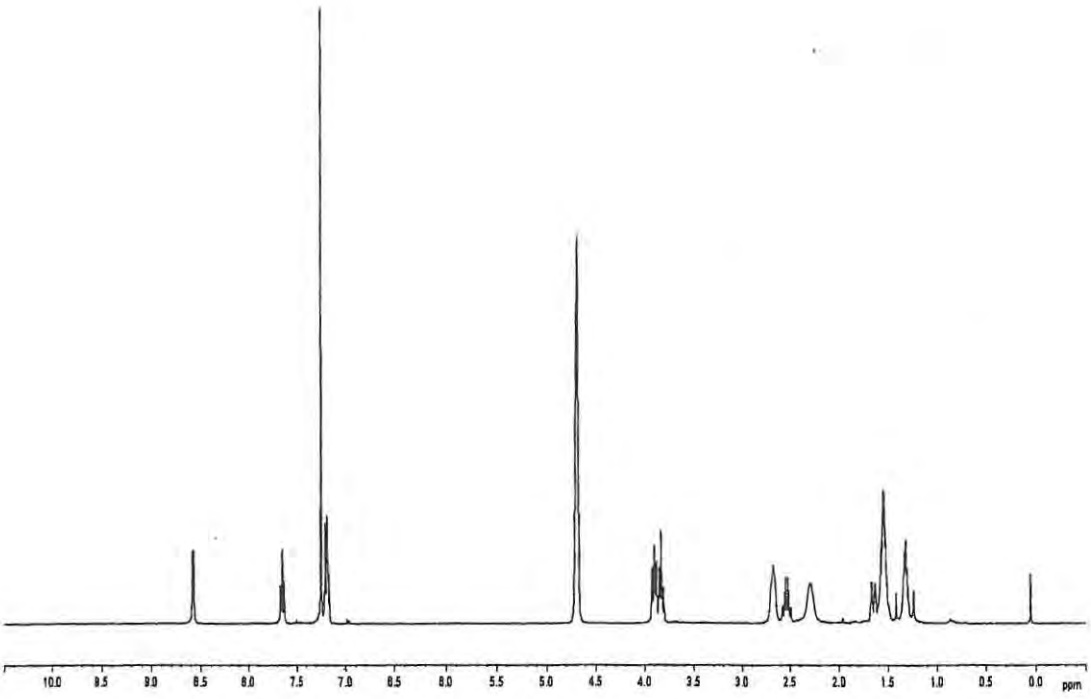

Figure 12b. 400 MHz ^{1}H NMR spectrum of the alcohol **34** after addition of D_2O.

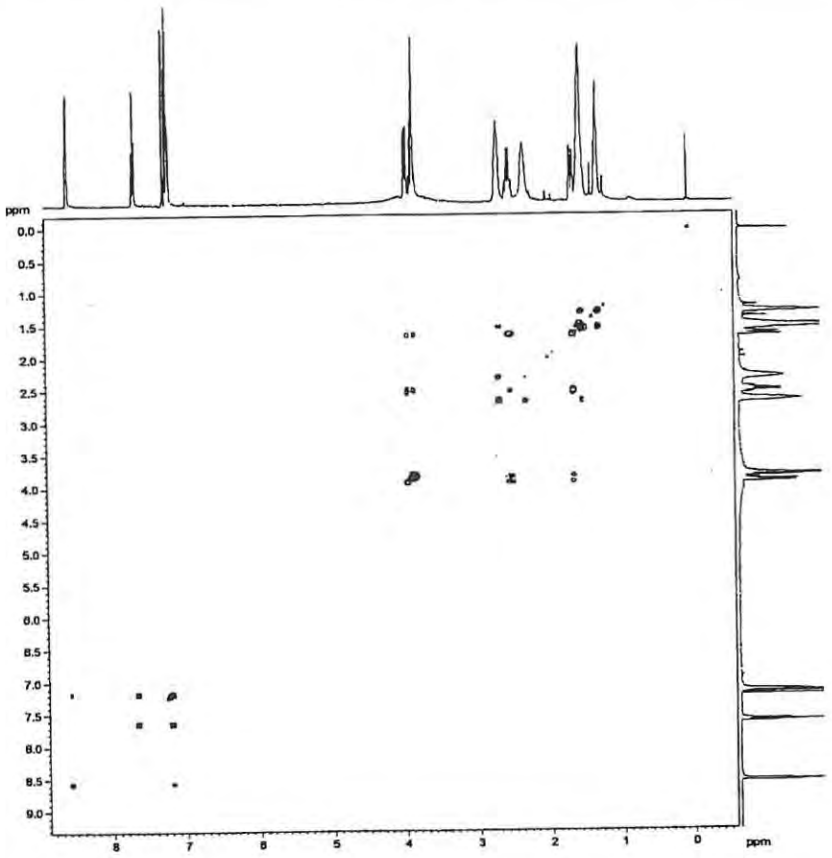

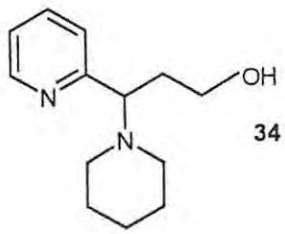

34

Figure 12c. COSY spectrum of the alcohol **34** in $CDCl_3$.

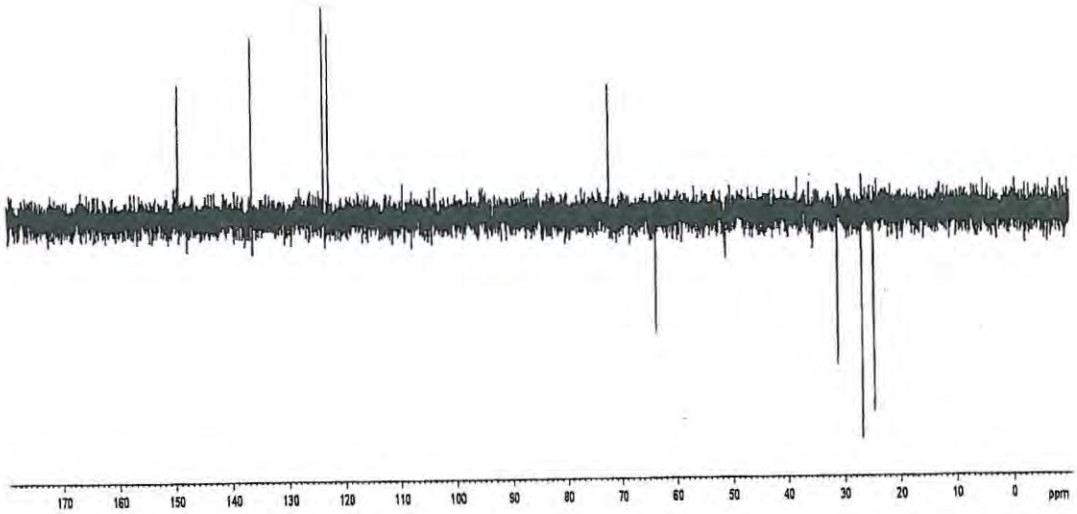

Figure 12d. DEPT-135 NMR spectrum of the alcohol **34** in $CDCl_3$.

2.2.2 Modification of the ligand design

It became apparent that some alteration of the initial target system **TM 1 (Figure 7)** was necessary. A literature survey [79-84] was conducted to establish suitable methods for achieving dehydration of the primary alcohol **34** to the target molecule **40** under mild conditions. The literature methods for such dehydration of primary alcohols all appear to involve high temperatures which could effect isomerisation of the required product **40** to the conjugated system **41 (Scheme 5)**. Consequently, it was decided to redirect the synthesis to afford the allyl ether **42**, which also contains a polymerizable vinyl group, as the target molecule of type **TM 2 (Figure 7)**. It was expected that the allyl ether **42** could be obtained by reacting the alcohol **34** with sodium hydride to generate an alkoxide, which could then be treated with allyl bromide under mild conditions.

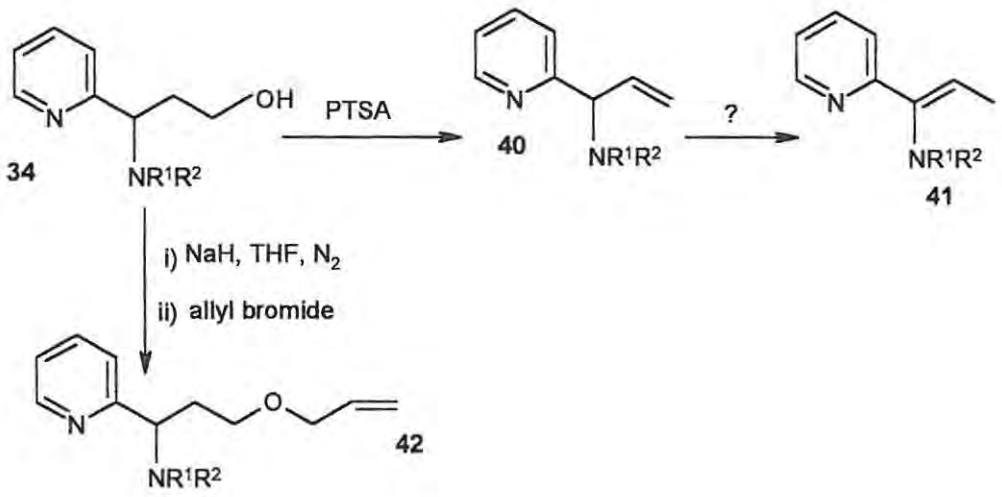

Scheme 5. Modification of ligand design (for NR^1R^2 = piperidino).

Scheme 6. Formation of the allyl ether products.

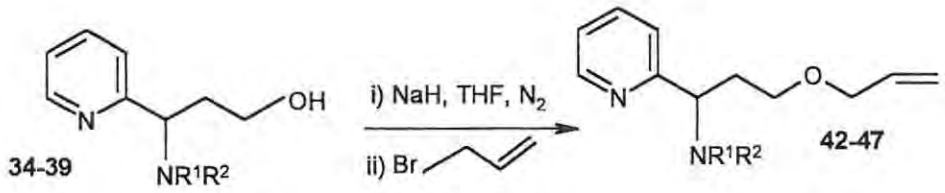

	NR^1R^2	
34	Piperidino	**42**
35	1-Pyrrolidinyl	**43**
36	Morpholino	**44**
37	Butylamino	**45**
38	Benzylamino	**46**
39	Isopentylamino	**47**

Formation of the allyl ether **42 (Scheme 6)** was achieved by treating the alcohol **34** with pre-washed NaH under nitrogen to give the alkoxide, followed by the addition of 1 equivalent of allyl bromide. The reaction mixture was stirred for 24 h at room temperature to afford the target ligand **42** in 86 % yield. This approach was then applied to the synthesis of the pyrrolidinyl and morpholino analogues. In the case of the allyl ether **43**, the reaction mixture was stirred for 28 h to afford compound **43** in 28 % yield. When the reaction period was increased to 30h, compound **43** was obtained in 35 % yield. The yield of the morpholino analogue was improved from 45 to 90 % by increasing the reaction period from 24 to 26h.

In an attempt to generate the allyl ether **45,** excess (4 equivalents) of NaH was used to generate the alkoxide, followed by excess (4 equivalents) of allyl bromide. The reaction, however, afforded the disubstituted ligand **48 (Scheme 7)**. This clearly suggested that the excess base (NaH) deprotonated both the alcohol and amine moieties, resulting in the formation of the disubstituted system following addition of allyl bromide. To effect monosubstitution, one equivalent of fresh NaH and one equivalent of allyl bromide were used in dry THF under nitrogen, and the expected product **45** was obtained in 64 % yield. The allyl ether **46** was obtained

following the same procedure but, in this case, the reaction mixture was stirred for 24h to afford compound **46** in 72 % yield. The low yield obtained for the allyl ether **47** is attributed to the loss of product during chromatographic purification.

Table 9. Yields for the allyl ether products.

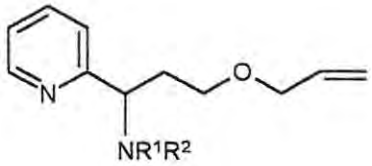

Compound	NR^1R^2	Yield [a] / %
42	Piperidino	86
43	1-Pyrrolidinyl	35
44	Morpholino	90
45	Butylamino	64
46	Benzylamino	72
47	Isopentylamino	17

[a] Based on pure product obtained from flash chromatography.

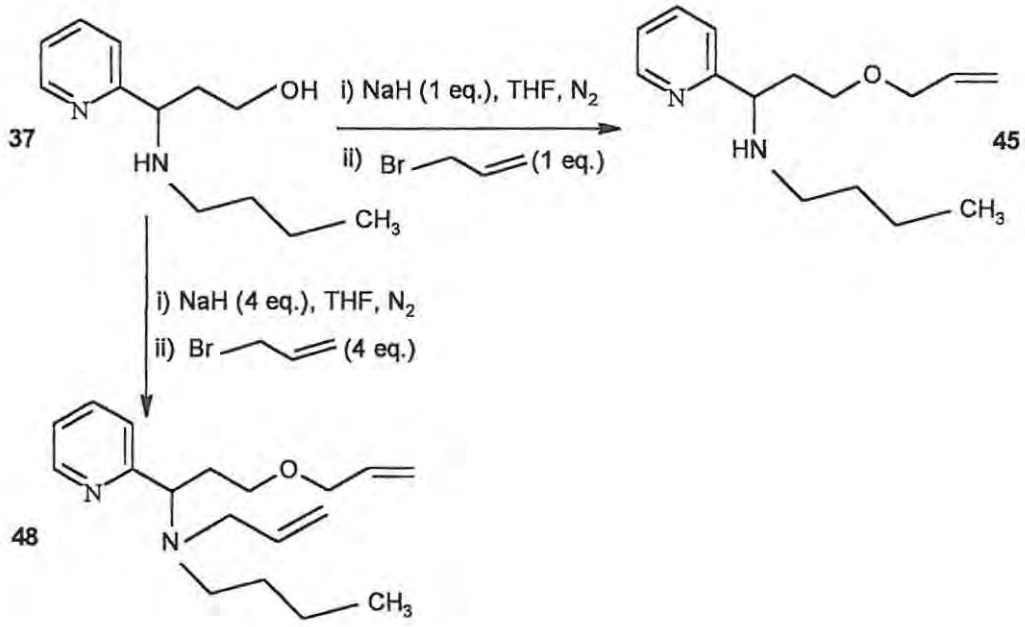

Scheme 7. Formation of the mono- and disubstituted products **45** and **48**.

All the allyl ether products appear to be new compounds and were fully characterised by elemental (high-resolution electron-impact MS) and spectroscopic (IR and ^{1}H and ^{13}C NMR) analysis. NMR spectra of the morpholine-containing ligand **44**, which are representative of the other allyl ether products, are illustrated in **Figures 13a, 13b** and **13c**. Two downfield multiplets at δ 5.80 and 5.06 ppm in the ^{1}H NMR spectrum **(Figure 13a)** are due to the vinylic methine and methylene protons respectively, while the corresponding carbon nuclei resonate at δ 135.9 and 116.5 ppm in the ^{13}C NMR spectrum **(Figure 13b)**. The DEPT-135 spectrum **(Figure 13c)** clearly reveals the presence of six methylene carbons and the chiral methine carbon, which resonates at δ 67.4 ppm.

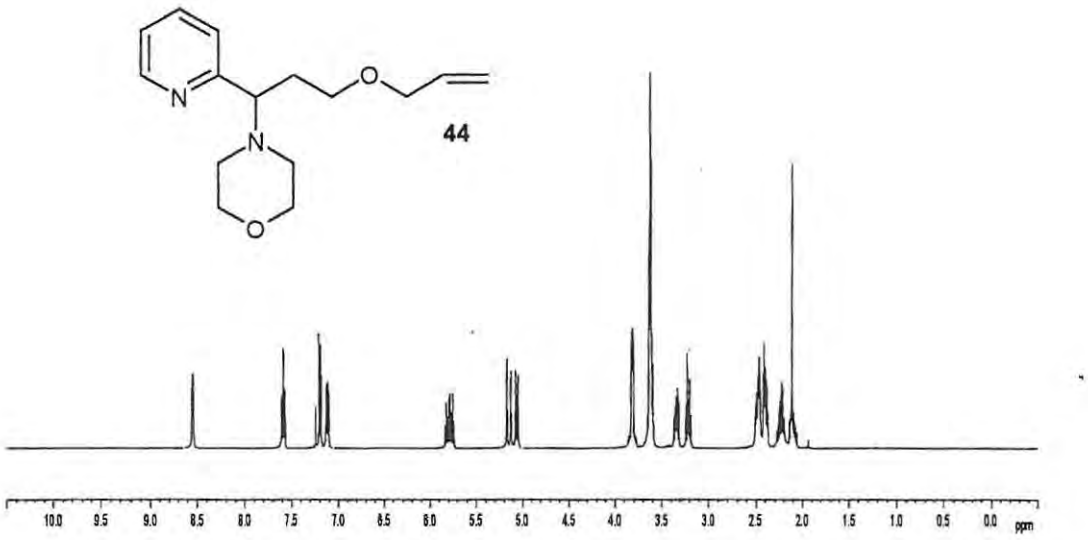

Figure 13a. 400 MHz ^{1}H NMR spectrum of the morpholino ligand **44** in $CDCl_3$.

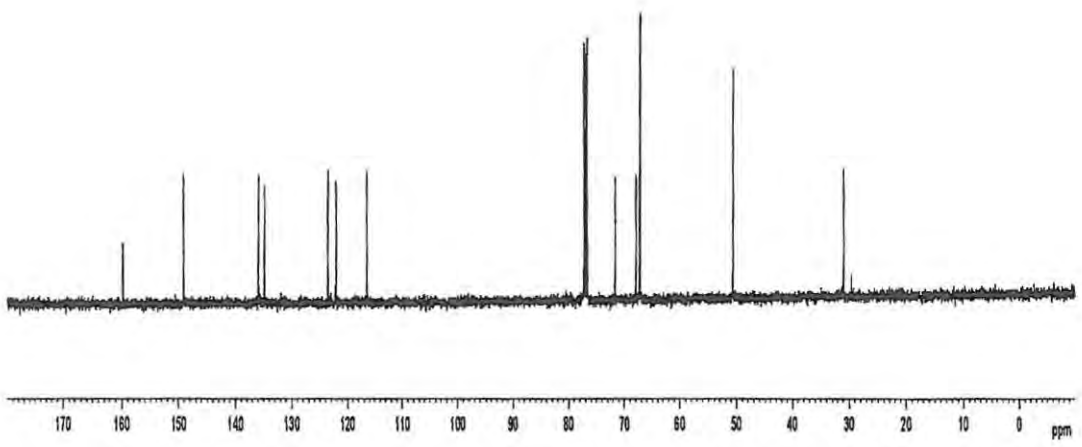

Figure 13b. 100 MHz ^{13}C NMR spectrum of the morpholino ligand **44** in $CDCl_3$.

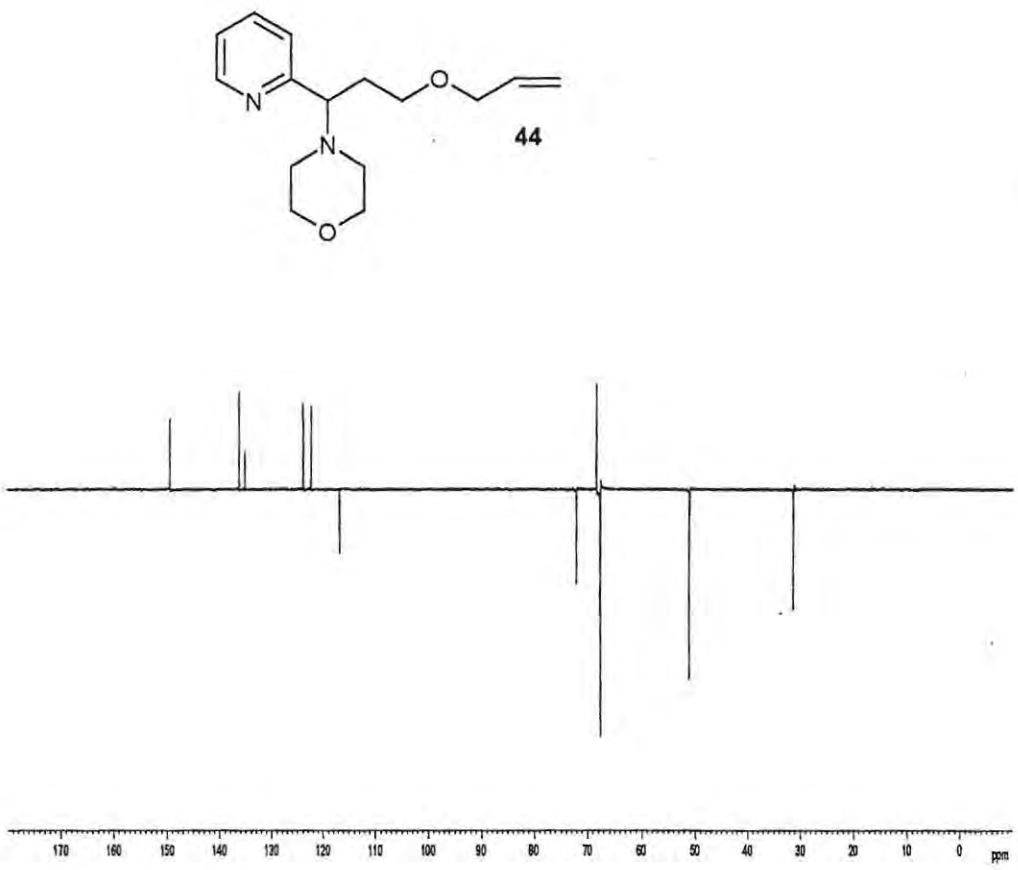

Figure 13c. DEPT-135 NMR spectrum of the morpholino ligand **44** in $CDCl_3$.

2.2.3 Use of 6-methylpyridine-2-carbaldehyde as precursor

In order to explore the effect of the methyl substituent on the donor capacity of the pyridyl nitrogen, 6-methyl-2-carbaldehyde **49** was substituted for pyridine-2-carbaldehyde **24** as the precursor. In a Wittig reaction **(Scheme 8)**, the ylide **20** was treated with one equivalent of 6-methylpyridine-2-carbaldehyde **49** in boiling CH_2Cl_2 to give the *trans*-isomer **50** in 68 % yield after refluxing the reaction mixture for 26h. Successful conjugate addition of morpholine to the α,β unsaturated compound **50** was achieved by using morpholine as both solvent and nucleophile. The addition product **51** was obtained in 66 % yield after the reaction mixture had been heated under reflux for 25h. Reduction of the ester **51** to the alcohol **52** was achieved in 80 % yield using 5 equivalents of fresh $LiAlH_4$, and heating the reaction mixture for 3h. The allyl ether **53** was finally obtained in 71 % yield by treating the alcohol **52** with sodium hydride and allyl bromide as described previously.

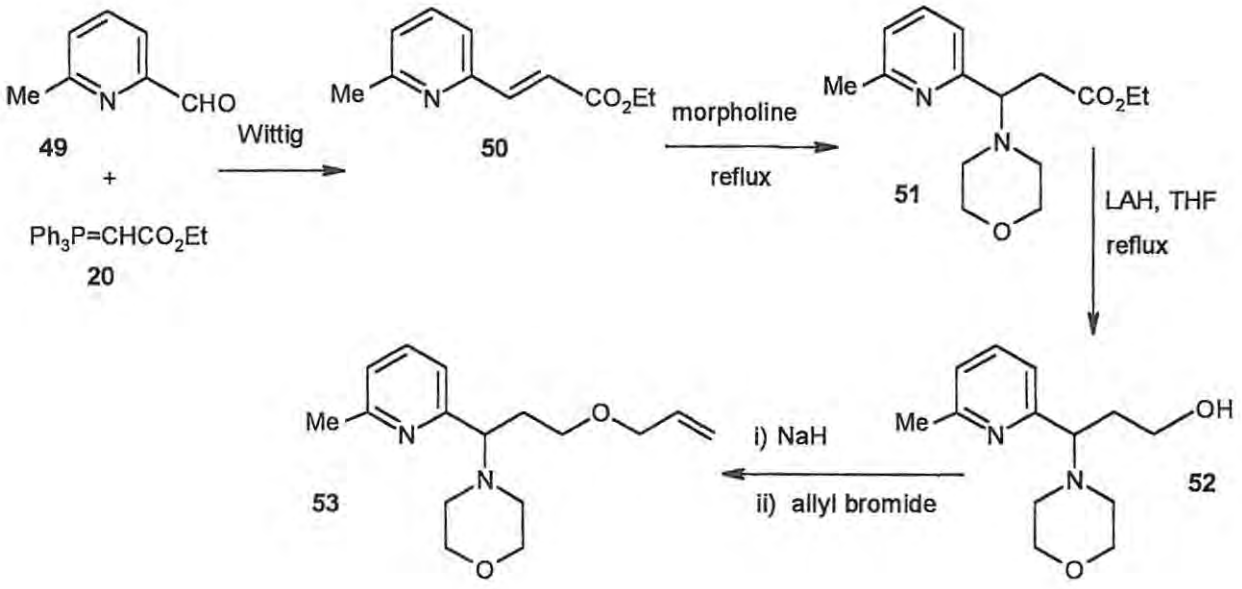

Scheme 8. Reaction sequence for the formation of allyl ether **53**.

The ligand **53** was fully characterised from the elemental (high-resolution MS) and spectroscopic (IR and ^{1}H and ^{13}C NMR) data. The ^{1}H, ^{13}C and DEPT NMR spectra for this compound are illustrated in **Figures 14a, 14b**, and **14c**, respectively. The ^{1}H NMR spectrum **(Figure 14a)** reveals the presence of a methyl singlet at δ 2.38 ppm and two downfield multiplets at δ 5.85 and 5.05 ppm due to the vinylic methine and methylene protons respectively; the corresponding carbons resonate at δ 24. 9, 135.4 and 116.9 ppm in the ^{13}C NMR **Figure 14b**. The DEPT-135 spectrum **(Figure 14c)** clearly shows the presence of six methylene carbons and the chiral methine carbon which resonates at δ 68.7 ppm.

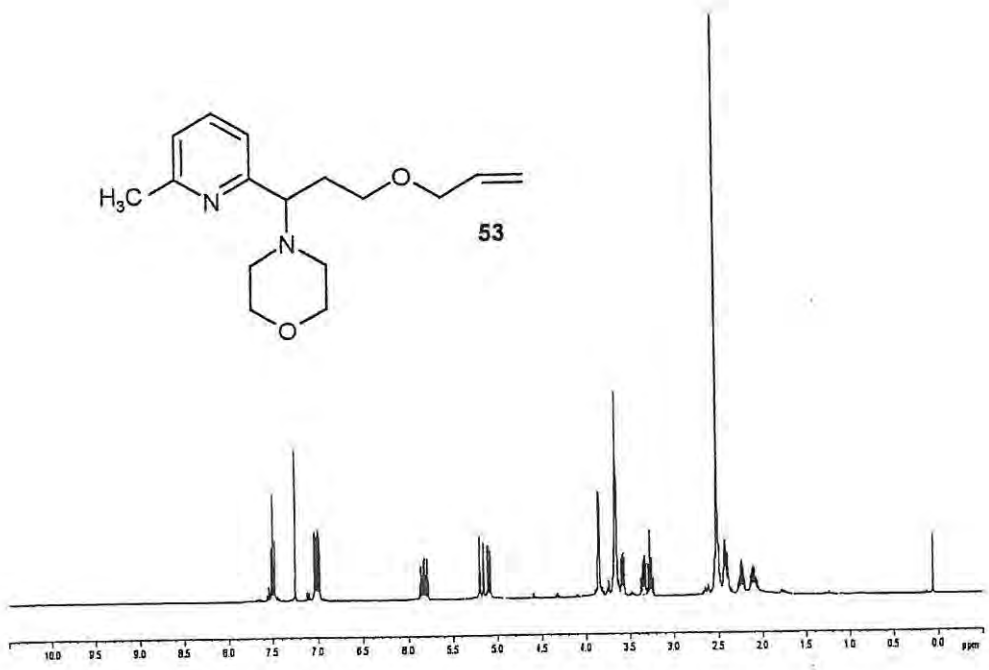

Figure 14a. 400 MHz ^{1}H NMR spectrum of the ligand **53** in $CDCl_3$.

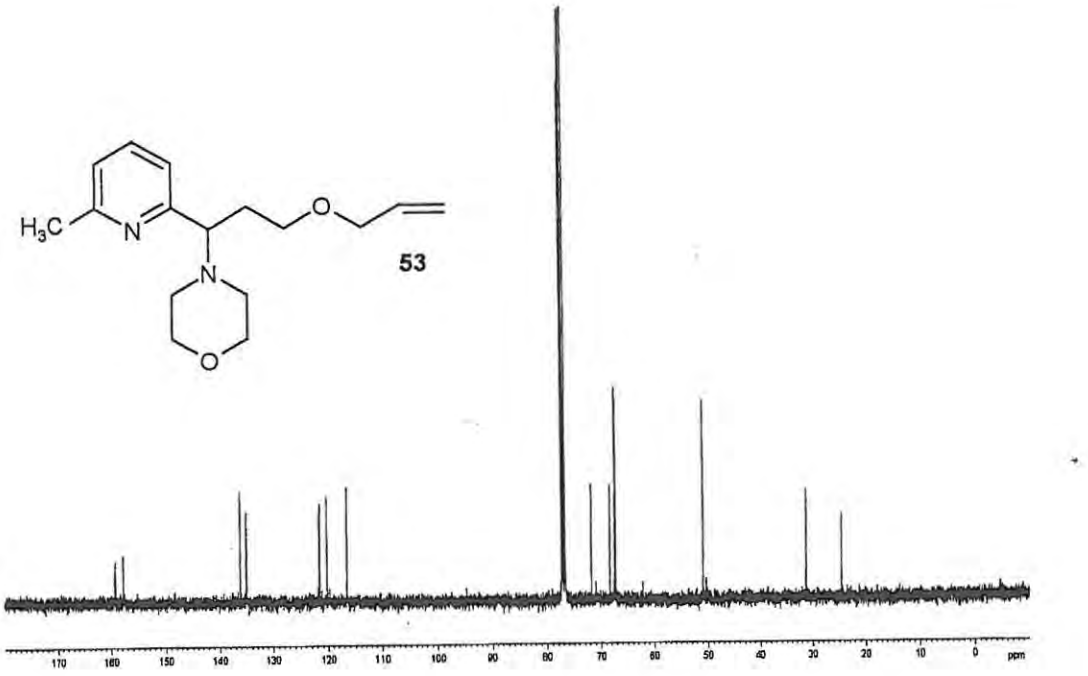

Figure 14b. 100 MHz ^{13}C NMR spectrum of the ligand **53** in $CDCl_3$.

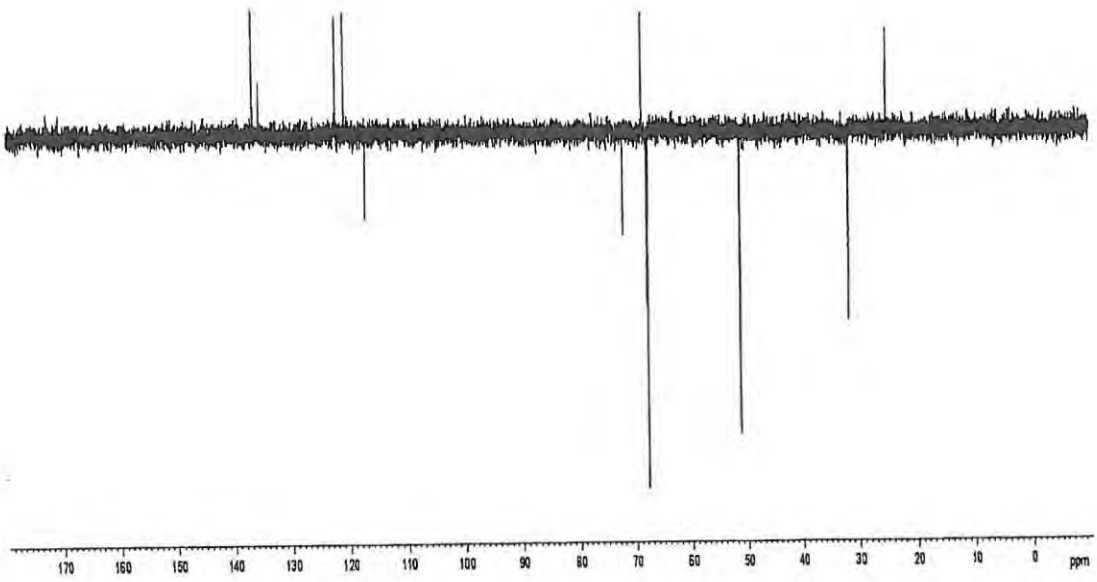

Figure 14c. DEPT-135 NMR spectrum of the morpholine ligand **53** in $CDCl_3$.

2.3 Fragmentation patterns in the electron-impact mass spectra of selected ligands

High-resolution electron-impact (EI) mass spectra (illustrated for compound **42**; Figure **15**) and B/E linked scan data were obtained to investigate the fragmentation patterns exhibited by selected target ligands. In all cases, the molecular ions were observed to lose a hydrogen atom to produce well-stabilized ions of one mass unit less (M-1). The stability of the M-1 ions is attributed to the availability of the adjacent pyridyl ring and the adjacent nitrogen, both of which permit resonance stabilization of the picolinic carbocation. Thus, the molecular ion (*m/z* 260) for compound **42** (Scheme **9**) loses hydrogen atom, to afford an M-1 species with *m/z* 259, which subsequently fragments to the resonance-stabilised cations at *m/z* 84 and 201; elimination of acetylene from the latter fragment would account for the formation of the even-electron species with *m/z* 175. In an alternative pathway, elimination of a piperidinyl imine from the molecular ion would account for the formation of the radical-cation (*m/z* 177); subsequent loss of acrolein would afford the radical-cation (*m/z* 121). Further fragmentation involving elimination of ethylene affords the α-picoline radical-cation (*m/z* 93), while loss of a methyl radical (*m/z* 121 ⇨ *m/z* 106) affords the base peak, formulated as a secondary carbocation (*m/z* 106). Further loss of an ethyl radical would then account for the formation of the pyridine cation (*m/z* 78). All of these fragmentations are, in fact, supported by the B/E linked scan data. The other ligands exhibit similar fragmentation patterns; these patterns and the corresponding high-resolution data are detailed in Schemes **10-15** and Tables **11-16**.

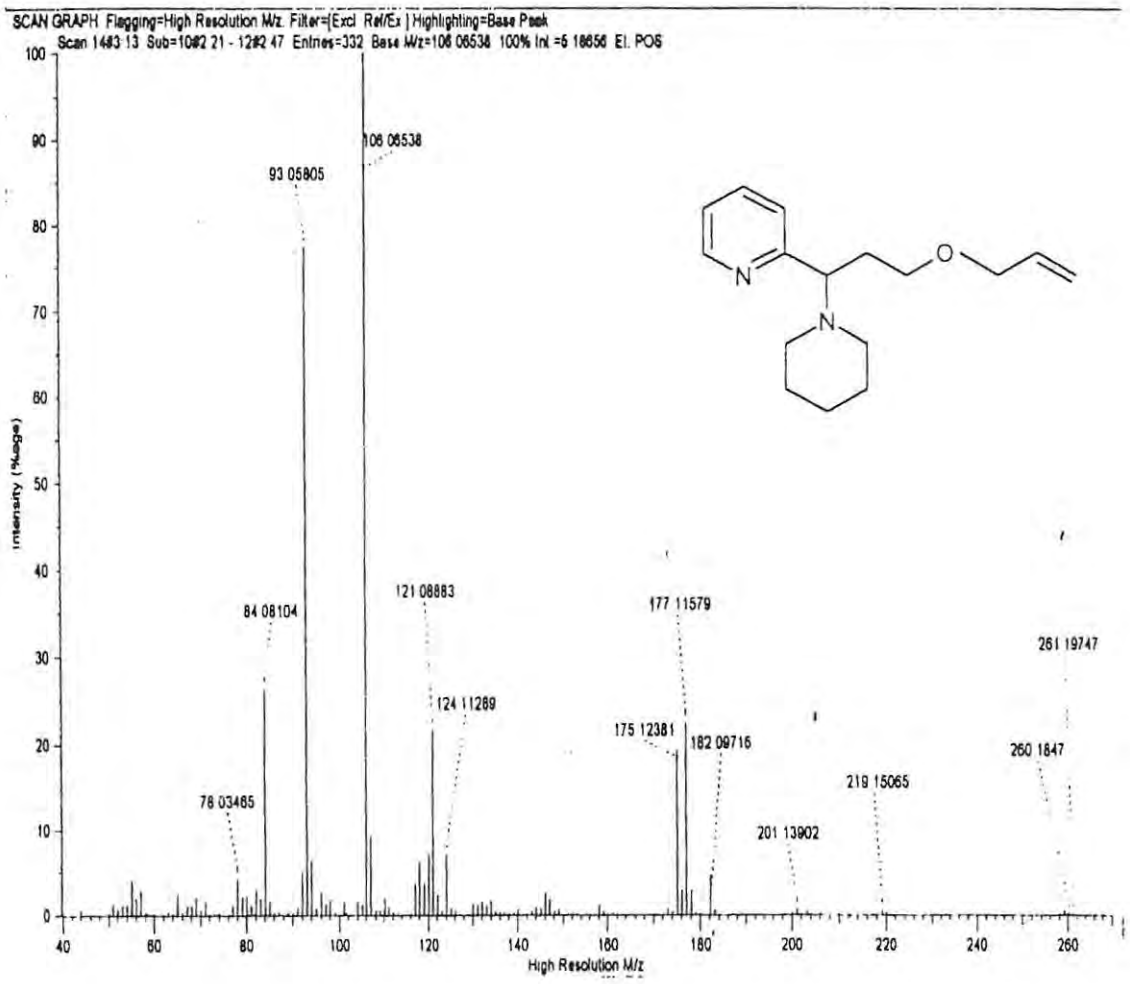

Figure 15. High-resolution electron-impact mass spectrum of compound **42**.

Scheme 9. Proposed fragmentation of compound **42**.

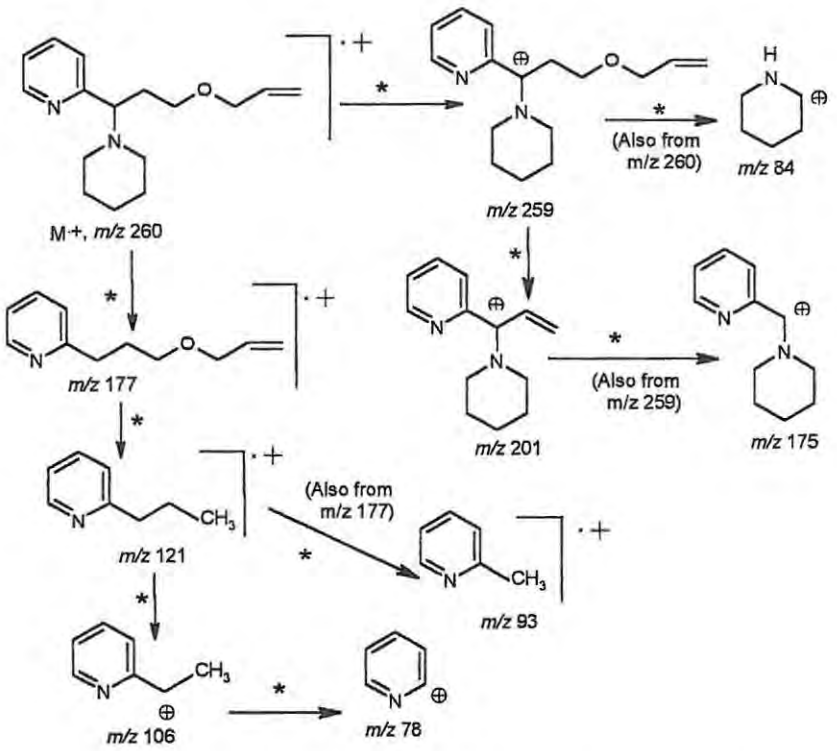

* = B/E Linked Scan connection; other such connections are indicated in parentheses.

Table 10. High-resolution and relative abundance data for selected fragments from compound **42**.

Observed	Formula	Calculated	Relative abundance/ %
260.18470	$C_{16}H_{24}N_2O$	260.18886	< 2.1
259.11846	$C_{16}H_{23}N_2O$	259.11844	< 2.1
201.13902	$C_{13}H_{17}N_2$	201.13917	< 0.2
177.11579	$C_{11}H_{15}NO$	177.11536	22.29
175.12381	$C_{11}H_{15}NO$	175.12352	19.03
121.08883	$C_8H_{11}N$	121.08915	21.51
106.06538	C_6H_7N	106.06567	100
93.05805	C_6H_7N	93.05785	77.66
84.08104	$C_5H_{10}N$	84.08132	26.40
78.03465	C_5H_4N	78.03437	5.05

Scheme 10. Proposed fragmentation of compound **43**.

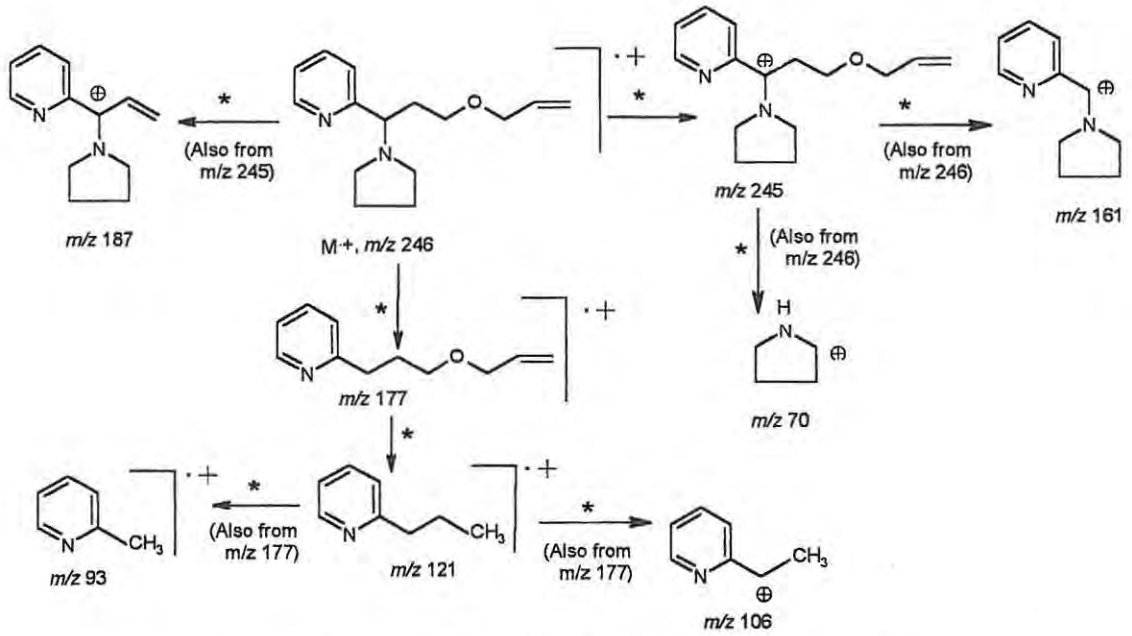

* = B/E Linked Scan connection; other such connections are indicated in parentheses

Table 11. High-resolution and relative abundance data for selected fragments from compound **43**.

Observed	Formula	Calculated	Relative abundance/ %
246.18780	$C_{15}H_{22}N_2O$	246.18866	< 0.2
245.16436	$C_{15}H_{21}N_2O$	245.11536	0.66
187.14974	$C_{12}H_{15}N$	187.15065	<0.2
177.11516	$C_{11}H_{15}NO$	177.11536	17.79
161.10794	$C_{10}H_{13}N_2$	161.10787	22.62
121. 08950	$C_8H_{11}N$	121.08915	10.08
106.06572	C_7H_8N	106.06567	100
93.05785	C_6H_7N	93.05792	59.42
70.08104	C_4H_8N	70.06567	6.88

Scheme 11. Proposed fragmentation of compound **44**.

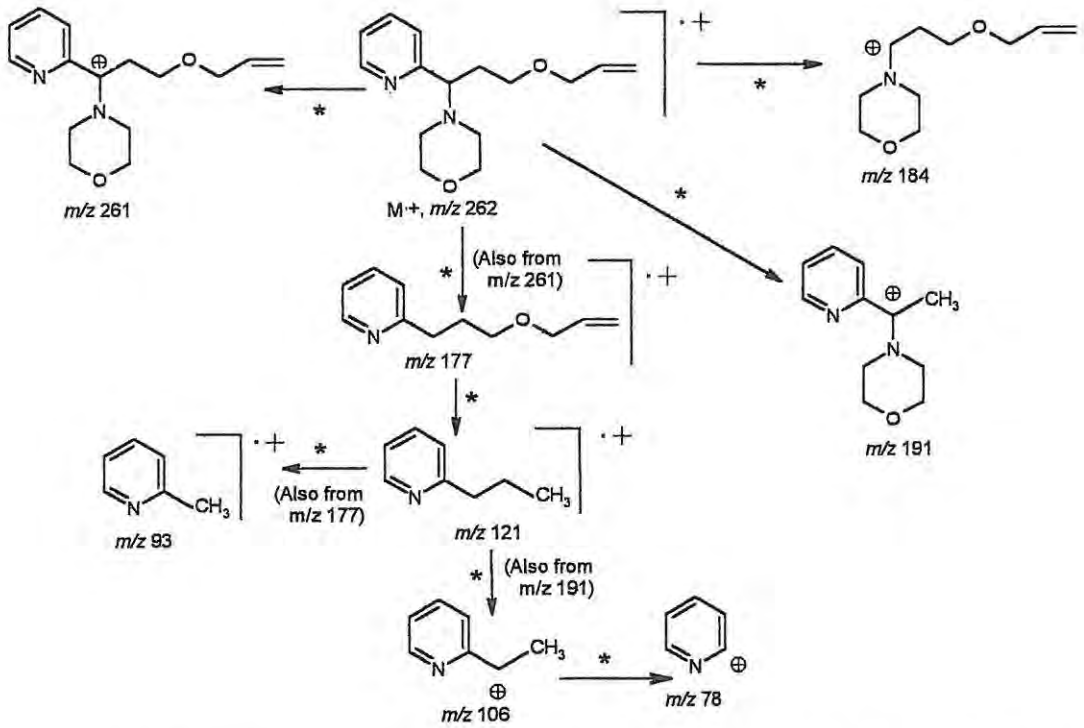

* = B/E Linked Scan connection; other such connections are indicated in parentheses

Table 12. High-resolution and relative abundance data for selected fragments from compound **44**.

Observed	Formula	Calculated	Relative abundance/ %
261.15969	$C_{15}H_{21}N_2O_2$	261.16030	0.35
191.11846	$C_{11}H_{15}N_2O$	191.11844	2.27
184.13403	$C_{10}H_{18}N_2O$	184.13375	3.82
177.11080	$C_{11}H_{15}NO$	177.11080	6.34
121.08919	$C_8H_{11}N$	121.08915	12.45
106.06550	C_6H_7N	106.06567	100
93.05798	C_6H_7N	93.05785	62.19
78.03437	C_5H_4N	78.03437	5.18

Scheme 12. Proposed fragmentation of compound **45**.

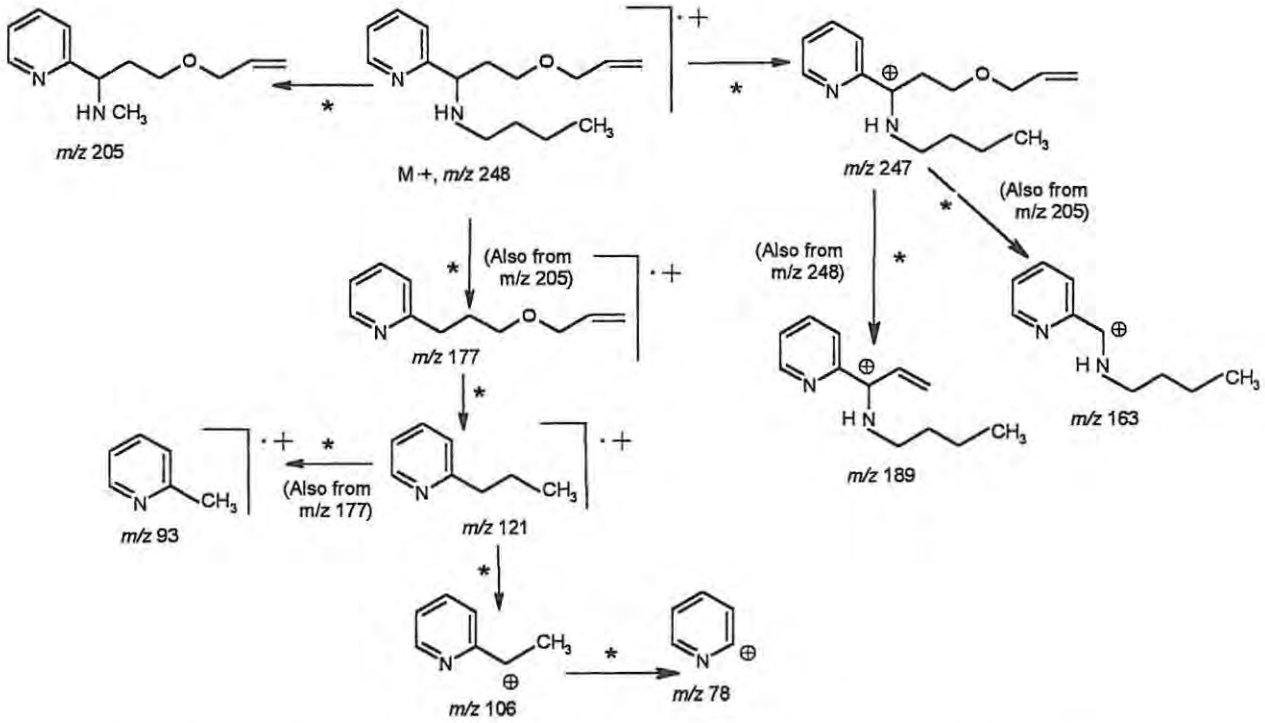

* = B/E Linked Scan connection; other such connections are indicated in parentheses.

Table 13. High-resolution and relative abundance data for selected fragments from compound **45**.

Observed	Formula	Calculated	Relative abundance/ %
248.19658	$C_{15}H_{24}N_2O$	248.19669	< 0.3
247.18050	$C_{15}H_{23}N_2O$	248.18104	1.24
205.13385	$C_{12}H_{17}N_2O$	205.13409	5.90
189.13770	$C_{12}H_{17}N_2$	189.13917	< 0.2
177.11741	$C_{11}H_{15}NO$	177.11536	33.80
163.12236	$C_{10}H_{15}N_2$	163.12352	99.30
106.06608	C_6H_7N	106.06567	100
93.05835	C_6H_7N	93.05785	84.93
78.03496	C_5H_4N	78.03437	14.60

Scheme 13. Proposed fragmentation of compound **46**.

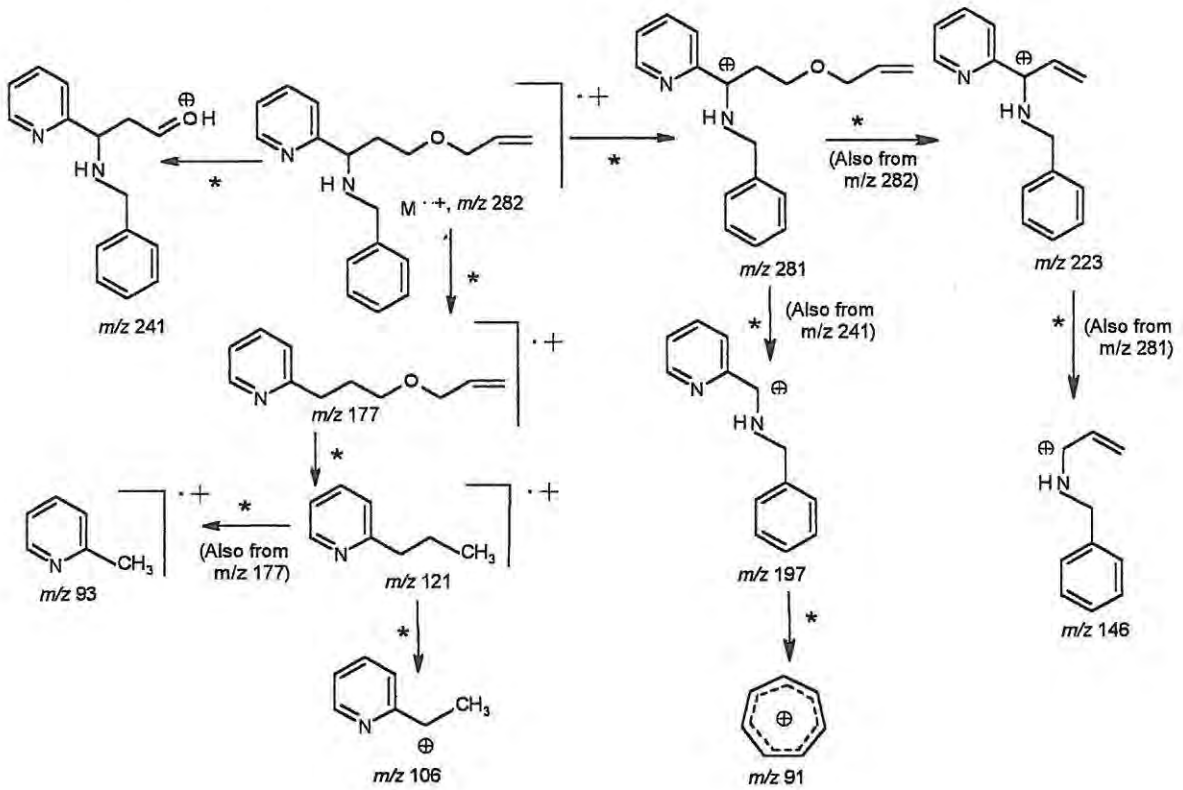

* = B/E Linked Scan connection; other such connections are indicated in parentheses.

Table 14. High-resolution and relative abundance data for selected fragments from compound **46**.

Observed	Formula	Calculated	Relative abundance/ %
282.18380	$C_{18}H_{22}N_2O$	282.18866	< 0.2
281.16368	$C_{18}H_{21}N_2O$	281.16539	0.66
241.13490	$C_{15}H_{17}N_2O$	241.13409	1.05
223.12345	$C_{15}H_{15}N_2$	223.12352	2.36
197.10794	$C_{13}H_{13}N_2$	197.10787	52.84
177.11544	$C_{11}H_{15}NO$	177.11536	53.13
146.09668	$C_{10}H_{12}N$	146.09697	2.72
121. 08861	$C_8H_{11}N$	121.08915	21.23
106.06538	C_7H_8N	106.06567	100
93.05838	C_6H_7N	93.05785	92.04

Scheme 14. Proposed fragmentation of compound **47**.

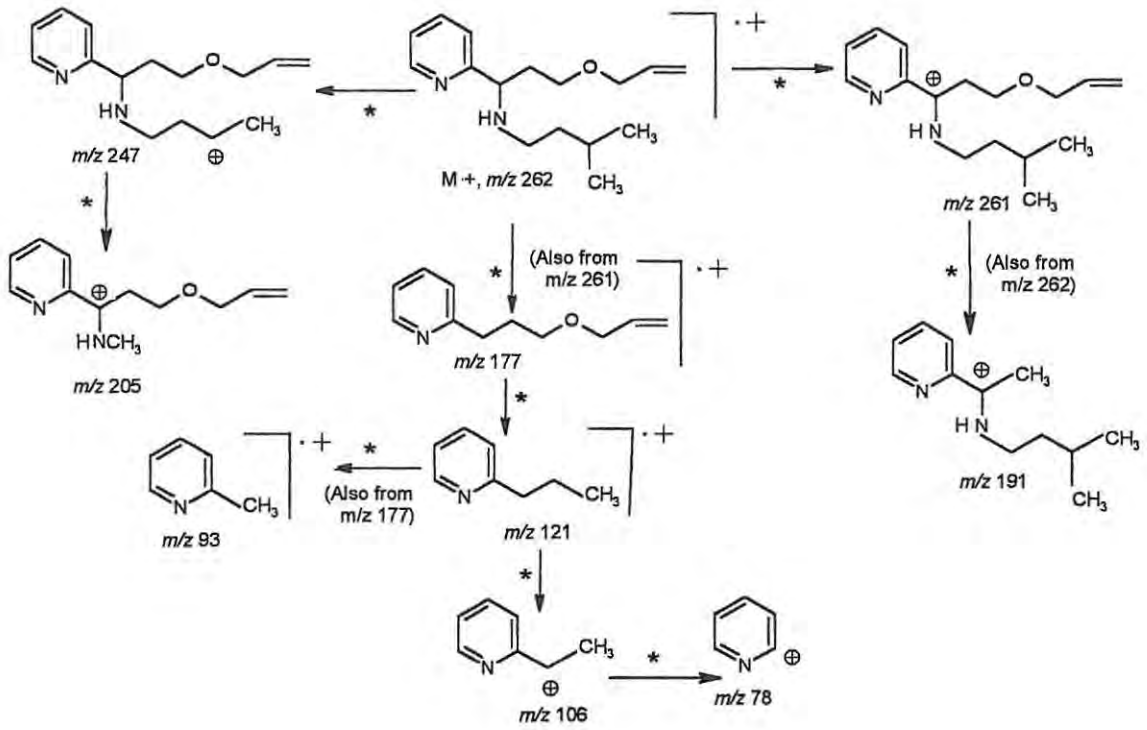

* = B/E Linked Scan connection; other such connections are indicated in parentheses.

Table 15. High-resolution and relative abundance data for selected fragments from compound **47**.

Observed	Formula	Calculated	Relative abundance/ %
262.19658	$C_{16}H_{26}N_2O$	262.19669	0.39
261.19571	$C_{15}H_{25}N_2O$	261.19669	0.86
247.18092	$C_{15}H_{23}N_2O$	247.18104	1.45
205.13455	$C_{12}H_{17}N_2O$	205.13409	13.30
191.14723	$C_{12}H_{19}N_2$	191.14526	42.31
177.11741	$C_{11}H_{15}NO$	177.11536	66.80
121.12236	$C_{10}H_{15}N_2$	121.12352	73.30
106.06542	C_6H_7N	106.06567	100
93.05777	C_6H_7N	93.05785	92.93
78.03496	C_5H_4N	78.03437	6.60

Scheme 15. Proposed fragmentation of compound **53**.

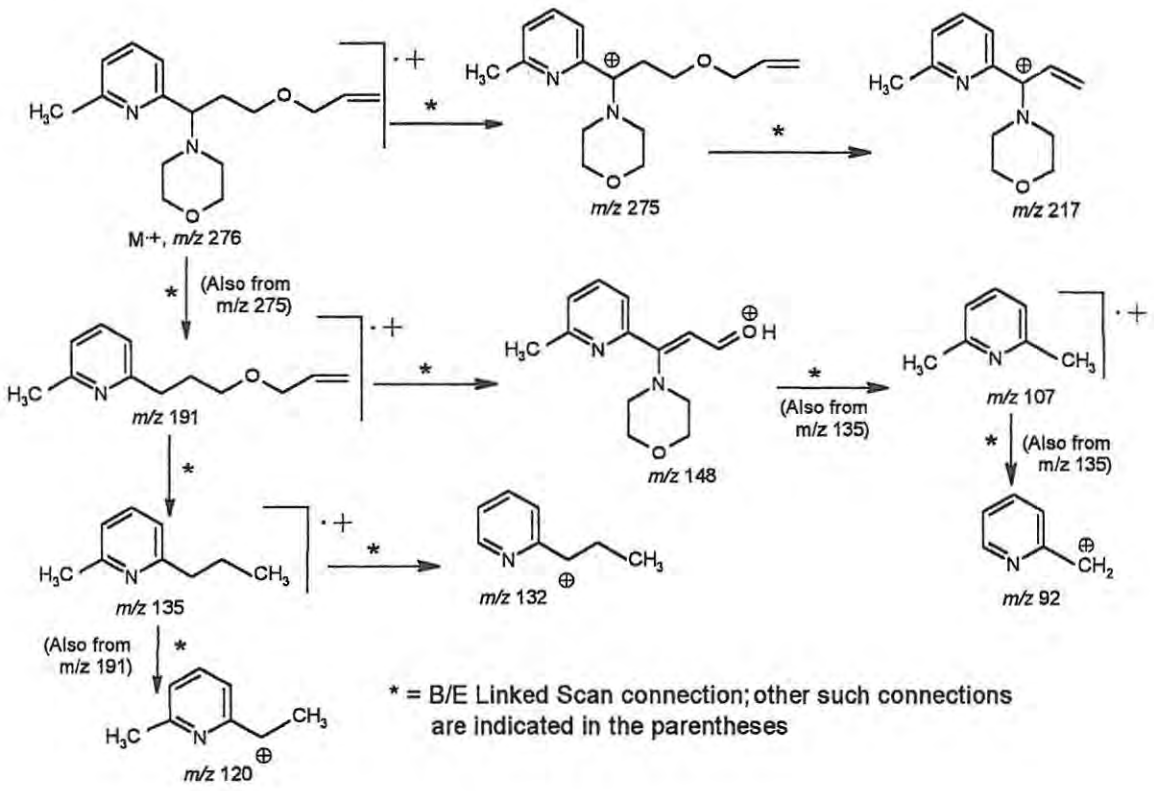

Table 16. High-resolution and relative abundance data for selected fragments from compound **53**.

Observed	Formula	Calculated	Relative abundance/ %
276.18117	$C_{16}H_{24}N_2O_2$	276.18378	0.03
275.99114	$C_{16}H_{23}N_2O_2$	275.16030	0.04
217.14881	$C_{13}H_{17}N_2O$	217.14974	0.71
191.12926	$C_{12}H_{17}NO$	191.13101	33.7
148.07680	$C_9H_{10}NO$	148.07778	2.55
135.10408	$C_9H_{13}N$	135.18480	3.99
132.07965	$C_9H_{10}N$	132.08132	6.00
120.08123	$C_8H_{10}N$	120.08131	100
107.07390	C_7H_9N	107.07350	0.06
92.03860	C_6H_6N	92.05002	4.20

2.4 Formation and analysis of nickel complexes

2.4.1 Formation of complexes

Complexation studies were carried out to investigate the chelation of nickel by the selected ligands:- **42- 44, 46** and **53 (Scheme 16)**. Various nickel(II) salts were employed to observe the effect of different counterions on the formation (Equation **4**) and coordination geometry of the complexes.

$MX_2 + nL \rightleftharpoons ML^{2+}_n + 2X^-$ (eq. **4**)

Where: $MX_2 = NiCl_2$; $Ni(OAc)_2$; $Ni(NO_3)_2$; *etc*; L = ligand **42-44, 46, 53**.

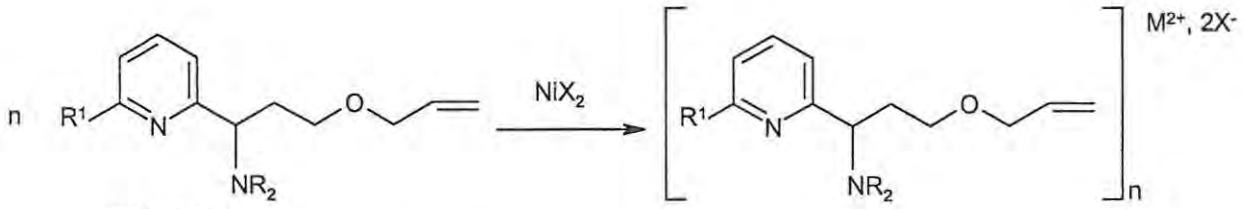

42-44, 46,53 **54-65**

	NR_2	R^1	
42		H	**54**(X=Cl), **55**(X=OAc); **56**($X=BF_4$)
43	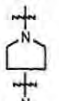	H	**57**(X=Cl), **58**(X=OAc)
44		H	**59**(X=Cl); **60**(X=Br); **61**($X=BF_4$); **62**($X=ClO_4$); **63**(X=OAc)
46	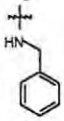	H	**65**(X=Cl)
53		Me	**64**(X=Cl)

Scheme 16. Formation of the nickel(II) complexes.

2.4.1.1 Complexation with the piperidinyl ligand **42**

Two equivalents of compound **42** in methanol were added to a stirred solution containing one equivalent of $NiCl_2.6H_2O$ in MeOH and, after stirring for 48 h. diethyl ether was added to precipitate the complex. To reduce contamination, the precipitate was re-dissolved in methanol and re-precipitated again with diethyl ether. The re-precipitation process was repeated three times to afford complex **54** as a green, hygroscopic, semi-solid product. When only 1 equivalent of compound **42** was used, co-precipitation of $NiCl_2.6H_2O$ was observed.

The piperidinyl ligand **42** was then treated with Ni(II)acetate.$4H_2O$ and $Ni(BF_4)_2.4H_2O$ under various conditions, the complex being precipitated in each case, by the addition of diethyl ether. Thus, four equivalents of compound **42** in MeOH were added to a solution of nickel(II) acetate.$4H_2O$ in warm MeOH. There was an immediate colour change and after stirring the reaction mixture for 6h, diethyl ether was added to induce precipitation. Repeated re-precipitation after drying at high vacuum, afforded a brownish hygroscopic product **55**. The same product was isolated when 2 equivalents of ligand **42** was used. Complexation with $Ni(BF_4)_2.4H_2O$ was effected in methanol to afford the brownish complex **56**.

2.4.1.2 Complexation with the pyrrolidinyl ligand **43**

Following the general approach described for the preparation of the Ni(II) complexes of the piperidinyl ligand **42**, two equivalents of ligand **43** were treated with $NiCl_2.6H_2O$. Mixing of the reagents was, again, accompanied by an immediate colour change from light yellow to light green, and the reaction mixture was stirred overnight prior to precipitation and purification of the complex. Extensive drying at high vacuum afforded complex **58** as a greenish, shiny hygroscopic solid. Similar complexation with Ni(II) acetate.$6H_2O$ afforded the corresponding complex **58** as a yellowish solid.

2.4.1.3 Complexation with the morpholino ligands **44** and **53**

The morpholino ligand **44** was used to investigate the effect of a range of different counterions (Cl^-; Br^-; BF_4^-; ClO_4^-; $CH_3CO_2^-$). Thus, two equivalents of the ligand **44**,dissolved in MeOH, were treated with $NiCl_2.6H_2O$ to give, as a light green hygroscopic semi-solid, complex **59**; with Ni(II) $Br_2.6H_2O$ to give, as a brownish hygroscopic solid, complex **60**; with $Ni(BF_4)_2.4H_2O$ to give, as dark brown semi-solid,complex **61**; with nickel(II)perchlorate.$6H_2O$ to give, as a brown semi-solid complex **62**; with nickel(II)acetate.$4H_2O$ to give, as a light-green semi-solid complex **63**. Ligand **53** was used to chelate with $NiCl_2.6H_2O$ to give, as a light-green hygroscopic semi-solid, complex **64.**

2.4.1.4 Complexation with the benzylamino ligand **46**

Following the general approach described for the preparation of the Ni(II) complexes of the piperidinyl ligand **42**, two equivalents of ligand **46** were treated with $NiCl_2.6H_2O$ to give, as a light green hygroscopic semi-solid, complex **65**.

2.4.2 Analysis of the complexes

As pointed out in the Introduction (Section **1.1.5.1**) nickel(II) complexes may undergo certain structural and conformational changes in solution depending on factors, such as the nature of the counterions, exposure to atmospheric moisture *etc.* In this investigation, such "anomalous" behaviour involving square-tetrahedral or square-octahedral ambivalence was observed, thus complicating analysis. All of the nickel complexes obtained were analyzed by NMR, IR and UV techniques, while some were also analyzed by FAB MS and HREIMS. From the IR and NMR data, it appears that co-ordination did not occur when the ligands were treated with $NiSO_4.6H_2O$ or $Ni(NO_3)_2.6H_2O/NH_3PF_6$. In most cases, however complexes were obtained using $NiCl_2.6H_2O$, nickel(II)acetate.$4H_2O$, nickel(II)perchlorate. $6H_2O$, $NiBr_2.6H_2O$ and $Ni(BF_4)_2$.

The two, broad and intense bands observed at *ca.* 405cm^{-1} and 605cm^{-1} in the mid-IR spectra of all of free ligands were assigned to the pyridine ring. [89, 90] Following complexation, these bands shifted, in most cases, to *ca.* 430 and 630 cm^{-1}, respectively; furthermore, Ni-N stretches (200-370 cm^{-1}) and, when $NiCl_2.6H_2O$ was used, Ni-Cl stretches (170-250 cm^{-1}) were also observed. Low intensity absorption bands were observed in the UV spectra of the complexes. In some cases, dissolution of the coloured complexes in MeOH resulted in a pale "straw-coloured" solution, suggesting co-ordination by the solvent and a change in the coordination geometry from square-planar to octahedral.

The ^{1}H NMR spectrum **Figure 18b** of the Ni(II) complex **59** obtained when ligand **44** was treated with $NiCl_2.6H_2O$, is typical of the complexes obtained. Comparison of the spectra for the free ligand **44** (**Figure 18a**) and the Ni(II) complex **(Figure 18b)** reveal broadening of the aromatic peaks, and the morpholine proton signals in the spectrum of the complex. The fact that the aromatic peaks remain well defined in the spectrum of the complex suggest strong pyridine Ni-N diamagnetic co-ordination, However, broadening of peaks indicates some change in the co-ordination geometry to afford systems containing the paramagnetic d^8 metal ion. The ^{1}H NMR spectra of some of the other complexes indicated a complete shift to the paramagnetic octahedral geometry.

Elemental (combustion and high-resolution MS) analyses of the complexes did not correspond closely with the predicted structures, and extensive re-precipitation and washing of the complexes appeared to worsen the situation. The difficulties encountered in the analysis of the Ni(II) complexes is attributed to the existence of dynamic equilibria in solution [18], involving changes in the metal coordination geometry and the species in the coordination shell **(Figure 19)**.

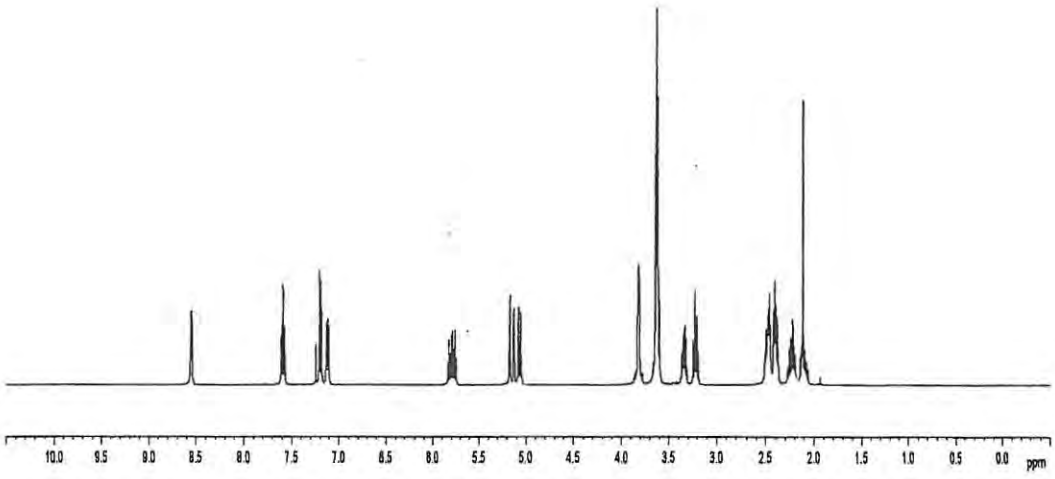

Figure 18a. 400 MHz ^{1}H NMR spectrum of the morpholino ligand **44** in $CDCl_3$.

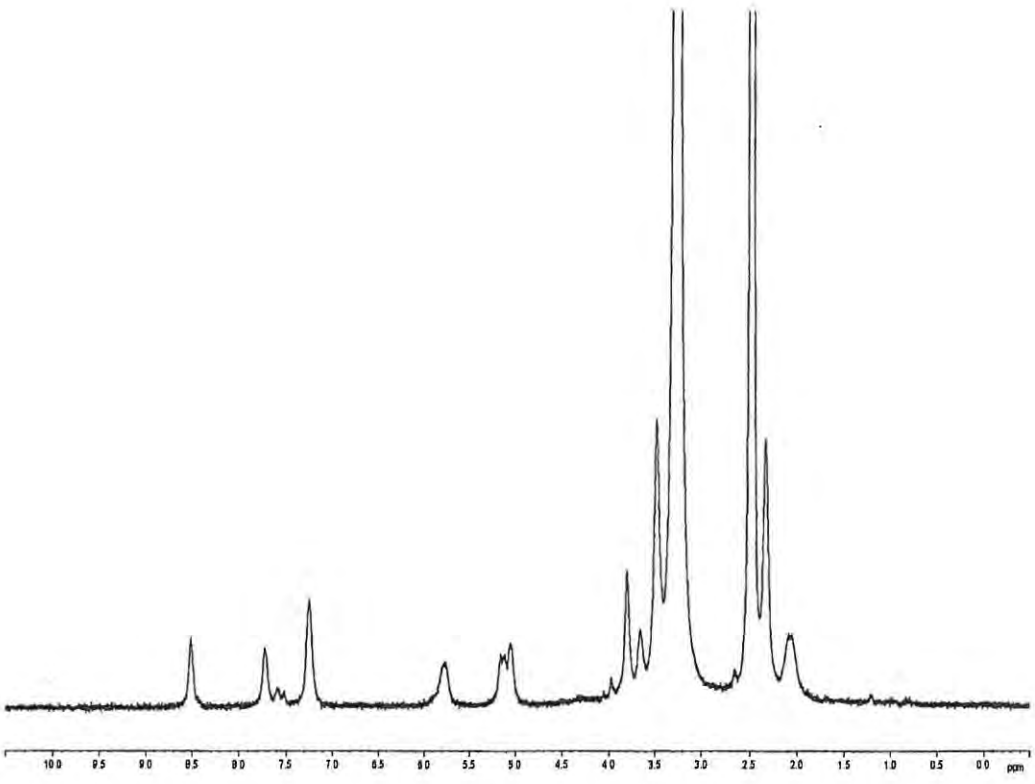

Figure 18b. 400 MHz ^{1}H NMR spectrum of the morpholino complex **59** in $CDCl_3$.

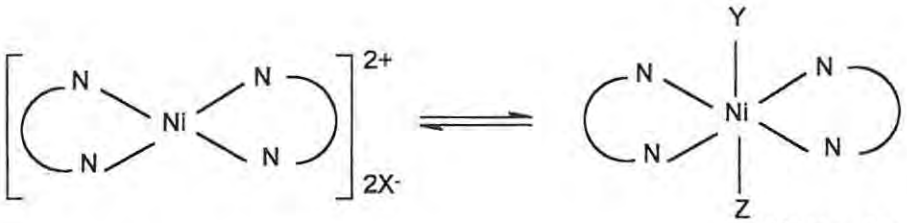

(Y,Z = X or solvent molecule)

Where:  represent bidentate ligands, **42, 43, 44** *etc.*

Figure 19. Dynamic equilibria of Ni(II) complexes.

Note: Other octahedral arrangements could also be involved.

2.5 Computer modelling studies

Organic molecules react and interact in 3-dimensional space. While physical models may be useful in analyzing 3-D structures, they have obvious limitations and cannot provide quantitative data on conformational energies, molecular dimensions, H-bonding effects *etc*. Many of these properties can be explored using appropriate computer modelling programmes.[85]

In the present study, a Molecular Mechanics (MM) approach has been followed. The "steric energy" E_{steric} of a particular conformation of a molecular system, as determined by a typical molecular mechanics programme is made up of a number of components [86]:-

$$E_{\text{steric}} = E_{\text{bonds}} + E_{\text{angles}} + E_{\text{vdw}} + E_{\text{torsion}} + E_{\text{charge}} + E_{\text{miscellaneous}}$$

Where: E_{bonds} is the total stretching energy,
E_{angles} is the total valence angle deformation energy,
E_{vdw} is the total van der Waals interaction energy,
E_{torsion} is the total torsion angle deformation energy,
E_{charge} is the total charge-charge interaction energy and
$E_{\text{miscellaneous}}$ is the total miscellaneous interactions energy.

Because of its relative simplicity and speed, Molecular Mechanics has been used to model even complex structures, but its application to metal complexes can be problematic. Establishing parameters for metal ions is not always straight forward and, consequently, the modelling data should be interpreted with caution. In this project, a Molecular Mechanics approach was used to explore likely conformation for each of the complexes. The modelling was carried out using the MSI Cerius2 package,[87] and the general protocol, which was followed, is outlined in the experimental section. The universal force field option was chosen and the overall charge distribution was set to zero (neutral) for ligands and to +2 for the complexes containing nickel. Steepest descent and Newton-Raphson techniques [88] were employed successively to obtain energy-minimised structures, which were then subjected to Dynamic Simulation in an attempt to

establish, in each case, the structure corresponding to the global minimum.

The structures of selected complexes were built to explore their possible square-planar and octahedral geometries. In the octahedral environment (in which the pyridine and amine nitrogen donor atoms are *cis*- or *trans*- to each other), the counterions within the coordination sphere were limited to chloride. Both *cis*-and *trans*-structures were modelled for each of the possible coordination geometries, square-planar and octahedral.

In the case of the Ni(II) complex **59**, containing the morpholino ligand **44**, the *trans*-structures are favoured over *cis*, in each case, with the *trans*-octahedral geometry being considerably more stable (ΔE= 173 kcal/mol) than *trans*-square-planar **(Figure 16 a and b)**. In the case of the pyrrolidino complex **57**, however, the *cis*-structures appear to be favoured with the *cis*-octahedral geometry being more stable (ΔE= 31 kcal/mol) than the *cis*-square-planar geometry **(Figure 16 c and d)**.While *cis*-structures of the piperidino complex **54** are also favoured; in this case, the *cis*-octahedral geometry appears to be more stable than the *cis*-square-planar **(Figure 17 e and f)**, by 6.3 kcal/mol.

It should be noted, however, that the computer modelled structures represent isolated (gas phase) systems and that, in solution, the situation may be more complicated due to solvation, ligand exchange and *cis*/*trans* and octahedral/square-planar equilibria

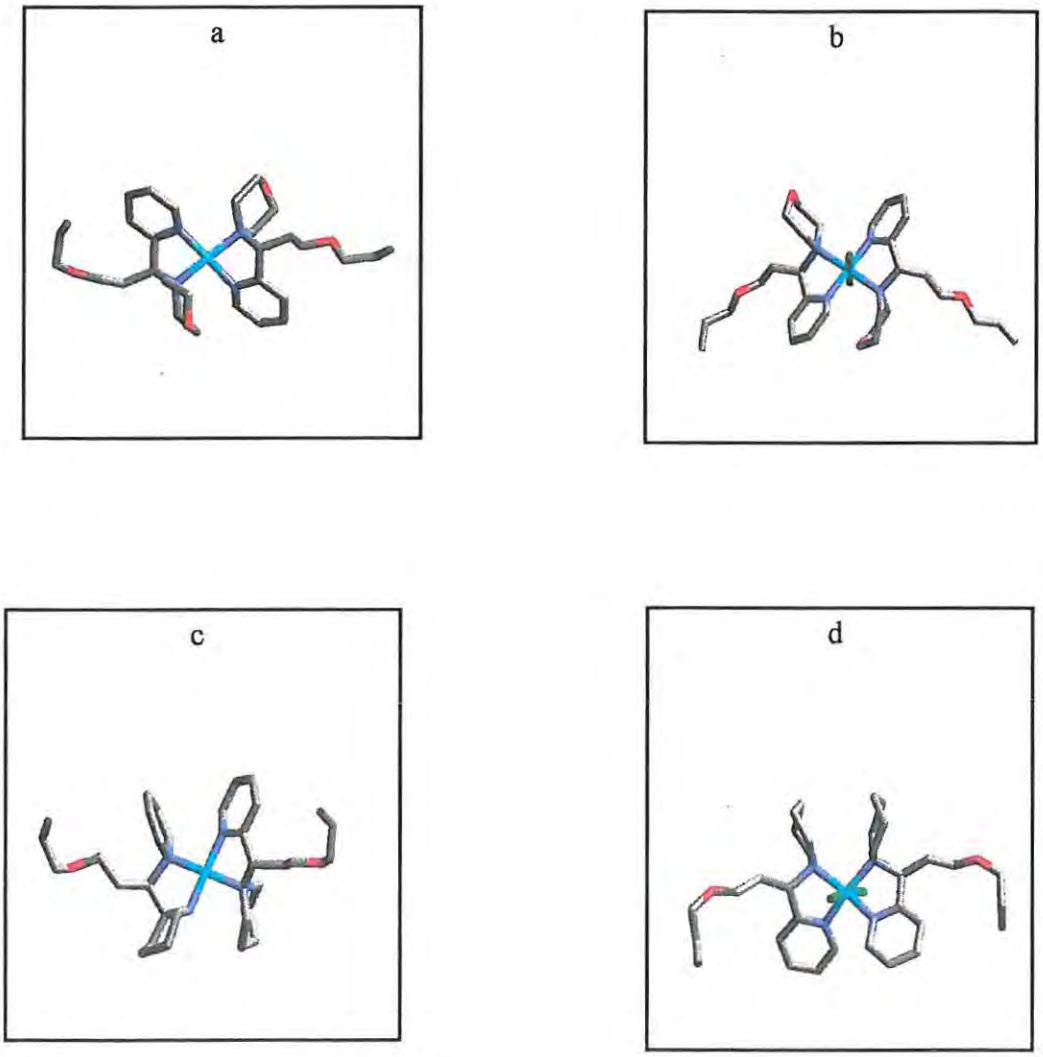

Figure 16. Computer-modelled structures of:- the morpholino ligand complexes, **a)** *trans*-square-planar and **b)** *trans*-octahedral; and the pyrrolidino complexes, **c)** *cis*-square-planar, and **d)** *cis*-octahedral.

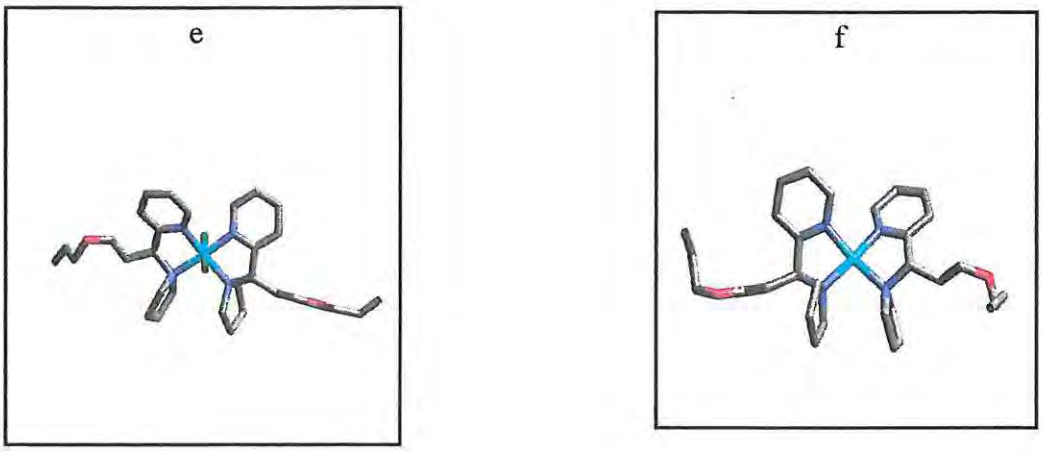

Figure 17. Computer-modelled structures of the piperidino ligand complexes **e)** *cis*-octahedral and **f)** *trans*-square-planar.

2.6 Preparation and evaluation of molecularly imprinted polymers (MIP's)

2.6.1 Preparation of nickel-selective MIP's

The primary aim of this project has been to design and synthesize selected ligands for use in the construction of MIP's containing nickel-specific cavities. The general approach to the MIP's, outlined in **Scheme 17**, involves several important stages, *viz.*, mixing, polymerization, grinding, leaching and, finally, drying. The different stages will be discussed separately.

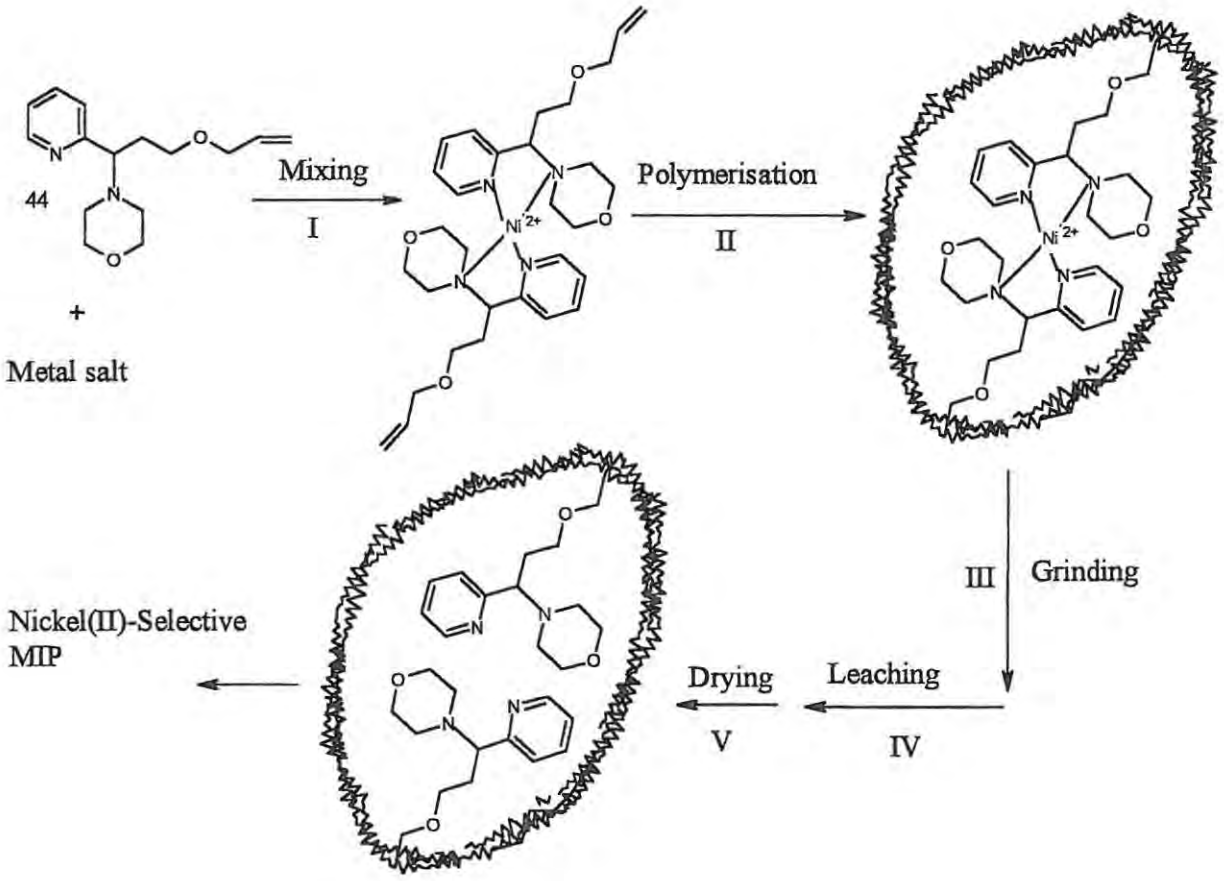

Scheme 17. Schematic representation of the processes involved in the preparation of the nickel-selective MIP's, using ligand **44**.

2.6.1.1 Mixing

The first stage of the MIP synthesis involved mixing of the polymerisable ligand and the metal ion to generate the metal complex. Initially, 2 equivalents of the ligand system **44**, as the "functional monomer," were treated with the "print species," nickel(II) acetate, in methanol as the "porogenic" solvent. The reaction mixture was stirred overnight. On mixing, it was noted that the light-yellow solution underwent an immediate colour change to light-green. The proportion of the functional monomer **44** and the nickel acetate concentration was varied (from 2:1 to 3:1 and 1:2), while in other experiments, nickel(II) acetate was replaced by different metal salts, *viz.*, nickel(II) chloride, nickel(II) perchlorate, nickel(II) tetrafluoroborate, cobalt(II) chloride and ferric(III) chloride. MIP's were also prepared using nickel(II) acetate and each of the ligands **42**; **46** and **53**.

2.6.1.2 Polymerization

A large volume of the cross-linker, ethylene glycol dimethacrylate (EGDMA), was then added under nitrogen to give an EGDMA : monomer molar ratio of 95:5 to permit nickel-cavities in the polymer to retain their shape even after removal of the template. In one case, using nickel(II) acetate and ligand **44**, the relative proportion of the EGDMA was reduced by half. A small amount of the radical initiator, azobis(isobutyronitrile) (AIBN), was then added, and polymerization was achieved by increasing the temperature of the stirred reaction mixture to 60 °C. At this temperature AIBN decomposes to form radicals, which then initiate co-polymerization of the functional monomer and cross-linker to form solid, glassy polymers.

2.6.1.3 Grinding

After cooling, the test tube containing the MIP was wrapped in a cloth and then shattered. After retrieving the solid, greenish polymer from the test tube fragments, the polymer was pulverized into three different "mesh" sizes (fine, medium and course), using a pestle and mortar.

2.6.1.4 Leaching studies

Different options were explored to obtain an ideal solvent capable of extracting the coordinated nickel ions from the MIP's. This initially involved washing polymeric material of different particles sizes with conc. acetic acid or with a 1:1 mixture of acetic acid and MeOH. In these attempts, however, the greenish colour of the particles (which is believed to indicate the presence of nickel ion) never disappeared. Finally, prolonged washing, through suction filtration, with conc. HCl was found to be effective, although leaving the ground MIP's to stand overnight in conc. HCl was found to be the best option.

2.6.1.5 Drying

The leached MIP's were washed throughly with MeOH prior to drying under high vacuum for 2 days. At this stage, the MIP's were comprised largely of shiny white particles. It was noticed, however, that incompletely leached particles retained their original colour even after extensive drying.

All of the MIP's prepared following the general protocol are listed in **Table 17**; in each case, the polymeric product was pulverized to afford the corresponding, rough "mesh" sizes (fine, medium and course). For reference purposes, a "blank MIP" was obtained by excluding a nickel(II) salt (the "imprint" species) in the preparation.

Table 17. Nickel-Selective MIP's prepared in this study [a]

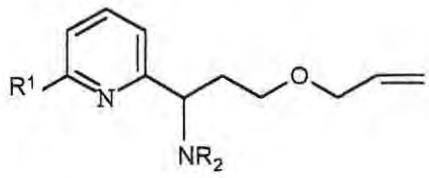

Ligand	NR_2	R^1	Metal salt	Colour on mixing	Colour of MIP prior to leaching	MIP Code
44	morpholino	H	Ni(II)acetate	greenish	greenish	**MIP 44A**
44	morpholino	H	Ni(II)acetate [b]	greenish	greenish	**MIP 44B**
44	morpholino	H	Ni(II)acetate [c]	greenish	greenish	**MIP 44C**
44	morpholino	H	Ni(II)acetate [d]	greenish	greenish	**MIP 44D**
44	morpholino	H	Ni(II)chloride	dark-brown	yellow-brown	**MIP 44E**
44	morpholino	H	Ni(II)perchlorate	yellow-brown	brick-red	**MIP 44F**
44	morpholino	H	Ni(II)tetrafluoro-borate	dark-brown	brown	**MIP 44G**
44	morpholino	H	Co(II)chloride	black-brown	brown	**MIP 44H**
44	morpholino	H	Fe(III)chloride	dark-red	red-brown	**MIP 44I**
42	piperidino	H	Ni(II)acetate	dark-brown	brown	**MIP 42A**
46	benzylamino	H	Ni(II)chloride	light-green	brown	**MIP 46A**
53	morpholino	Me	Ni(II)acetate	light-green	blue-brown	**MIP 53A**

[a] Following the "standard" protocol, using an EGDMA: functional monomer molar ratio of 95:5 and a functional monomer: metal molar ratio of 2:1. [b] Using functional monomer: metal molar ratio of 3:1. [c] Using functional monomer: metal molar ratio of 1:2. [d] Using EGDMA: functional monomer ratio of 48:5.

Scanning electron microscopy (SEM) was used to examine the physical dimensions of the particles corresponding to the different "mesh" sizes. Dried imprinted polymer particles obtained using ligand **44** and nickel(II)tetrafluoroborate and blank polymer particles were dusted on to conductive double sided adhesive tape on SEM specimen stubs. Sputter-coating with gold was effected on a Balzero Union sputtering device, and the samples viewed on the Scanning Electron Microscope. The general distribution of the fine and medium size particles is clearly shown in the low magnification (33 x) micrographs (**Figures 20a** and **20b**, respectively). It is evident from the high magnification (120 x) micrographs that there are numerous cavities in the nickel-imprinted polymer particles **(Figure 20c)**, but these are absent in the case of the blank polymer particles **(Figure 20d)**.

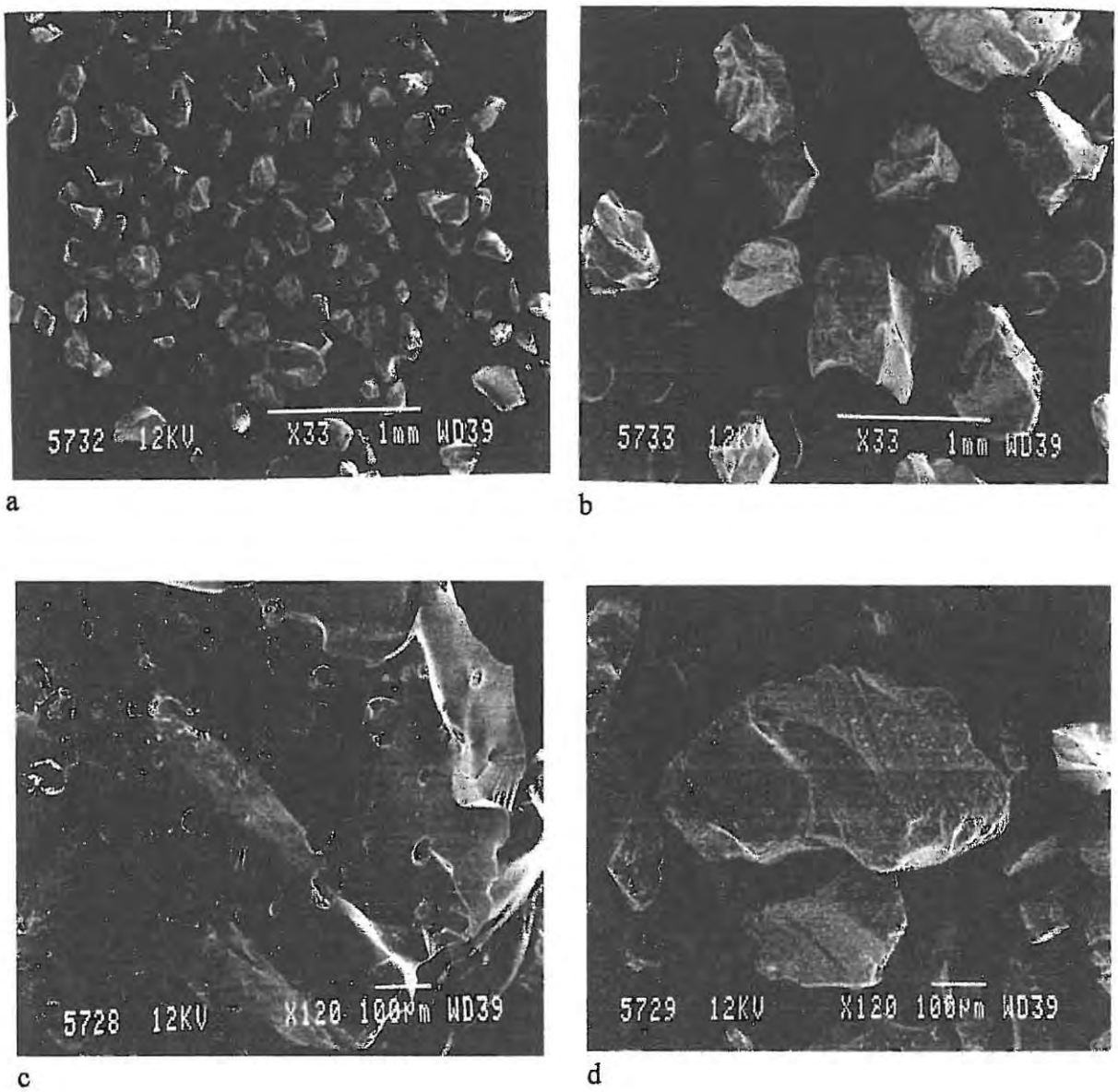

Figure 20. Scanning Electron Micrographs of **MIP 44G**;- **a**) fine particles (33 x magnification); **b**) medium size particles (33 x magnification); **c**) medium size particles (120 x magnification ; and **d**) blank polymer particles (120 x magnification).

2.6.2 Evaluation of the molecularly imprinted polymers

Evaluation of the nickel-imprinted polymers was initially carried out by stirring the dried particles at room temperature for 3 days with a known concentration of nickel(II) acetate dissolved in MeOH as described in the experimental section. Significant changes in the colour of the highly concentrated solutions were observed, and the supernatant liquid was analyzed, in each case, using flame Atomic Absorption Spectroscopy (AAS).It was noted that, on stirring for extended periods, the MIP particles began to disintegrate, and the AA spectrophotometer was found to give inconsistent results. In the second method, standard solutions of Ni(II)acetate, Ni(II)chloride and Fe(III) chloride, or mixtures of Ni(II) chloride and Fe(III) chloride, in methanol-water[1:1(v/v)] and 1% nitric acid, were passed through pasteur pipettes containing polymer particles as the stationary phase, and the eluents were analyzed by AAS. In the third method, standard solutions were prepared as in the second method, the only difference being that, after adding the MIP, the mixtures were shaken mechanically. Samples of the supernatant liquid were removed for ICP-MS analysis at various time intervals. The intention was to determine:-

i) the extraction efficiency of MIP's prepared using selected ligand monomers;
ii) the time required to establish equilibrium;
iii) the influence of mesh-size on extraction; and
iv) the effect of different metals and counterions (used in the formation of the MIP's) on extraction efficiency.

The ICP-MS analysis results are tabulated in the experimental section and reflect the concentration of Fe(III) and isotopes of Ni(II) present after equilibration. Organic solvents are known to affect ICP analysis[69] and small anomalies in the results [increases in Fe(III) concentration and small negative values for the Ni(II) concentration after equilibration] are attributed to the presence of methanol in the analyte solutions. The MIP's selected for evaluation were those prepared from:- the morpholino ligand **44** (**MIP 44E**); the piperidinyl analogue **42** (**MIP 42A**); the benzylamino analogue **46** (**MIP 46A**); and the 6-methyl pyridine-2-carbaldehyde morpholino substituted analogue **53** (**MIP 53A**) (**Table 17**).

The nickel-selective behaviour of these ligands is illustrated in **Figure 21**. While all of the MIP's examined exhibit significant selectivity for nickel(II) over iron(III), MIP **44G** is clearly the most selective, the concentration of nickel present in solution after equilibration in this case being almost zero. Nickel(II)-selectivity [relative to Fe(III)] for the ligands appear to follow the following trend, MIP **44G** > MIP **53A** > MIP **46A** > MIP **42A**.

To explore the time needed to reach equilibrium, it seems that shaking for 5 minutes is generally sufficient to reach equilibrium. When the shaking exceeded 5h, the nickel concentration in solution was found to increase, an observation attributed to the disintegration of the polymeric matrix during extended mechanical shaking. When MIP **44I** [prepared using ligand **44** and $FeCl_3$] was used to monitor the time required to reach equilibrium, it was observed that equilibration was achieved within 10 min.

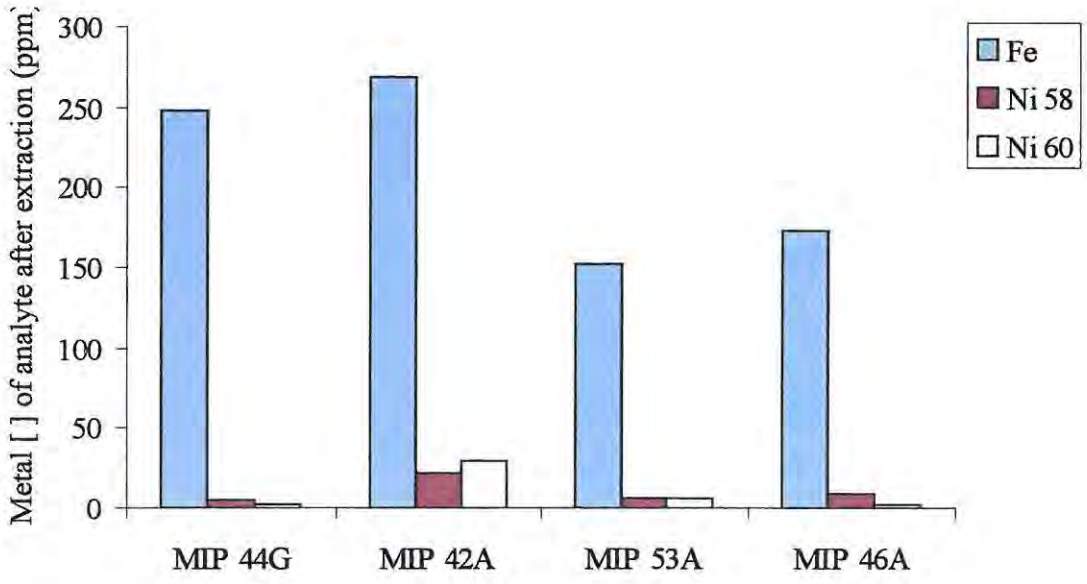

Figure 21. ICP-MS analysis results, comparing the metal selectivities of various MIP's.

The molecularly imprinted polymer **MIP 44G** prepared using the morpholino ligand **44** was used to investigate the influence of mesh size on absorption capacities, and the results detailed in **Table 19c** (Experimental Section) indicate that the fine particles(which have a large surface area) trap the nickel(II) ions more efficiently than the medium or coarse particles. In another set of experiments, which were conducted to determine the nickel-selectivity of MIP's prepared using different metal chlorides **(Table 19d)**, it appears that the Fe(III) and Co(II) imprinted polymers (**MIP 44I** and **MIP 44G**, respectively) are even more selective for nickel(II) than the nickel-imprinted analogue **MIP 44E**. **Table 19f** details the effects of varying:-i) the counterion and ii) the ligand and metal concentrations used in preparing the MIP's; these results may be summarized as follows. The use of nickel tetrafluoroborate and acetate salts appears to afford MIP's with greater nickel-selectivity than the MIP prepared using the chloride salt, while use of a high nickel concentration appears to reduce selectivity, suggesting that the polymer does not contain sufficient nickel-selective cavities.

2.7 Conclusions

An extensive literature search provided insights into the chemistry of nickel, its geology, mining and extractive metallurgy, and indicated the preferred stereochemistry of nickel(II) complexes to be square-planar or octahedral. These insights provided the basis for designing bidentate ligand systems, containing amine and pyridyl moieties to permit the formation of 5-membered nickel(II) chelates which would be stable at low pH. A vinyl group was also incorporated to permit co-polymerisation to afford the required MIP's. A synthetic pathway to the novel target ligands was established on the basis of a retrosynthetic analysis. Using this pathway (which had to be modified to permit replacement of the vinyl group by an allyl ether moiety), ligand systems were successfully prepared and fully characterized. The mass fragmentation patterns exhibited by selected ligands were explored using high-resolution electron-impact MS and B/E linked scan data, and common fragments were identified in the spectra of most of the ligands investigated.

Complexation studies were undertaken employing various nickel salts. Use of nickel(II) chloride, nickel(II) acetate, nickel(II)perchlorate and nickel(II) tetrafluoroborate afforded hygroscopic, semi-solid complexes, ruling out their characterization using X-ray crystallography. In some cases dissolution of the coloured complexes in MeOH afforded pale straw-coloured solutions, suggesting coordination by the solvent and a change in the coordination geometry from square-planar to octahedral. Computer modelling of the complexes was undertaken to explore possible structures.

A range of molecularly imprinted polymers containing nickel-specific cavities was successfully prepared using selected ligands. Ethylene glycol dimethacrylate (EGDMA) was used as the cross-linking agent and azobis(isobutyronitrile) (AIBN) was employed as a radical initiator to induce polymerization; methanol was used as the porogenic solvent and glassy solid polymers were obtained. Concentrated hydrochloric acid was found to be the best solvent for leaching out the coordinated nickel in the polymer. Different polymer mesh sizes were produced by manual grinding and Scanning Electron Micrographs of such particles clearly showed the presence of cavities on the surface of the nickel-imprinted polymer. ICP-MS analysis was used to evaluate

the extraction potential of the MIP's. The results suggested that the morpholino ligand was the most selective and that the use of tetrafluoroborate and acetate counterions in the preparation of the MIP's appeared to enhance nickel-selectivity. The MIP's examined showed good to excellent selectivity for Ni(II) over Fe(III).

The aims of the project have thus been realized, and future research in this area is expected to include the following.

i) Conclusive structural elucidation of the nickel(II) complexes and the corresponding polymers.

ii) An extensive investigation of the ICP analysis protocol to explore the effects of nitric acid and the organic phase on the results.

iii) Evaluation of the mechanical and thermal stability of the nickel-imprinted polymers to explore their applications under various conditions.

iv) An investigation of the selectivity of the MIP's for nickel(II) in the presence of other metals in addition to Fe(III).

3 EXPERIMENTAL

3.1 General

Solvents were dried following methods described by Perrin and Armarego.[93] Reagents were purchased from Aldrich or Merck, and were used without further purification. Thin layer chromatography (TLC) was conducted using Merck pre-coated silica gel 60 PF_{254} plates, preparative layer chromatography using silica gel 60 PF_{254} and flash chromatography[94] using silica gel 60 (particle sizes 0.040-0.063 mm).

Low resolution mass spectra were recorded on a Finnigan-MAT GCQ mass spectrometer, while high resolution and FAB-MS analyses were conducted by the Cape Technikon Mass Spectrometry Unit and at the University of Potchefstroom, respectively. A Bruker 400 MHz AVANCE spectrometer was used to record all NMR spectra. Chemical shifts are quoted relative to the solvent signals (δ_H : 7.25 ppm for $CDCl_3$ or 2.50 ppm for DMSO-d_6; δ_C: 77.0 ppm for $CDCl_3$ and 39.43 ppm for DMSO-d_6). UV-visible spectra were recorded on a Cary 500 UV-Visible NIR spectrophotometer.

IR spectra were recorded on a Perkin-Elmer FT-IR spectrum 2000 spectrometer using KBr discs or as thin films between NaCl plates for the mid-IR range (4000-400 cm^{-1}), and polyethylene discs for the far-IR range (650-30 cm^{-1}). Atomic Absorption Spectroscopy (AAS) data were obtained using Varian AA-1275 series spectrophotometer, and ICP analyses were conducted at the University of Port Elizabeth. Scanning electron micrographs were obtained using a JEOL JSM 840 SEM instrument. Computer modelling was conducted on SGI O^2 computer using the MSI Cerius^2 software platform. Microanalysis (combustion analysis) was conducted at the University of Cape Town.

3.2 Synthetic procedures

Ethyl 3-(2-pyridyl)acrylate **25** [76, 78]

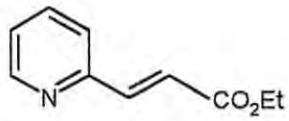

A solution of pyridine-2-carbaldehyde **24** (9.00 ml, 96.0 mmol) in dry CH_2Cl_2 (54 ml) was added dropwise to (carbethoxymethyl)triphenylphosphorane **20** (30.4 g, 86.4 mmol) in dry CH_2Cl_2 (90 ml) in a two-necked flask protected from light. The reaction mixture was stirred at *ca.*15 °C for 15 min, and then boiled under reflux for 26h. The solvent was evaporated from the resulting mixture *in vacuo,* and the crude product was extracted with boiling hexane (6 x 30 ml). The hexane extracts were combined and evaporated under reduced pressure to afford, as a viscous amber oil, ethyl 3-(2-pyridyl)acrylate **25** (14.2 g, 93 %) (Found: M^+, 177.07866. $C_{10}H_{11}NO_2$ requires *M*, 177.07898); ν_{max} (NaCl)/cm^{-1} 1721 (CO); δ_H (400 MHz; $CDCl_3$) 1.23 (3H, t, *J* 7.1 Hz, OCH_2CH_3), 4.19 (2H, q, *J* 7.1 Hz, OCH_2CH_3), 6.82 (1H, d, *J* 15.7 Hz, Ar C*H*=CH), 7.16 (1H, t, *J* 4.2 Hz, ArH), 7.33 (1H, d, *J* 7.7 Hz, ArH), 7.66 (2H, overlapping multiplet, ArH and ArCH=C*H*), 8.56 (1H, d, *J* 4.5 Hz, ArH); δ_C (100 MHz; $CDCl_3$) 14.6 (CH_2CH_3), 61.1 (CH_2CH_3), 124.5 (ArCH=CH), 124.6 (ArCH=CH), 123.0, 137.2, 143.5, 149.9 and 152.9 (ArC) and 166.7 (CO).

Ethyl 3-(1-piperidyl)-3-(2-pyridyl)propanoate **26** [95, 96]

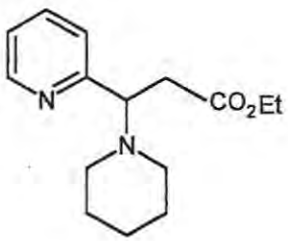

Method A: Piperidine (28.6 ml, 288 mmol) was added dropwise to ethyl 3-(2-pyridyl)acrylate **25** (4.20 g, 23.7 mmol) and the reaction mixture was boiled under reflux for 24h. The volatiles were evaporated from the resulting mixture *in vacuo* to yield, as a light-yellow oil, *ethyl 3-(piperidino)-*

3-(2-pyridyl)propanoate **26** (6.05 g, 100 %) (Found: M^+-H, 261.16082. $C_{15}H_{22}N_2O_2$ requires *M*-1, 261.16030); ν_{max} (NaCl)/cm^{-1} 1724 (CO); δ_H (400MHz; $CDCl_3$) 1.14 (3H, t, *J* 7.1 Hz, CH_2CH_3), 1.16 (2H, m, $CH_2CH_2CH_2$), 1.35 (4H, m, CH_2CH_2N), 2.27 (4H, m, CH_2N), 2.79 (2H, m, $CHCH_2CO_2$), 3.90 (2H, q, *J* 7.2 Hz, $CO_2CH_2CH_3$), 4.09 (1H, m, $NCHCH_2$), 7.09 (1H, t, *J* 5.2 Hz, ArH), 7.29 (1H, d, *J* 7.3 Hz, ArH), 7.60 (1H, t, *J* 6.0 Hz, ArH) and 8.54 (1H, d, *J* 4.2 Hz, ArH); δ_C (100 MHz; $CDCl_3$) 14.5 (CH_2CH_3), 24.9 ($CH_2CH_2CH_2$), 26.8 (NCH_2CH_2), 35.0 ($CHCH_2CO_2$), 51.1 (NCH_2CH_2), 60.5 ($CO_2CH_2CH_3$), 67.1 ($NCHCH_2$), 122.3, 124.0, 136.2, 148.1 and 158.9 (ArC) and 172.8 (C=O).

Method B: A mixture of piperidine (1.5 ml, 9 mmol) and ethyl 3-(2-pyridyl)acrylate **25** (0.33 g, 2.0 mmol).was allowed to stand at room temperature for 3.5d. Work-up afforded, as a light-yellow oil, ethyl 3-(1-piperidyl)-3-(2-pyridyl)propanoate **26** (0.10 g, 19 %).

Attempted preparation: A solution of piperidine (0.2 ml, 1.2 mmol) in dry THF (1 ml) was added dropwise to a stirred solution of ethyl 3-(2-pyridyl)acrylate **25** (0.35 g, 2.0 mmol) in dry THF (1 ml). The reaction mixture was stirred for 9d, and the solvent was removed *in vacuo*. ^{1}H NMR spectroscopic analysis of the crude product revealed that only starting material was present.

Ethyl 3-(2-pyridyl)-3-(1-pyrrolidinyl)propanoate **27**

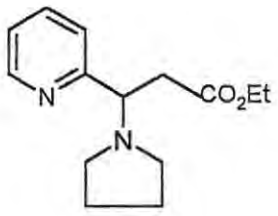

The experimental procedure described for the synthesis of ethyl 3-(1-piperidyl)-3-(2-pyridyl)propanoate **26** was followed, using pyrrolidine (29.0 ml, 34.0 mmol) and ethyl 3-(2-pyridyl)acrylate **25** (4.29 g, 24.0 mmol). The reaction mixture was boiled under reflux for 5d and, after work-up, afforded, as a yellow oil, *ethyl 3-(2-pyridyl)-3-(1-pyrrolidinyl)propanoate* **27** (4.12

g, 69 %) (Found: M^+-H, 247.14493. $C_{14}H_{20}N_2O_2$ requires *M*-1, 247.14465); ν_{max} (NaCl)/cm^{-1} 1722 (CO); δ_H (400 MHz; $CDCl_3$) 1.05 (3H, t, *J* 7.6 Hz, CH_2CH_3), 1.65 (4H, m, NCH_2CH_2), 2.37 (4H, m, CH_2NCH_2), 2.94 (2H, m, $CH_2CH_2CO_2$), 3.90 (1H, m, $NCHCH_2$), 3.91 (2H, m, $CO_2CH_2CH_3$), 7.09 (1H, t, *J* 4.9 Hz, ArH), 7.26 (1H, d, *J* 7.5 Hz, ArH), 7.56 (1H, t, *J* 7.6 Hz, ArH) and 8.53 (1H, d, *J* 4.0 Hz, ArH); δ_C (100 MHz; $CDCl_3$) 14.4 (CH_2CH_3), 23.6 (NCH_2CH_2), 39.3 ($CH_2CH_2CO_2$), 51.7 (NCH_2CH_2), 60.4 ($CO_2CH_2CH_3$), 66.6 ($NCHCH_2$), 122.5, 123.6, 136.3, 149.5 and 161.0 (ArC) and 172.0 (C=O).

Ethyl 3-(morpholino)-3-(2-pyridyl)propanoate **28**

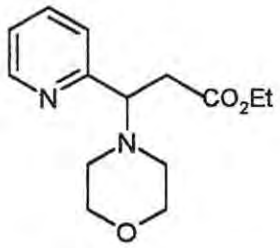

The experimental procedure described for the synthesis of ethyl 3-(1-piperidyl)-3-(2-pyridyl)propanoate **26** was followed, using morpholine (25.9 ml, 290 mmol) and ethyl 3-(2-pyridyl)acrylate **25** (3.71 g, 21.0 mmol). The reaction mixture was boiled under reflux for 18h. The solvent was evaporated from the resulting mixture in *vacuo* to yield, as a yellow oil, *ethyl 3-(morpholino)-3-(2-pyridyl)propanoate* **28** (4.89 g, 88 %) (Found: M^+, 264.14720. $C_{14}H_{20}N_2O_3$ requires *M*, 264.14739); ν_{max} (NaCl)/cm^{-1} 1725 (CO); δ_H (400 MHz; $CDCl_3$) 1.08 (3H, t, *J* 7.5 Hz, CH_2CH_3), 2.35 (4H, m, CH_2N), 2.90 (2H, m, $CHCH_2CO_2$), 3.59 (4H, m, CH_2O), 4.01 (2H, q, *J* 7.1 Hz, $CO_2CH_2CH_3$), 4.08 (1H, m, $NCHCH_2$), 7.11 (1H, m, ArH), 7.25 (1H, d, *J* 7,3 Hz, ArH), 7.55 (1H, m, ArH) and 8.49 (1H, d, *J* 4.2 Hz, ArH); δ_C (100 MHz; $CDCl_3$) 14.5 (CH_2CH_3), 35.5 (CH_2N), 50.5 ($CHCH_2CO_2$), 67.4 (CH_2OCH_2), 67.6 ($NCHCH_2$), 68.5 ($CO_2CH_2CH_3$), 122.7, 124.1, 136.4, 149.3 and 158.8 (ArC) and 172.6 (C=O).

Ethyl 3-butylamino-3-(2-pyridyl)propanoate **29**

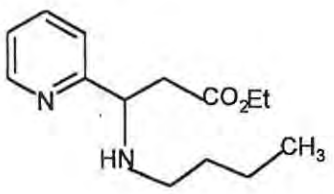

A solution of butylamine (12 ml, 0.12 mol) in THF (5 ml) was added dropwise to a solution of ethyl 3-(2-pyridyl)acrylate **25** (4.4 g, 30 mmol) in THF (6 ml). The reaction mixture was boiled under reflux for 26h. ^{1}H NMR analysis confirmed completion of the reaction and the excess butylamine was evaporated in *vacuo* during 24h to afford, as a light-yellow oil, *ethyl 3-butylamino-3-(2-pyridyl)propanoate* **29** (6.07 g, 87 %) (Found: MH^+, 251.17745. $C_{14}H_{22}N_2O_2$ requires M+1, 251.17595); ν_{max} (NaCl)/cm^{-1} 3301 (NH) and1720 (CO); δ_H (400 MHz; $CDCl_3$) 0.89 (3H, t, J 7.4 Hz, $CH_2CH_2CH_3$), 1.17 (3H, t, J 7.1 Hz, $CO_2CH_2CH_3$), 1.21 (2H, m, $CH_2CH_2CH_3$), 1.38 (2H, m, CH_2CH_2NH), 1.98 (2H, m, $NHCH_2$), 2.00 (1H, br s, $NHCH_2$), 2.36 (2H, m, $CHCH_2CO_2$), 4.03 (1H, m, NHC*H*), 4.12 (2H, m, $CO_2CH_2CH_2$), 7.02 (1H, m, ArH), 7.31 (1H, d, J 7.7 Hz, ArH), 7.60 (1H, m, ArH) and 8.52 (1H, d, J 3.4 Hz, ArH); δ_C (100 MHz; $CDCl_3$) 13.8 ($CH_2CH_2CH_3$), 14.1 ($CO_2CH_2CH_3$), 20.9 ($CH_2CH_2CH_3$), 32.2 ($CH_2CH_2CH_2$), 41.3 ($NHCH_2$), 47.2 ($CH_2CH_2CO_2$), 60.3 ($NHCHCH_2$), 60.5 (CO_2CH_2CH), 122.1, 122.3, 136.3, 149.5 and 162.0 (ArC) and 171.8 (C=O).

Ethyl 3-benzylamino-3-(2-pyridyl)propanoate **30**

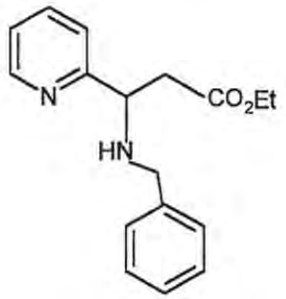

The experimental procedure described for the synthesis of ethyl 3-(1-piperidyl)-3-(2-pyridyl)propanoate **26** was followed, using benzylamine (12.0 ml, 110 mmol) and ethyl 3-(2-pyridyl)acrylate **25** (5.0 g, 28 mmol). After the reaction mixture had been boiled under reflux for 26h, work-up afforded, as a yellow oil, *ethyl 3-benzylamino-3-(2-pyridyl)propanoate* **30** (2.6 g, 32 %) (Found: M^+-2, 282.13565. $C_{17}H_{20}N_2O_2$ requires M-2, 282.13683); ν_{max} (NaCl)/cm^{-1} 3327 (NH) and 1737 (CO); δ_H (400 MHz; $CDCl_3$) 1.15 (3H, t, J 7.1 Hz, CH_2CH_3), 2.02 (1H, br s, N*H*), 2.78 (2H, d, J 6.9 Hz, $CHCH_2$), 3.50 (2H, m, $NHCH_2$), 4.01 (2H, q, J 6.8 Hz, CH_2CH_3), 4.13 (1H, t, J 7.1 Hz, NHC*H*), 7.12-7.31 (7H, m, ArH), 7.59 (1H, t, J 7.5 Hz, ArH) and 8.55 (1H, d, J 4.0 Hz, ArH); δ_C (100 MHz; $CDCl_3$) 13.8 (CH_2CH_3), 23.6 ($CHCH_2$), 41.1 ($NHCH_2$), 60.2 ($CHCH_2$),

60.8 (CH_2CH_3), 121.9, 122.1, 126.5, 127.8, 127.9, 135.9, 139.8, 149.3, 161.4 (ArC) and 171.3 (C=O).

Ethyl 3-isopentylamino-3-(2-pyridyl)propanoate **31**

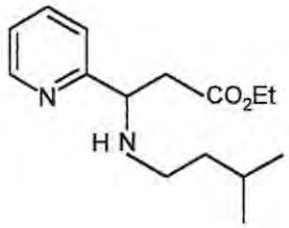

The experimental procedure described for the synthesis of ethyl 3-butylamino-3-(2-pyridyl)propanoate **29** was followed, using ethyl 3-(2-pyridyl)acrylate **25** (6.0 g, 33 mmol) and isopentylamine (12 ml, 0.10 mol). The reaction mixture was boiled under reflux for 24h to afford, as a light-yellow oil, *ethyl 3-isopentylamino-3-(2-pyridyl)propanoate* **31** (8.2 g, 92 %) (Found: MH^+, 263.17544. $C_{15}H_{24}N_2O_2$ requires *M*+1, 263.17595); ν_{max}(NaCl)/cm^{-1} 2956 (NH) and 1737 (CO); δ_H (400 MHz; $CDCl_3$) 0.78 [6H, m, $CH(CH_3)_2$], 1.15 (3H, t, *J* 7.2 Hz, CH_2CH_3), 1.48 (2H, m, CH_2CH_2CH), 1.55 (1H, m, $CHCH_3$), 1.92 (1H, br s, NH), 2.38 (2H, m, CH_2CO_2), 2.74 (2H, m, CH_2NH), 4.03-4.10 (3H, m, CH_2CH_3 and NHCH), 7.11 (1H, t, *J* 6.6 Hz, ArH), 7.30 (1H, d, *J* 7.6 Hz, ArH), 7.60 (1H, t, *J* 7.45 Hz, ArH) and 8.53 (1H, d, *J* 2.8 Hz, ArH); δ_C (100 MHz; $CDCl_3$) 14.5 (CH_2CH_3), 22.8 and 23.7 [$CH(CH_3)_2$], 26.3 ($CHCH_3$), 39.6 (CH_2CH_2CH), 41.7 (CH_2CO_2), 46.1 (CH_2NH), 60.7 (CH_2CH_3), 61.0 (NHCH), 122.5, 122.6, 136.6, 149.9 and 162.0 (ArC) and 172.0 (C=O).

Attempted synthesis of ethyl 3-(3-pentylamino)-3-(2-pyridyl)propanoate **32**

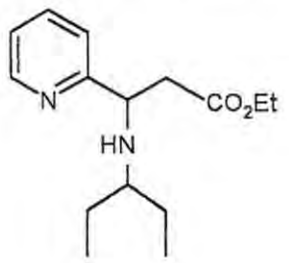

The methods described for the synthesis of ethyl 3-(1-piperidyl)-3-(2-pyridyl)propanoate **26**

(methods **A** and **B**) were followed, using 3-pentylamine (8.0 ml, 67 mmol) and ethyl 3-(2-pyridyl)acrylate **25** (6.0 g, 34.0 mmol). After boiling the reaction mixture under the reflux for 2 weeks, ^{1}H NMR analysis revealed that, in each case, only starting materials were present.

Attempted synthesis of ethyl 3-anilino-3-(2-pyridyl)propanoate **33**

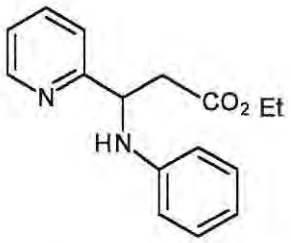

All three methods described for the synthesis of ethyl 3-(1-piperidyl)-3-(2-pyridyl)propanoate **26** were followed, using ethyl 3-(2-pyridyl)acrylate **25** and aniline. In each case, the reaction mixture was boiled under reflux for 10-14d. Work-up and ^{1}H NMR spectroscopic analysis of the crude products revealed that only starting materials were present.

3-(1-Piperidyl)-3-(2-pyridyl)propanol ***34*** [97, 98]

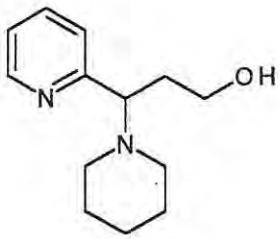

To a suspension of $LiAlH_4$ (3.26 g, 86.6 mmol) in dry Et_2O (30 ml), a solution of ethyl 3-(1-piperidyl)-3-(2-pyridyl)propanoate **26** (5.70 g, 21.6 mmol) in dry Et_2O (10 ml) was added dropwise under nitrogen, and the reaction mixture was boiled under reflux for 2h. Excess $LiAlH_4$ was quenched by the successive, dropwise addition of H_2O and 10 % NaOH, and the resulting mixture was extracted with boiling EtOAc (6 x 50 ml). The combined extracts were dried over anhydrous $MgSO_4$, and the solvent was evaporated under reduced pressure. The residual material was chromatographed [flash chromatography on silica gel: elution with MeOH-EtOAc (1:1)] to give, as a light-yellow oil, *3-(piperidino)-3-(2-pyridyl)propanol* **34** (2.96 g, 62 %) (Found: M^+,

220.15670.$C_{13}H_{20}N_2O$ requires *M*, 220.15756); ν_{max} (NaCl)/cm^{-1} 3389 (OH); δ_H (400 MHz; $CDCl_3$) 1.23 (2H, m, $CH_2CH_2CH_2$), 1.50 (4H, m, NCH_2CH_2), 2.46 (4H, m, NCH_2), 2.51 (2H, m, $CHCH_2$), 3.82 (2H, m, CH_2OH), 3.80-3.94 (1H, br overlaps, CH_2OH), 3.94 (1H, m, $NCHCH_2$), 7.17-7.21(2H, m, ArH), 7.63 (1H, t, *J* 7.6 Hz, ArH) and 8.56 (1H, d, *J* 4.9 Hz, ArH); δ_C (100 MHz; $CDCl_3$) 24.5 ($CH_2CH_2CH_2$), 26.6 (NCH_2CH_2), 30.8 ($CHCH_2CH_2$), 51.0 (NCH_2CH_2), 63.6 (CH_2CH_2OH), 72.1 ($NCHCH_2$), 122.6, 123.4, 136.2, 149.1 and 157.8 (ArC).

3-(2-Pyridyl)-3-(1-pyrrolidinyl)propanol **35**

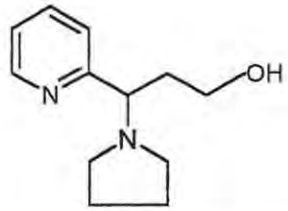

The experimental procedure described for the synthesis of 3-(1-piperidyl)-3-(2-pyridyl)propanol **34** was followed, using LAH (0.92 g, 21.0 mmol) in dry Et_2O (5 ml) and ethyl 3-(2-pyridyl)-3-(1-pyrrolidyl)propanoate **27** (3.0 g, 12 mmol) in dry Et_2O (4 ml). The reaction mixture was boiled under reflux for 2.5h, and the residual LAH quenched by the successive, dropwise addition of H_2O and 10 % NaOH. The resulting mixture was extracted with boiling EtOAc (6 x 25 ml), the combined extracts were dried (anhyd.$MgSO_4$), and the solvent was evaporated *in vacuo*. The residual material was chromatographed [flash chromatography on silica gel: elution with MeOH-EtOAc (4:6)] to give, as a yellow oil, *3-(2-pyridyl)-3-(1-pyrrolidinyl)propanol* **35** (0.46 g, 14 %) (Found: M^+-1, 205.13409. $C_{12}H_{18}N_2O$ requires *M*-H, 205.13302); ν_{max} (NaCl)/cm^{-1} 3390 (OH); δ_H (400 MHz; $CDCl_3$) 1.69 (4H, m, NCH_2CH_2), 1.89 and 2.25 (2H, 2 x m, $CHCH_2CH_2$), 2.53 (4H, m, NCH_2CH_2), 3.44 (1H, s, CH_2CH_2OH), 3.52 (2H, m, CH_2CH_2OH), 3.76 (1H, t, *J* 6.1 Hz, $NCHCH_2$), 7.14 (1H, t, *J* 1.2 Hz, ArH), 7.32 (1H, d, *J* 7.8 Hz, ArH), 7.63 (1H, t, *J* 5.7 Hz, ArH) and 8.51 (1H, d, *J* 2.7 Hz, ArH); δ_C (100 MHz; $CDCl_3$) 23.5 (NCH_2CH_2), 35.2 ($CHCH_2CH_2$), 51.6 (NCH_2CH_2), 61.4 (CH_2CH_2OH), 69.4 ($NCHCH_2$), 122.6, 123.3, 136.8, 149.2 and 160.8 (ArC).

3-(Morpholino)-3-(2-pyridyl)propanol **36**

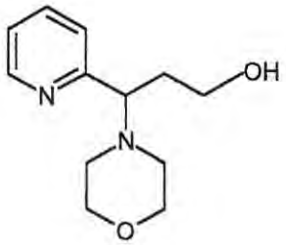

The experimental procedure described for the synthesis of 3-(1-piperidyl)-3-(2-pyridyl)propanol **34** was followed, using ethyl 3-(4-morpholino)-3-(2-pyridyl)propanoate **28** (4.62 g,17.0 mmol) in dry Et_2O (6 ml) and $LiAlH_4$ (3.22 g, 85.0 mmol) in dry Et_2O (17 ml). The reaction mixture was boiled under reflux for 2h, and the residual material was chromatographed [flash chromatography on silica gel: elution with MeOH-EtOAc (5:7)] to give, as a yellow oil, *3-(morpholino)-3-(2-pyridyl)propanol* **36** (2.9 g, 76 %) (Found: M^+-H, 221.12947. $C_{12}H_{18}N_2O_2$ requires *M*-1, 221.12960); ν_{max} (NaCl)/cm^{-1} 3396 (OH); δ_H (400 MHz; $CDCl_3$) 1.68 (1H, br s, CH_2OH), 2.30 (4H, m, CH_2OCH_2), 2.51 (2H, m, $CHCH_2CH_2$), 3.50 (4H, m, CH_2N), 3.68 (2H, m, CH_2OH), 3.78 (1H, m, $NCHCH_2$), 7.11 (1H, m, ArH), 7.13 (1H, d, *J* 6.8 Hz, ArH), 7.51 (1H, m, ArH) and 8.56 (1H, d, J 3.1 Hz, ArH); δ_C (100 MHz; $CDCl_3$) 31.8 ($CHCH_2CH_2$), 50.8 (CH_2OCH_2), 61.2 (CH_2N), 67.5 (CH_2OH), 71.0 ($NCHCH_2$), 122.8, 123.5, 136.6, 149.3 and 158.8 (ArC).

3-Butylamino-3-(2-pyridyl)propanol **37**

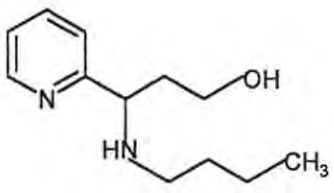

A solution of ethyl 3-butylamino-3-(2-pyridyl)propanoate **29** (4.5 g, 18 mmol) in dry Et_2O (6 ml) was added dropwise to a suspension of LAH (6.0 g, 0.16 mol in Et_2O (35 ml) under nitrogen. The reaction mixture was boiled under reflux for 4 d, and then the excess LAH was quenched by the successive, dropwise addition of water and 10 % aq. NaOH. The resulting mixture was extracted

with boiling EtOAc (6 x 50 ml), the combined extracts were dried (anhyd. $MgSO_4$) and the EtOAc was removed *in vacuo.* The residual material was purified by chromatography [flash chromatography on silica gel; elution with MeOH-EtOAc (6:5)] to give, as a yellow oil, *3-butylamino-3-(2-pyridyl)propanol* **37** (1.5 g, 43 %) (Found: M^+-H, 207.14916. $C_{12}H_{20}N_2O_2$ requires *M*-1, 207.14974); ν_{max} (NaCl)/cm^{-1} 3359 (OH) and 3301 (NH); δ_H (400 MHz; $CDCl_3$) 0.78 (3H, m, CH_2CH_3), 1.15 (2H, m, CH_2CH_3), 1.16 (2H, m, $CH_2CH_2CH_3$), 1.60 (1H, br d, CH_2OH), 1.88 (2H, m, $CHCH_2$), 2.35 (2H, m, $NHCH_2$), 2.51 (1H, br m, NHCH), 3.71 (1H, m, $CHCH_2$), 3.80 (2H, m, CH_2CH_2OH), 7.05 (2H, m, ArH), 7.56 (1H, m, ArH) and 8.51 (1H, d, *J* 4.1 Hz, ArH); δ_C (100 MHz; $CDCl_3$) 14.2 (CH_2CH_3), 20.7 (CH_2CH_3), 32.7 (CH_2CH_2NH),38.2 ($CHCH_2$), 47.5 ($NHCH_2$), 63.3 (CH_2OH), 65.5 ($CHCH_2$), 122.0, 122.5,136.8, 149.9 and 162.0 (ArC).

3-Benzylamino-3-(2-pyridyl)propanol **38**

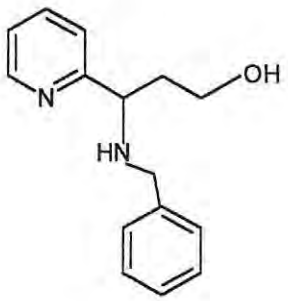

The experimental procedure described for the synthesis of 3-(1-piperidyl)-3-(2-pyridyl)propanol **34** was followed, using ethyl 3-benzylamino-3-(2-pyridyl)propanoate **30** (2.3 g, 8.0 mmol) in dry Et_2O (4 ml) and LAH (4.30 g, 110 mmol) in dry Et_2O (40 ml). Work-up and purification of the residual material afforded, as a yellow oil, *3-benzylamino-3-(2-pyridyl)propanol* **38** (0.90 g, 46 %) (Found: MH^+, 243.14965. $C_{15}H_{18}N_2O$ requires *M*+1, 243.14974); ν_{max} (NaCl)/cm^{-1} 3400 (OH) and 3310 (NH); δ_H (400 MHz; $CDCl_3$), 1.65 and 1.86 (2H, 2 x m, $CHCH_2CH_2$), 3.30-3.44 (2H, br s, NH and OH), 3.60 (2H, m, $NHCH_2$), 3.89 (2H, m, CH_2OH), 3.96 (1H, m, CHNH), 7.15-7.51(7H, m, ArH), 7.60 (1H, t, *J* 7.5 Hz, ArH) and 8.53 (1H, d, *J* 4.3 Hz, ArH); δ_C (100 MHz; $CDCl_3$) 38.5 ($CHCH_2$), 52.1(CH_2NH), 62.9 (CH_2OH), 64.2 (NHCH), 122.4, 122.6, 127.5, 128.6, 128.8, 136.9, 150.0, 151.3 and 162.1 (ArC).

3-Isopentylamino-3-(2-pyridyl)propanol **39**

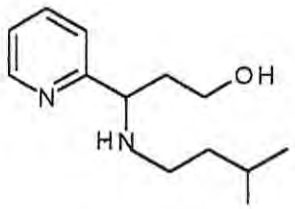

The method described for the synthesis of 3-butylamino-3-(2-pyridyl)propanol **37** was followed, using ethyl 3-isopentylamino-3-(2-pyridyl)propanoate **31** (8.0 g, 30 mmol) in dry Et_2O (20 ml) and LAH (3.4 g, 90 mmol) in dry Et_2O (15 ml). The reaction mixture was stirred at 0 °C for 1h, and then boiled under reflux for 3,5h. Work-up yielded, as a brown oil, *3-isopentylamino-3-(2-pyridyl)propanol* **39** (6.3 g, 94 %) (Found: MH^+, 223.18115. $C_{13}H_{22}N_2O$ requires *M*+1, 223.181104); ν_{max}(NaCl)/cm^{-1} 3500-3300 (overlapping NH and OH); δ_H (400 MHz; $CDCl_3$) 0.7 [6H, m, $CH(CH_3)_2$,] 0.8 (1H, br m, N*H*), 1.20 (2H, m, $NHCH_2CH_2$), 1.50 (1H, m, CH_3CH), 1.63 and1.74 (2H, 2 x m, CH_2CH_2OH), 2.30 (2H, m, CH_2NH), 3.67-3.71 (2H, m, NHC*H* and CH_2OH), 3.77 (2H, m, CH_2CH_2OH), 7.12 (2H, m, ArH), 7.60 (1H, m, ArH) and 8.50 (1H, d, *J* 4.7 Hz, ArH); δ_C (100 MHz; $CDCl_3$) 22.7 and 23.0 [$CH(CH_3)_2$], 26.3 ($CHCH_3$), 38.2 ($NHCH_2CH_2$), 39.6 (CH_2CH_2OH), 46.2 (CH_2NH), 63.3 (CH_2CH_2OH), 65.5 (NHCH), 122.1, 122.5, 136.8, 149.9 and 162.3 (ArC).

3-Allyloxy-1-(piperidino)-1-(2-pyridyl)propane **42** [99, 100]

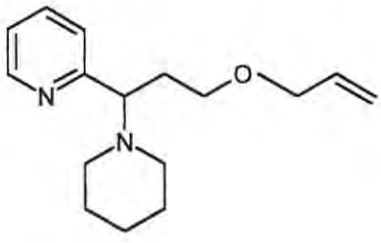

A solution of 3-(piperidino)-3-(2-pyridyl)propanol **34** (0.10 g, 4.5 mmol) in dry THF (4 ml) was added dropwise under N_2 to a stirred suspension of pre-washed NaH (50 % dispersion in oil; 0.25 g, 8.4 mmol). The reaction mixture was stirred at r.t. for 1h, and then allyl bromide (0.50 ml, 4.5

mmol) was added dropwise. The resulting mixture was stirred overnight and completion of the reaction was confirmed by TLC. After quenching by the dropwise addition of water, the mixture was extracted with boiling EtOAc (3 x 15 ml), the combined extracts were dried over anhydrous $MgSO_4$ and the solvent was removed *in vacuo*. The residual material was purified by chromatography [flash chromatography on silica gel; elution with MeOH-EtOAc (4:6)] to afford, as a light-yellow oil, *3-allyloxy-1-(piperidino)-1-(2-pyridyl)]propane* **42** (0.10 g, 86 %) (Found: M^+, 261.19747. $C_{16}H_{24}N_2O$ requires *M*, 261.19669); ν_{max} (NaCl)/cm^{-1} 1504 (C=C) and 1123 (C-O-C); δ_H (400MHz; $CDCl_3$) 1.25 (2H, m, $CH_2CH_2CH_2$), 1.43 (4H, m, NCH_2CH_2), 2.17 (2H, m, $CHCH_2CH_2$), 2.39 (4H, m, CH_2N), 3.27 and 3.39 (2H, 2 x m, CH_2CH_2O), 3.66 (1H, m, $NCHCH_2$), 3.82 (2H, m, OCH_2CH), 5.06 (2H, m, $CH=CH_2$), 5.74 (1H, m, $CH=CH_2$), 7.05 (1H, t, *J* 5.1 Hz, ArH), 7.16 (1H, d, *J* 7.4 Hz, ArH), 7.52 (1H, t, *J* 6.58 Hz, ArH) and 8.50 (1H, d, *J* 4.2 Hz, ArH); δ_C (100 MHz; $CDCl_3$) 25.1 $CH_2CH_2CH_2$), 26.8 (NCH_2CH_2), 31.6 ($CHCH_2CH_2$), 51.6 (NCH_2), 68.2 (CH_2CH_2O), 68.4 ($NCHCH_2$), 72.1 ($CHCH_2O$), 116.8 ($CH=CH_2$), 135.5 ($CH=CH_2$), 122.2, 123.9, 136.1, 149.2 and 160.8 (ArC).

3-Allyloxy-1-(2-pyridyl)-1-(1-pyrrolidinyl)propane **43**

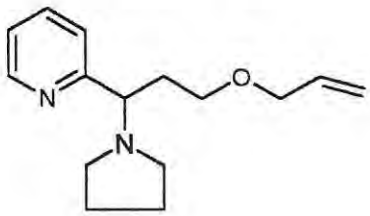

The experimental procedure described for the synthesis of 3-allyloxy-1-(piperidino)-1-(2-pyridyl)propane **42** was followed, using 3-(2-pyridyl)-3-(1-pyrrolidinyl)propanol **35** (0.60 g, 2.9mmol) in dry THF (4 ml) and pre-washed NaH (50 % dispersion in oil; 0.14 g, 2.9 mmol). The reaction mixture was stirred at r.t. for 1h prior to the addition of allyl bromide (0.50 ml, 5.0 mmol). The resulting mixture was stirred overnight and completion of the reaction was confirmed by TLC. After quenching by the dropwise addition of water, the mixture was extracted with boiling EtOAc (3 x 10 ml). The combined extracts were dried over anhydrous $MgSO_4$, and the solvent was removed *in vacuo*. The residual material was purified by chromatography [flash chromatography on silica gel; elution with MeOH-EtOAc (5:6)] to yield, as a yellow oil, *3-allyloxy-1-(2-pyridyl)-1-*

(1-pyrrolidinyl)propane **43** (0.20 g, 28 %) (Found: M^+-H, 245.16436. $C_{15}H_{22}N_2O$ requires *M*-1, 245.16539); ν_{max} (NaCl)/cm^{-1} 1455 (C=C) and 1104 (C-O-C); δ_H (400 MHz; $CDCl_3$) 1.71 (4H, br, NCH_2CH_2), 2.13 and 2.31(2H, 2 x m, $CHCH_2CH_2$), 2.35 and 2.61 (4H, 2 x m, CH_2NCH_2), 3.15 (2H, m, CH_2CH_2O), 3.43 (1H, m, $NCHCH_2$), 3.80 (2H, d, *J* 4.8 Hz, OCH_2CH), 5.06 (2H, m, $CH_2CH=CH_2$), 5.79 (1H, m, $CH_2CH=CH_2$), 7.10 (1H, m, ArH), 7.25 (1H, d, *J* 7.2 Hz, ArH), 7.58 (1H, t, *J* 7.6 Hz, ArH) and 8.54 (1H, d, *J* 4.1 Hz, ArH); δ_C (100 MHz; $CDCl_3$) 23.1 (NCH_2CH_2), 34.6 ($CHCH_2CH_2$), 51.2 (CH_2NCH_2), 67.3 (CH_2CH_2O), 68.8 ($NCHCH_2$), 71.7 ($CH_2CH=CH_2$), 116.6 ($CH=CH_2$), 134.8 ($CH=CH_2$), 121.8, 122.9, 136.3, 148.8 and 162.1 (ArC).

3-Allyloxy-1-(morpholino) -1-(2-pyridyl)propane **44**

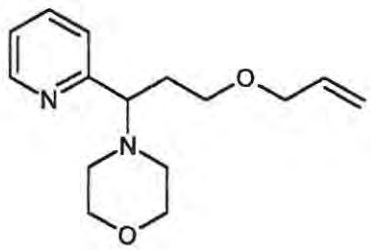

The experimental procedure described for the synthesis of 3-allyloxy-1-(2-pyridyl)-1-(1-pyrrolidinyl)propane **43** was followed, using 3-(4-morpholino)-3-(2-pyridyl)propanol **36** (2.8 g, 13. mmol) in dry THF (15 ml), pre-washed NaH (50 % dispersion in oil; 0.60 g, 13. mmol) in dry THF and allyl bromide (2.9 ml, 26 mmol). Work-up and chromatography [flash chromatography on silica gel; elution with MeOH-EtOAc (1:1)] afforded, as a yellow oil, *3-allyloxy-1-(morpholino -1-(2-pyridyl)propane* **44** (1.5 g, 44 %) (Found: M^+-H, 261.15969. $C_{15}H_{22}N_2O_2$ requires *M*-1, 261.16030); ν_{max} (NaCl)/cm^{-1} 1430 (C=C) and 1110 (C-O-C); δ_H (400 MHz; $CDCl_3$) 2.13 and 2.25 (2H, 2 x m, $CHCH_2CH_2$), 2.40 (4H, m, NCH_2), 3.22 and 3.28 (2H, 2 x m, $CHCH_2CH_2O$), 3.64 (4H, m, NCH_2CH_2O), 3.66 (1H, br s, $NCHCH_2$), 3.85 (2H, m, $CH_2CH=CH_2$), 5.07 (2H, m, $CH=CH_2$), 5.78 (1H, m, $CH=CH_2$), 7.12 (1H, t, *J* 4.9 Hz, ArH), 7.15 (1H, m, ArH), 7.58 (1H, t, *J* 7.5 Hz, ArH) and 8.56 (1H, d, *J* 4.0 Hz, ArH); δ_C (100 MHz; $CDCl_3$), 31.0 ($CHCH_2CH_2$), 50.7 (NCH_2), 67.2 (CH_2OCH_2), 67.4 (CH_2OCH_2), 67.9 ($NCHCH_2$), 71.7 ($CH_2CH=CH_2$), 116.6 ($CH=CH_2$), 134.9 ($CH=CH_2$), 122.1, 123.6, 135.9, 149.1 and 159.8 (ArC).

3-*Allyloxy-1-butylamino-1-(2-pyridyl)propane* **45**

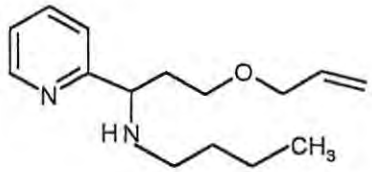

The experimental procedure described for the synthesis of 3-allyloxy-1-(*N*-allylbutylamino)-1-(2-pyridyl)propane **48** was followed, using 3-butylamino-3-(2-pyridyl)propanol **37** (2.94 g, 10.0 mmol) and NaH (60 % dispersion in oil; 0.56 g, 20 mmol). After the reaction mixture had been boiled under reflux for 1h, allyl bromide (1.3 ml, 10 mmol) was added dropwise. Work-up and chromatography [flash chromatography on silica gel; elution with MeOH-EtOAc (1:1)] afforded, as a yellow oil, 3-*allyloxy-1-butylamino-1-(2-pyridyl)propane* **45** (1.6 g, 64 %) (Found: M^+-H, 223.06668.$C_{15}H_{24}N_2O$ requires *M*-1, 223.06670); ν_{max} (NaCl)/cm^{-1}, 1456 (C=C) and 1104 (C-O-C); δ_H (400 MHz; $CDCl_3$) 0.81 (3H, t, *J* 7.3 Hz, CH_2CH_3),1.22 (2H, m, CH_2CH_3), 1.37 (2H, m, $CH_2CH_2CH_3$) 1.89 and 1.97 (2H, 2 x m, $CHCH_2CH_2$), 2.32-2.45 (3H, complex of multiplets, N*H* and CH_2NH), 3.31 and 3.43 (2H, 2 x m, $CH_2CH{=}CH_2$), 3.82 (2H, m, CH_2CH_2O), 3.87 (1H, m, $CHCH_2CH_2$), 5.09-5.22 (2H, m, $CH{=}CH_2$), 5.80 (1H, m, $CH{=}CH_2$), 7.09 (1H, m, ArH), 7.28 (1H, m, ArH), 7.57 (1H, m, ArH) and 8.52 (1H, m, ArH); δ_C (100 MHz; $CDCl_3$) 13.86 (CH_2CH_3), 20.3 (CH_2CH_3), 31.9 ($CH_2CH_2CH_2$), 36.4 ($CHCH_2CH_2$), 47.4 (NCH_2), 61.9 (CH_2CH_2O), 67.7 (NCH), 71.8 ($CH_2CH{=}CH_2$), 1164 ($CH{=}CH_2$), 134.5 ($CH{=}CH_2$), 122.1, 122.3, 136.3, 149.1 and 158.9 (ArC).

3-Allyloxy-1-benzylamino-1-(2-pyridyl)propane **46**

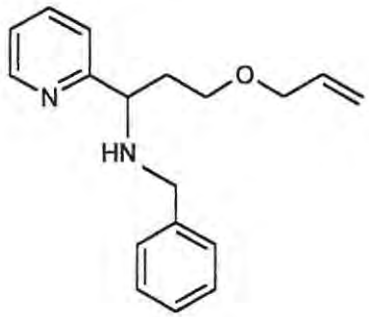

The experimental procedure described for the synthesis of 3-allyloxy-1-(N-allylbutylamino)-1-(2-pyridyl)propane **45** was followed, using 3-benzylamino-3-(2-pyridyl)propanol **38** (0.6 g, 2 mmol) in THF (2 ml) and NaH (60 % dispersion in oil; 0.04 g, 2 mmol) in THF (2 ml). The reaction mixture was stirred at r.t. for 1h, prior to adding allyl bromide (0.20 ml, 2.0 mmol). The resulting mixture was then stirred for 24 h. Work-up yielded, as a light-yellow oil, *3-allyloxy-1-butylamino-1-(2-pyridyl)propane* **46** (0.50 g, 75 %) (Found: M^+-H, 281.16368. $C_{18}H_{22}N_2O$ requires *M*-1, 281.16539); ν_{max}(NaCl)/cm^{-1} 3350 (NH), 1470 (C=C) and 1104 (C-O-C); δ_H (400 MHz; $CDCl_3$) 1.92 and 1.95 (2H, 2 x m, CHC*H*$_2$CH$_2$), 2.02 (1H, br s, N*H*), 3.36 (2H, m, NHC*H*$_2$), 3.38(1H, m, NHC*H*), 3.40 (2H, m, CH$_2$C*H*$_2$O), 3.86 (2H, m, C*H*$_2$CH=CH$_2$), 5.09(2H, m, CH=C*H*$_2$), 5.79 (1H, m, C*H*=CH$_2$), 7.10-7.40 (7H, m, ArH), 7.61 (1H, t, *J* 7.6 Hz, ArH) and 8.56 (1H, d, *J* 4.1 Hz, ArH); δ_C (100 MHz; $CDCl_3$) 36.9 (CH*C*H$_2$), 52.1 (CHCH$_2$*C*H$_2$), 61.7 (NH*C*H$_2$), 68.3 (NH*C*H), 72.2 (O*C*H$_2$CH=CH$_2$), 117.0 (CH=*C*H$_2$), 127.1 (*C*H=CH$_2$), 122.3, 122.7, 128,5, 128.6, 134.9, 136.6, 140.6, 149.9 and 163.5 (ArC).

3-Allyloxy-1-isopentylamino-1-(2-pyridyl)propane **47**

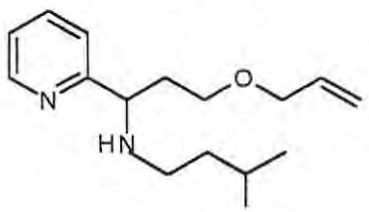

The method described for the synthesis of 3 allyloxy-1-(*N*-allylbutylamino)-1-(2-pyridyl)propane

45 was followed, using 3-isopentylamino-3-(2-pyridyl)propanol **39** (6.40 g, 28.8 mmol) in dry THF (15 ml) and NaH (60 % dispersion in oil;1.15 g, 28.6 mmol) in dry THF (10 ml). The reaction mixture was stirred for 1h, prior to adding allyl bromide (3.20 ml, 28.8 mmol). Work-up yielded, as a yellow-brown oil, *3-allyloxy-1-isopentylamino-1-(2-pyridyl)propane* **47** (1.30 g, 17 %) (Found: (M^+-H), 261.19571. $C_{16}H_{26}N_2O$ requires *M*-1, 261.19669); ν_{max}(NaCl)/cm^{-1} 3350 (NH), 1471 (C=C) and 1105 (C-O-C); δ_H (400 MHz; $CDCl_3$) 0.79 [6H, m, $CH(CH_3)_2$], 1.29 (2H, m, $NHCH_2CH_2$), 1.55 (1H, m, CH_3CH), 1.90-2.10 (3H, br m, CH_2NH and CH_2CH_2O), 2.34 (2H, m, CH_2NH), 3.34 and 3.48 (2H, 2 x m, $OCH_2CH=CH_2$), 3.82 (1H, t, *J* 6.8 Hz, $NHCHCH_2$), 3.89 (2H, m, CH_2CH_2O), 5.11 (2H, m, $CH=CH_2$), 5.75 (1H, m, $CH=CH_2$), 7.11 (1H, t, *J* 6.6 Hz, ArH), 7.28 (1H, d, *J* 7.6 Hz, ArH), 7.59 (1H, t, *J* 7.6 Hz, ArH) and 8.54 (1H, d, *J* 4.2 Hz, ArH); δ_C (100 MHz; $CDCl_3$) 22.4 and 22.7 [$CH(CH_3)_2$], 25.9 (CH_3CH), 30.8 ($NHCH_2CH_2$), 39.1 ($NHCHCH_2$), 45.8 (CH_2NH), 60.4 (CH_2CH_2O), 67.2 (NHCH), 71.8 ($CH_2CH=CH_2$), 116.6 ($CH=CH_2$), 134.9 ($CH=CH_2$), 121.9, 122.2, 136.2, 149.4 and 162.1 (ArC).

3-Allyloxy-1-(N-allyl butylamino)-1-(2-pyridyl)propane **48**

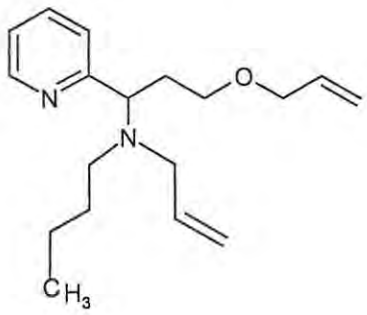

A solution of 3-butylamino-3-(2-pyridyl)propanol **37** (1.5 g,10 mmol) in dry THF (5 ml) was added dropwise to a stirred suspension of pre-washed NaH (50 % dispersion in oil; 4.5 g, 90 mmol), in dry THF (10 ml) under nitrogen. The reaction mixture was stirred at r.t. for 1h, prior to the addition of allyl bromide (3.0 ml, 30 mmol). The mixture was then stirred overnight. After excess NaH had been quenched by the dropwise addition of water, the mixture was extracted with boiling EtOAc (4 x 10 ml), and the combined extracts were dried over anhydrous $MgSO_4$.The EtOAc was removed *in vacuo*, and the residual material was purified by chromatography [flash chromatography on silica gel; elution with MeOH-EtOAc (1:9)] to afford, as a light-yellow oil,

allyloxy-1-(N-allyl butylamino)-1-(2-pyridyl)propane **48** (0.60 g, 20 %) (Found: M^+, 288.22120. $C_{18}H_{28}N_2O$ requires *M*, 288.22016); ν_{max} (NaCl)/cm^{-1} 1456 (C=C) and 1104 (C-O-C); δ_H (400 MHz; $CDCl_3$) 0.83 (3H, t, *J* 7.3 Hz, $CH_2CH_2CH_3$), 1.22 (2H, m, $CH_2CH_2CH_3$), 1.38 (2H, m, $CH_2CH_2CH_3$), 2.16 (2H, m, $CHCH_2CH_2$), 2.26 and 2.30 (2H, 2 x m, NCH_2CH_2), 2.89 and 3.25 (2H, 2 x m, $CH_2CH{=}CH_2$), 3.37 and 3.48 (2H, 2 x m, CH_2CH_2O), 3.89 (1H, t, *J* 7.7 Hz, $CHCH_2CH_2$), 3.91 (2H, m, $NCH_2CH{=}CH_2$), 5.09-5.23 (4H, complex of multiplets, 2 x $CH{=}CH_2$), 5.89-5.87 (2H, complex of multiplets, 2 x $CH{=}CH_2$), 7.09 (1H, t, *J* 4.8 Hz, ArH), 7.21 (1H, d, *J* 7.7 Hz, ArH), 7.57 (1H, t, *J* 7.6 Hz, ArH) and 8.54 (1H, d, *J* 3.1 Hz, ArH); δ_C (100 MHz; $CDCl_3$) 14.4 ($CH_2CH_2CH_3$), 20.6 ($CH_2CH_2CH_3$), 30.7 ($CH_2CH_2CH_2$), 30.8 ($CHCH_2$), 50.1 (NCH_2CH_2), 53.9 ($CH_2CH{=}CH_2$), 61.9 ($NCHCH_2$), 68.5 (CH_2CH_2O), 72.1 ($CH_2CH{=}CH_2$), 116.4 and 116.8 (2 x $CH{=}CH_2$), 135.5 and 136.0 (2 x $CH{=}CH_2$), 122.1, 124.2, 138.2, 149.1 and 161.0 (ArC).

Ethyl 3-(6-methyl-2-pyridyl)acrylate **50**

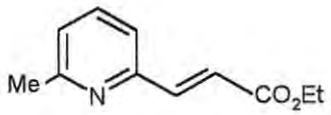

The method described for the synthesis of ethyl 3-(2-pyridyl)acrylate **25** was followed, using 6-methylpyridine-2-carbaldehyde **49** (5.0 g, 40 mmol) in dry CH_2Cl_2 (50 ml) and (carbethoxymethyl) triphenylphosphorane **20** (14.2 g, 40 mmol) in dry CH_2Cl_2 (45 ml). The reaction mixture was boiled under reflux for 10h, and the crude product was extracted with boiling hexane (5 x 35 ml). The hexane extracts were combined and evaporated *in vacuo*, to afford, as a yellow-brown oil, *ethyl 3-(6-methyl-2-pyridyl)acrylate* **50** (5.2 g, 68 %) (Found: M^+, 191.09537. $C_{11}H_{13}NO_2$ requires *M*, 191.09463); ν_{max}(NaCl)/cm^{-1} 3406 (NH) and 1714 (CO); δ_H (400 MHz; $CDCl_3$) 1.25 (3H, t, *J* 5.9 Hz, CH_2CH_3), 2.51(3H, s, $ArCH_3$), 4.20 (2H, m, CH_2CH_3), 6.82 (1H, d, *J* 14.0 Hz, $CH{=}CHCO_2$), 7.06 (1H, d, *J* 7.3 Hz, ArH), 7.16 (1H, d, *J* 8.1 Hz, ArH) and 7.56 (1H, m, ArH), 7.60 (1H, d, *J* 15.1 Hz, $CH{=}CHCO_2$); δ_C (100 MHz; $CDCl_3$) 14.6 (CH_2CH_3), 24.9 ($ArCH_3$) 60.1 (CH_2CH_3),120.9 and 122.0 (CH=CH), 123.8, 136.7, 143.6, 152.3 and158.9 (ArC) and 166.7 (C=O).

Ethyl 3-(6-methyl-2-pyridyl)-3-(morpholino)propanoate **51**

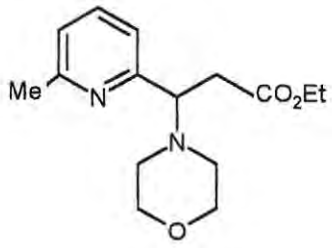

The method described for the synthesis of ethyl 3-(piperidino)-3-(2-pyridyl)propanoate **26** (method **A**) was followed, using ethyl 3-(6-methyl-2-pyridyl)acrylate **50** (5.0 g, 26 mmol) and morpholine (12 ml, 0.13 mol). The reaction mixture was boiled under reflux for 25h to yield, as a brown oil, *ethyl 3-(6-methyl-2-pyridyl)-3-morpholino propanoate* **51** (4.8 g, 66 %) (Found: MH^+, 279.17295. $C_{15}H_{22}N_2O_2$ requires M+1, 279,19087); ν_{max}(NaCl)/cm^{-1} 1733 (CO); δ_H (400 MHz; $CDCl_3$) 1.11 (3H, t, J 7.2 Hz, CH_2CH_3), 1.70 (3H, s, $ArCH_3$), 2.49 (4H, m, CH_2N), 2.99 (2H, m, CH_2CO_2), 3.60 (4H, m, CH_2OCH_2), 4.05 (2H, m, CH_2CH_3), 4.08 (1H, m, NCH), 6.98 (1H, d, J 7.2 Hz, ArH), 7.11 (1H, d, J 6.8 Hz, ArH) and 7.49 (1H, t, J 6.8 Hz, ArH); δ_C (100 MHz; $CDCl_3$) 14.5 (CH_2CH_3), 24.8 ($ArCH_3$), 46.1 (CH_2CH_3), 49.9 (CH_2NCH_2), 51.3 ($CHCH_2$), 67.0 (NCH), 67.9 (CH_2OCH_2), 120.6, 122.0, 136.5, 149.5 and 159.3 (ArC) and 171.6 (CO).

3-(6-methyl-2-pyridyl)-3-morpholino propanol **52**

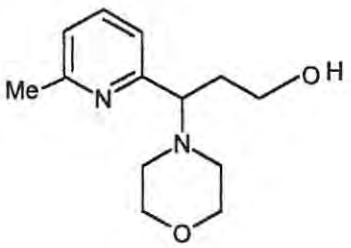

The method described for the synthesis of 3-(piperidino)-3-(2-pyridyl)propanol **34** was followed, using 3-(6-methyl-2-pyridyl)-3-morpholino propanoate **51** (4.2 g, 15 mmol) in dry Et_2O (10 ml) and LAH (2.3 g, 60 mmol) in dry Et_2O (25 ml). The reaction mixture was boiled under reflux for 2h, and work-up by chromatography [flash chromatography on silica gel; elution with MeOH-EtOAc (6:5)] to give, as light-yellow oil, *3-(6-methyl-2-pyridyl)-3-morpholino propanol* **52** (2.8

g, 80 %) (Found: MH^+, 237.16083. $C_{13}H_{20}N_2O_2$ requires *M*+1, 237.16030; ν_{max}(NaCl)/cm^{-1} 3320 (OH); δ_H (400 MHz; $CDCl_3$) 1.64 (3H, m, CH_3), 2.10 (1H, s, OH), 2.40 and 2.58 (2H, 2 x m, $CHCH_2$), 2.41 (4H, m, CH_2N), 3.61 (4H, m, CH_2OCH_2), 3.69 (2H, m, CH_2OH), 3.70 (1H, t, *J* 6.1 Hz, NC*H*), 7.05 (1H, d, *J* 7.6 Hz, ArH), 7.09 (1H, d, *J* 7.5 Hz, ArH) and 7.51 (1H, t, *J* 7.6 Hz, ArH); δ_C (100 MHz; $CDCl_3$) 24.8 ($ArCH_3$), 31.7 ($CHCH_2$), 50.6 (CH_2NCH_2), 62.6 (CH_2CH_2OH), 67.1 (CH_2OCH_2),71.3 (NCH), 120.1, 122.2, 136.8, 157.3 and 160.1 (ArC).

3-Allyloxy-1-(6-methyl-2-pyridyl)-1-(4-morpholino)propane **53**

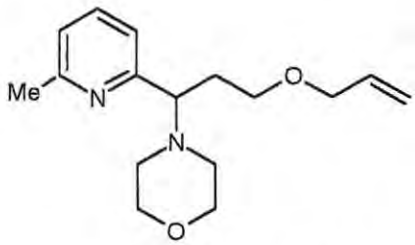

The experimental procedure described for the synthesis of 3-allyloxy-1-(piperidino)-1-(2-pyridyl)propane **42** was followed, using 3-(6-methyl-2-pyridyl)-3-morpholino propanol **52** (2.6 g, 11 mmol) in dry THF (20 ml) and NaH (60 % dispersion in oil; 0.44 g, 18 mmol). The reaction mixture was stirred for 1h, prior to the addition of allyl bromide (1.23 ml, 11.0 mmol). The crude product was purified by chromatography [flash chromatography on silica gel; elution with MeOH-EtOAc (5:6)] to afford, as a light-yellow oil, *3-allyloxy-1-(6-methyl-2-pyridyl)-1-morpholino propane* **53** (2.15 g, 71 %) (Found: M^+, 276.18117. $C_{16}H_{24}N_2O_2$ requires *M*, 276.18378); ν_{max} (NaCl)/cm^{-1} 1455 (C=C) and 1071 (C-O-C); δ_H (400 MHz; $CDCl_3$) 2.08 and 2.18 (2H, 2 x m, $CHCH_2CH_2$), 2.34 (3H, m, $ArCH_3$), 2.48 (4H, m, CH_2NCH_2), 3.20 (2H, m, CH_2CH_2O), 3.54 (1H, m, NCH), 3.59 (4H, m, CH_2OCH_2), 3.83 (2H, m, $CH_2CH{=}CH_2$), 5.09 (2H, m, $CH{=}CH_2$), 5.78 (1H, m, $CH{=}CH_2$), 7.01 (2H, m, ArH) and 7.42 (1H, t, *J* 8.0 Hz, ArH); δ_C (100 MHz; $CDCl_3$) 24.6 ($ArCH_3$), 31.2 ($CHCH_2CH_2$), 50.8 (CH_2NCH_2), 67.3 (CH_2OCH_2), 67.5 (CH_2CH_2O), 68.3 (NCH), 71.7 ($CH_2CH{=}CH_2$), 116.5 ($CH{=}CH_2$), 135.4 ($CH{=}CH_2$), 120.2, 121.5, 136.0, 157.7 and 159.2 (ArC).

3.3 Procedures for the preparation of the nickel complexes

The nickel complex **59**

A solution of 3-allyloxy-1-morpholino-1-(2-pyridyl)propane **44** (0.10 g, 0.38 mmol) in MeOH (1 ml) was added to a stirred solution of $NiCl_2.6H_2O$ (0.05 g, 0.19 mmol) in MeOH (2 ml). After noting an immediate colour change, the mixture was stirred for 3 days, and the suspension formed was re-dissolved by adding MeOH. Et_2O was then added to the crude mixture; the resulting precipitate was re-dissolved by adding MeOH and re-precipitated by Et_2O (3 x) and dried under high vacuum to yield, as a light-green, hygroscopic semi-solid, complex **59** (0.21 g, 94 %) (Found: C, 59.9; H, 7.0; N, 10.3. $C_{30}H_{44}N_4O_4Cl_2Ni$ requires C, 55.2; H, 6.7; N, 8.6 %);ν_{max} (polyethylene disc)/cm^{-1} 245 and 186 (Ni-Cl),157 (Cl-Ni-Cl).

The nickel complex **54**

The experimental procedure described for the preparation of complex **59** was followed, using 3-allyloxy-1-(1-piperidyl)-1-(2-pyridyl)propane **42** (0.10 g, 0.38 mmol) in MeOH (5 ml) and $NiCl_2.6H_2O$ (0.22 g, 0.90 mmol) in MeOH (5 ml). A suspension was formed after stirring for 48h, and work-up afforded as a green, hygroscopic semi-solid complex **54**.

The nickel complex **57**

The experimental procedure described for the preparation of complex **59** was followed, using 3-allyloxy-1-(2-pyridyl)-1-(pyrrolidino)propane **43** (0.09 g, 0.4 mmol) and $NiCl_2.6H_2O$ (0.043 g, 0.18 mmol). The mixture was stirred for 3 days, and work-up afforded, as a greenish, shiny, hygroscopic semi-solid, complex **57**.

The other nickel complexes which were prepared following the procedure described for the synthesis of complex **59**. are tabulated in **Table 18**.

Table 18. Summary of the other nickel complexes prepared in the study.

Ligand	Nickel salt	Solvent	Product
42 (0.03 g, 0.11 mmol)	nickel(II)acetate.$4H_2O$ (0.01 g, 0.06 mmol)	MeOH (5 ml)	**55** (brownish hygroscopic product)
42 (0.03 g, 0.11 mmol)	$Ni(BF_4)_2$ (0.01 ml, 0.07 mmol)	MeOH (5 ml)	**56** (brownish hygroscopic solid)
43 (0.010 g, 0.040 mmol)	nickel(II)acetate.$4H_2O$ (0.005 g, 0.020 mmol	MeOH (2 ml)	**58** (yellowish solid)
44 (0.050 g, 0.11 mmol	$NiBr_2.6H_2O$ (0.004 ml, 0.009 mmol)	Warm MeOH (5 ml)	**60** (brownish semi-solid)
44 (0.003 g, 0.011 mmol)	$Ni(BF_4)_2$ (0.004 ml, 0.009 mmol)	CH_3CN/MeOH (1:1) (1 ml)	**61** (dark-brown semi-solid)
44 (0.03 g, 0.11 mmol)	Ni(II)perchlorate. $6H_2O$ (0.02 g, 0.06 mmol)	MeOH (5 ml)	**62**(brown semi-solid)
44 (0.003 g, 0.011 mmol)	$Ni(OAc)_2.4H_2O$ (0.002 g, 0.006 mmol)	CH_3CN/MeOH (2 ml)	**63** (light green semi- solid)
53 (0.10 g, 0.38 mmol)	$NiCl_2.6H_2O$ (0.05 g, 0.19 mmol)	MeOH (5 ml)	**64** (light-green semi-solid)
44 (0.003 g, 0.01 mmol)	$Ni(NO_3)_2.6H_2O$ (0.002 g, 0.006 mmol)[a]	CH_3CN/CH_2Cl (1:1) (2 ml)	**66** (brown-solid)
46 (0.06 g, 0.2 mmol)	$NiCl_2.6H_2O$.(0.159g, 0.11mmol)	MeOH (5 ml)	**65** (light green)

[a] Excess $NH_3(PF_6)$ was added after stirring for 2h.

Procedure for computer modelling

Computer modelling was conducted on a Silicon Graphics O^2 computer using the MSI Cerius^2 modelling platform. The method followed outlined in **Figure 22** was aimed at establishing the global minima for both ligands and nickel(II)complexes.

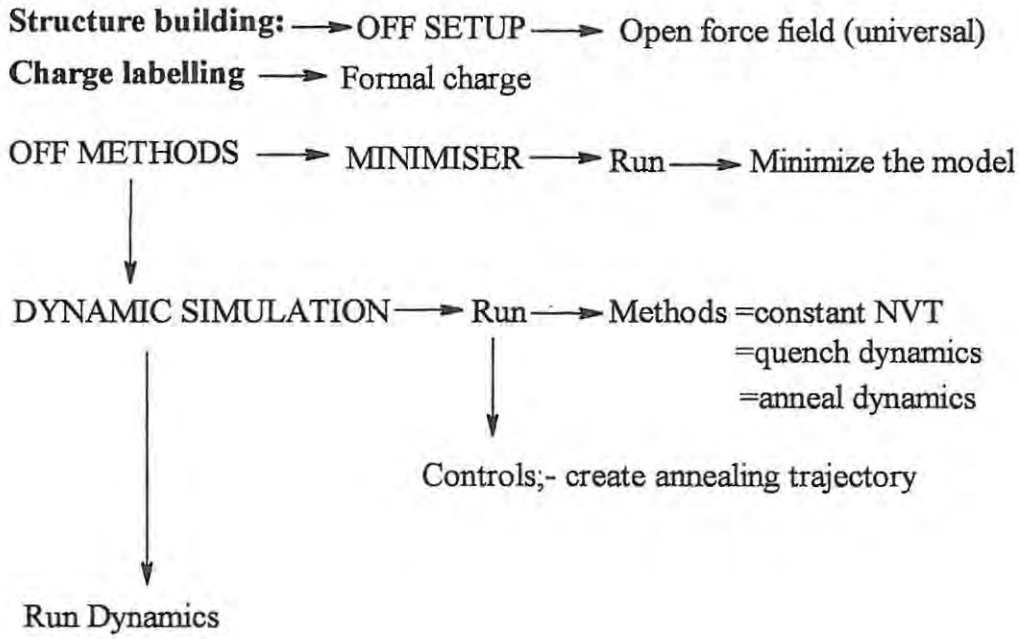

Figure 22. Procedure followed to carry out computer modelling studies.

In summary, the structure was built and "cleaned" prior to loading the universal force field. After labeling with appropriate formal charges, the model was then minimized using, initially, steepest descent and, finally, Newton Raphson methods. Dynamic simulation of the resulting minimized model was run using the dynamic simulation at constant NVT and with quenching and annealing (500 cycle).

3.5 Procedures for the synthesis of molecularly imprinted polymers (MIP's)

3-Allyloxy-1-(morpholino)-1-(2-pyridyl)propane-nickel(II)acetate.4H_2O **MIP 44A**

Method A

A solution of nickel(II)acetate.4H_2O (0.25 g, 1.0 mmol) in warm MeOH (2 ml) was added dropwise to a stirred solution of 3-allyloxy-1-morpholino-1-(2-pyridyl)propane **44** (0.52 g, 2.0 mmol) in MeOH (2 ml). A greenish complex was obtained after stirring overnight. Ethylene glycol dimethacrylate (EGDMA) (8.0 ml, 43 mmol) was then added under an atmosphere of nitrogen and, finally, azobis(isobutyronitrile) (AIBN) (0.03g, 0.2 mmol) was added. The reaction mixture was stirred at 60 °C for 3h, to afford a greenish glassy polymer (*ca.* 8 g). After standing at r.t. overnight, the solid was retrieved by hammering the test tube. The polymer was then ground into 3 rough particle sizes (fine, medium and coarse) using a pestle and mortar.

The polymeric material of each particle size was washed repeatedly (3 x) with MeOH, and then kept in conc. HCl overnight. After continued washing with conc. HCl through suction filtration, the particles were finally washed with MeOH and dried under high vacuum for 2 days to afford the respective MIP's as shiny, white particles.

3-Allyloxy-1-morpholino-1-(2-pyridyl)propane-nickel(II)acetate.4H_2O **MIP 44B**

Method B

The experimental procedure described for the synthesis of **MIP 44A** (method **A**) was followed, using 3-allyloxy-1-morpholino-1-(2-pyridyl)propane **44** (0.52 g, 2.0 mmol) in MeOH (2 ml) and nickel(II)acetate.4H_2O (0.19 g, 0.78 mmol) in warm MeOH (1.5 ml). Addition of EGDMA (4.0 ml, 21 mmol) and AIBN (0.03 g, 0.20 mmol) afforded a glassy, greenish polymer (*ca.* 4 g). Extensive washing and drying of the ground polymer yielded shiny, white particles of **MIP 44B**.

Method C

3-Allyloxy-1-morpholino-1-(2-pyridyl)propane-nickel(II)acetate.4H_2O **MIP 44C**

The experimental procedure described for the synthesis of **MIP 44A** (method **A**) was followed, using 3-allyloxy-1-morpholino-1-(2-pyridyl)propane **44** (0.49 g, 1.8 mmol) in MeOH (2 ml) and nickel(II)acetate.$4H_2O$ (1.0 g, 4.0 mmol) in warm MeOH (1.5 ml). Addition of EGDMA (8.0 ml, 43 mmol) and AIBN (0.03 g, 0.20 mmol) afforded a glassy greenish polymer (*ca.* 6 g). Washing and drying of the ground polymer yielded shiny, white particles of **MIP 44C**.

Method D

3-Allyloxy-1-(morpholino)-1-(2-pyridyl)propane-nickel(II)acetate.$4H_2O$ **MIP 44D**

The experimental procedure described for the synthesis of **MIP 44A** (method **A**) was followed, using 3-allyloxy-1-(morpholino)-1-(2-pyridyl)propane **44** (0.77 g, 2.8 mmol) in MeOH (3 ml) and nickel(II)acetate.$4H_2O$ (0.2 g, 0.99 mmol) in warm MeOH (1.0 ml). Addition of EGDMA (8.0 ml, 43 mmol) and AIBN (0.03 g, 0.20 mmol) afforded a glassy greenish polymer (*ca.* 7 g). Washing and drying of the ground polymer yielded shiny, white particles of **MIP 44D**.

3-Allyloxy-1-morpholino-1-(2-pyridyl)propane-$Ni(BF_4)_2$ **MIP 44G**

The experimental procedure described for the synthesis of **MIP 44A** (method **A**) was followed, using 3-allyloxy-1-morpholino-1-(2-pyridyl)propane **44** (0.56 g, 2.2 mmol) in MeOH (2 ml) and $Ni(BF_4)_2$ (0.17 g, 1.0 mmol) in MeOH (2 ml) to afford a dark-brown solution. Addition of EGDMA (8.0 ml, 43 mmol) and AIBN (0.027 g, 0.20 mmol) afforded a glassy brownish polymer (*ca.* 8 g). Washing and drying of the ground polymer yielded shiny, off-white particles of **MIP 24G**.

3-Allyloxy-1-morpholino-1-(2-pyridyl)propane-$NiCl_2.6H_2O$ **MIP 44E**

The experimental procedure described for the synthesis of **MIP 44A** (method **A**) was followed, using 3-allyloxy-1-(morpholino)-1-(2-pyridyl)propane **44** (0.20 g, 0.70 mmol) in MeOH (2 ml) and $NiCl_2.6H_2O$ (0.09 g, 0.4 mmol) in MeOH (2 ml). The reaction mixture was stirred for 4 days, to obtain a dark-brown solution. Addition of EGDMA (4.0 ml, 21 mmol) and AIBN (0.014 g, 0.10

mmol) yielded a yellow-brown, glassy polymer (*ca.* 4.5 g). Washing and drying of the ground polymer yielded shiny, milky-white particles of **MIP 44E**.

3-Allyloxy-1-morpholino-1-(2-pyridyl)propane-$CoCl_2.6H_2O$ **MIP 44H**

The experimental procedure described for the synthesis of **MIP 44A** (method **A**) was followed, using 3-allyloxy-1-(morpholino)-1-(2-pyridyl)propane **44** (0.20 g, 0.76 mmol) in MeOH (2 ml) and $CoCl_2.6H_2O$ (0.092 g, 0.38 mmol) in MeOH (2 ml) to obtain black-brown solution. Addition of EGDMA (4.0 ml, 21 mmol) and AIBN (0.013 g, 0.1 mmol) afforded a solid, brown polymer (*ca.* 8 g). Washing and drying of the ground polymer yielded shiny, off-white particles of **MIP 44H**.

3-Allyloxy-1-morpholino-1-(2-pyridyl)propane-nickel(II)perchlorate.$6H_2O$ **MIP 44F**

The experimental procedure described for the synthesis of **MIP 44A** (method **A**) was followed, using 3-allyloxy-1-(morpholino)-1-(2-pyridyl)propane **44** (0.20 g, 0.75 mmol) in MeOH (2 ml) and nickel(II)perchlorate.$6H_2O$ (0.14 g, 0.38 mmol) in MeOH (2 ml) to obtain a yellow-brown solution after the mixture had been stirred for 3 days. Addition of EGDMA (4.0 ml, 21 mmol) and AIBN (0.013 g, 0.1 mmol) yielded a brick-red solid polymer (*ca.* 4.6 g). Washing and drying of the ground polymer yielded shiny, white particles of **MIP 44F**.

3-Allyloxy-1-(piperidino)-1-(2-pyridyl)propane-nickel(II)acetate.$4H_2O$ **MIP 42A**

The experimental procedure described for the synthesis of **MIP 44A** (method **A**) was followed, using 3-allyloxy-1-(piperidino)-1-(2-pyridyl)propane **42** (0.120 g, 0.470 mmol) in MeOH (1 ml) and Ni(II) acetate.$4H_2O$ (0.059 g, 0.2 mmol) in MeOH (1 ml) to obtain a dark-brown solution. Addition of EGDMA (2.0 ml, 11 mmol) and AIBN (0.007 g, 0.05 mmol) yielded a glassy, brown polymer. Washing and drying of the ground polymer yielded shiny solid white particles of **MIP 42A**.

3-Allyloxy-1-benzylamino-1-(2-pyridyl)propane-nickel(II)acetate.4H_2O **MIP 46A**

The experimental procedure described for the synthesis of **MIP 44A** (method **A**) was followed, using 3-allyloxy-1-benzylamino-1-(2-pyridyl)propane **46** (0.042 g, 0.14 mmol) in MeOH (1 ml) and nickel(II) acetate.4H_2O (0.018 g, 0.070 mmol) in MeOH (0.5 ml) to obtain a light-green solution. Addition of EGDMA (0.5 ml, 3 mmol) and AIBN (0.002 g, 0.01 mmol) yielded a brown, glassy polymer after the reaction mixture had been stirred for 18h. Washing and drying of the ground polymer yielded shiny, white particles of **MIP 46A**.

3-Allyloxy-1-(6-methyl-2-pyridyl)-1-morpholinopropane-nickel*(II)acetate.4H_2O* **MIP 53A**

The experimental procedure described for the synthesis of **MIP 44A** (method **a**) was followed, using 3-allyloxy-1-(6-methyl-2-pyridyl)-1-morpholino propane **53** (0.14 g, 0.15 mmol) in MeOH (1 ml) and nickel(II) acetate.4H_2O (0.067g, 0.250 mmol) in MeOH (1 ml) to obtain a light-green solution. Addition of EGDMA (2.0 ml, 10 mmol) and AIBN (0.008 g, 0.05 mmol) yielded a blue-brown, glassy polymer. Washing and drying of the ground polymer yielded shiny, white particles of **MIP 53A**.

3-Allyloxy-1-morpholino-1-(2-pyridyl)propane-ferric chloride.6H_20 **MIP 44I**

The experimental procedure described for the synthesis of **MIP 44A** (method **A**) was followed, using 3-allyloxy-1-morpholino-1-(2-pyridyl)propane **44** (0.20 g, 0.76 mmol) in MeOH (2 ml) and $FeCl_3$.6H_2O (0.10 g, 0.4 mmol) in MeOH (2 ml). The reaction mixture was stirred for 2 days, to obtain dark-red solution. Addition of EGDMA (4.0 ml, 21 mmol) and AIBN (0.013 g, 0.10 mmol) yielded red-brown solid polymer. Washing and drying of the ground polymer yielded shiny, white particles of **MIP 44I**.

Blank polymer synthesis

The procedure described for the synthesis of **MIP 44A** (method **A**) was repeated, but without nickel(II)acetate.6H_2O.

3.6 Re-binding studies and determination of MIP extraction efficiency

Nickel stock solutions (1000-12000ppm) were prepared by dissolving nickel(II)acetate, $Ni(BF_4)_2$. or $Ni(II)Cl_2.6H_2O$ in MeOH or H_2O. These solutions were diluted to give standard solutions of various concentrations ranging from 2.5 to 300 ppm.

Method A. Ground, dried polymer particles (0.45 g) of each of the 3 different mesh sizes (fine, medium, and coarse) were treated with standard solutions (5-10 ml). The reaction mixtures were stirred at r.t. for 3 days, and the supernatant liquid was analyzed in each case, using flame Atomic Absorption Spectroscopy.

Method B. Standard solutions (*ca.* 5 ml) of nickel(II)acetate or $Ni(BF_4)_2$ were passed through Pasteur pipettes containing polymer particles (0.3 g) as the stationary phase and the eluents were analyzed.

Method C. The procedure described for method **A** was followed, the only difference being that the mixtures were mechanically shaken for 2 days or longer. In another set of experiments equilibration was monitored by analyzing the solutions after shaking for 5 min, 30 min, 1 h, 2 h, 5 h, 12 h, 24 h, 3 d and 4d period. All the solutions were analyzed by Inductively Coupled Plasma-Mass Spectroscopy (ICP-MS) and the results are detailed in **Table 19**. Each ICPMS result represents the mean of several determinations.

Table 19. ICP-MS analysis results.

(**a**) *Nickel-selectivity of various ligands imprinted polymers over iron*(ug/L).

MIP 44G	MIP 42A	MIP 53A	MIP 46A	metal ion
247.8	269.1	152.2	173.7	**Fe 57**
4.6	21.5	6.7	9.4	**Ni 58**
2.9	30.1	6.7	2.9	**Ni 60**

(**b**) *Equilibration experiment using* **MIP 44E** *medium particles.*

5 min	30 min	300 min	metal ion
2.4	45	57.6	**Fe 57**
-7.6	-12.5	-2.6	**Ni 58**
-7.1	-6.7	-2.1	**Ni 60**

(**c**) *Use of* ***MIP 24E*** *to compare mesh sizes (tetrafluoroborate salt)*

fine particles	medium particles	coarse particles	metal ion
16.4	247.8	65	**Fe 57**
-15.6	4.6	2.8	**Ni 58**
-9.6	2.9	8.2	**Ni 60**

(**d**) *Use of MIP's prepared using different metals (chloride salts)*

Ni(II)-polymer MIP 44E	**Co(II)-polymer MIP 44H**	**Fe(III)-polymer MIP 44I**	**metal ion**
-0.2	173.4	197	**Fe 57**
19.4	-0.3	-8.8	**Ni 58**
19.7	-0.07	0.05	**Ni 60**

(**e**) *Equilibration experiments using* **MIP 44I** *[medium (***M***) and coarse (***C***) particles]*

10min (M)	**3d**	**10 min (C)**	**3d**	**metal ion**
197.9	52	2528	3544	**Fe 57**
-8.8	-16	-7.5	-7.5	**Ni 58**
0.05	-10	-8.1	-1.1	**Ni 60**

(**f**) *Effect of varying the reagent ratio monomer: nickel (acetate salts)*

MIP 44D (3:1)	**MIP 44C (1:2)**	**metal ion**
356	1.4	**Fe 57**
71.7	104.7	**Ni 58**
70.1	101.8	**Ni 60**

4 REFERENCES

1. Nicholls, D. and Bailer, J. C., *Comprehensive Inorganic Chemistry*, 1st ed., Pergamon Press, Oxford, 1973, **3**, p.1109.
2. Smith, J. J. and Everson, R. C., *Executive summary: The extraction of nickel with the use of Supported Liquid Membrane (SLM)*, Department of Chemical Engineering, Potchefstroom University for C.H.E., a supplement to WRC Report No. K5/617, pp.3-12.
3. Joseph, R. B. and Queneau, P., *The winning of nickel*, Methuen and Co, London, 1967, pp. 3-16.
4. Lane, M., M.Sc. Thesis, Rhodes University, 1992.
5. Williams, B., *Nickel deposits of the world*, Wilgress, 1917, pp. 96-102.
6. Heslop, R. B. and Robinson, P. L., *Inorganic Chemistry*, 2nd ed., Elsevier, London, 1963, pp. 489-500.
7. Burelli, S. B., Steyl, J. T. and Lorio, G., *Mintek Technical Memorandum*, 1999, **18715**, p. 25.
8. Reference, 3, p.196.
9. Bowser, J. R., *Inorganic Chemistry*, Brookes/Cole, California, 1993, pp. 487-488.
10. Lee, J. D., *Concise Inorganic Chemistry*, 4th ed., Chapman and Hall, London, 1991, pp. 800-807.
11. Thompson, D., *Insights into Speciality Inorganic Chemicals*, Royal Society of Chemistry, Cambridge, 1995, pp. 15-18.
12. Reference, 2, pp.14-22.
14. Reference, 1, pp.1114.
15. Wilkinson, G., Gillard, R. D. and McCleverty, J. A., *Comprehensive Coordination Chemistry*, Pergamon Press, Oxford, 1987, **5**, pp. 3-5.
16. Cotton, F.A., Wilkinson, G., *Advanced Inorganic Chemistry, A Comprehensive Text*, 4th ed, John Wiley & Sons, New York, 1980, pp.784-793.
17. Reference, 1, pp.1139-1150.
18. Greenwood, N. N. and Earnshaw, A., *Chemistry of the Elements*, 1st ed., Pergamon Press, Oxford, 1984, pp.1328-1345.

19. Ballhause, C. J. and Liehr, A. D., *J. Am. Chem. Soc.*, 1959, **81**, 538.
20. Nyburg, S. C. and Wood, J. S., *J. Am. Chem. Soc.*, 1959, **81**, 468.
21. Holm, R. H., *J. Am. Chem. Soc.*, 1959, **81**, 4683.
22. Sacconi, L., Paoletti, P. and Chini, R.., *J. Am. Chem. Soc.*, 1958, **80**, 3583.
23. Jones, M. M., *J. Am. Chem. Soc.*, 1959, **81**, 3188.
24. Bullen, G. J., Mason, R. and Pauling, P., *Inorg. Chem.*, 1965, **4**, 456.
25. Hashagen, J. T., and Fackler, J. P., *J. Am. Chem. Soc.*, 1965, **87**, 2821.
26. Yaroslaw, D., Sergey, P. G., Robert, W. H., Tanja, E. and Phillip, L., *J. Chem. Soc. Dalton Trans.*, 2000, 2023-2029.
27. Viviene, J. T. and Robert D. H., *J. Chem. Soc. Dalton Trans.*, 1985, 1878.
28. Mathieu, W. A., Steenland, I. D., Gerrit, G. H., Bart, D., Werner, L., Andre, M. G., *J. Chem. Soc., Dalton Trans.*, 1997, 3637.
29. Marthur, M. A. and Scraton, A. B., *Separation and Technology*, 1999, **33** (5), 855.
30. Valeria, A., Luigi, F., Carlo, M., Piersando, P., Angelo, P. and Angelo T., *J. Chem. Soc., Dalton Trans.*, 2000, 185-189.
31. Grinstead, R. R., *Hydrometallurgy*,1984, **12**, 387.
32. Grinstead, R. R., *J. Metals.*, 1979, **31** (3), 13.
33. Kenneth, C. J. and Grinstead, R. R., *Chemistry and Industry.*, 1997, 637.
34 Skoog, A. D., West, M. D. and Holler, F. J., *Fundamentals of Analytical Chemistry*, 7th ed, Saunders, New York, 1996, pp. 660-662
35 Ramstrom, O., *Pure and Applied Biochemistry, Centre for Chemistry and chemical Engineering*, Lund University, *S*-221 00 LUND, Sweden. http://www.ng.hik.se/~SMI/story/What.htm
36. Reference, 35, http://www.ng.hik.se/~SMI/story/Hist.htm
37. Reference, 36, http://www.ng.hik.se/~SMI/story/Princ.htm
38. Wulff, G., *Angew. Chem. Int. Ed. Eng.*, 1995, **34**, 1820-1832.
39. Mosbatch, K., *Trends Biochem. Scie.*, 1994, **19**, 9-14.
40. Reference, 37, http://www.ng.hik.se/~SMI/story/How.htm
41 Muldoon, M.T. and Stanker, L.H., *Plastic antibodies: Molecularly Imprinted Polymers* Food Animal Protection Research laboratory, US Department of Agriculture,

Agricultural Research Services, College Station, TX 77845,US http://ci.mond.org/9606/960615.html, 1996, pp. 1-8

42. Reference, 37, http://www.ng.hik.se/~SMI/story/Gloss.htm
43. Whitcombe, M. J., Rodriguez, M. E., Villa, P. and Vulfson, E. N., *J. Am. Chem. Soc.*, 1995, **17**, 7105-7110.
44. Fieser, L. F. and Fieser, M., *Reagents for Organic Synthesis*, John Wiley and Sons, New York, *vol.* 1, 1967, p. 45.
45. Reference, 37, http://www.ng.hik.se/~SMI/story/Poro.htm
46. Gamex, P., Dunjie, B., Catherine P. and Mark L., *Tetrahedron Lett.*., 1995, **36** (48), 8779-8782.
47. Matsui, J., Teru, K., Toshifuni, T., Masayasu, S., Kenji, Y., Eichi, T. and Karube, I., *Anal. Chem.*,1993, **65**, 2223-2224.
48. Svenson, J. and Nicholls, I. A., *Analytical Chimica Acta*, 2001, **435**, 19-24.
49. Lai, J., Xian-Yu, L., Chun-Yang, L., Hong-Fang, J. and Xi-Wen, H., *Analytical Chimica Acta.*, 2001, **442**, 105-111.
50. Nicholls, I. A., Karina, A., Hakan, S. A., Per Ola, A., Jonas, A., Jimmy, H., Paivi, J., Jesper,. K., Linus, O., Rosengren, J., Shoravi, S., Svenson, J. and Wikman, S., *Analytical Chimica Acta*, 2001, **435**, 9-18.
51. Wen-Yih, C., Chin-Sung, C. and Fu-Yung, L., *J. Chromatogr.*, 2001, **923**, 1-6.
52. Bruggemann, O., Haupt, K., Ye, L., Yilmaz. and Klause, M., *Jounal of Chromatogr.*, 2000, **889**, 15-24.
53. Masahiro, Y., Yasuo, H., Kazuya, U., Masahiro, G. and Shintaro, F., *Colloids and Surfaces A: Physicochem. Eng. Aspects*, 2000, **169**, 259-269.
54. Kriz, D., Kriz, C. B., Andersson, L. I, and Mosbatch, K., *Anal. Chem.*,1994, **66**, 2636-2639.
55. Wulff, G, and Vietmeier, *J. Macromol. Chem.*, 1998, **190**, 1727-1735.
56. Lei, Y, and Mosbatch, K., *Reactive and Functional Polymers.*, 2001, **48**, 149-157.
57. Reference, 37, http://www.ng.hik.se/~SMI/story/Appl.htm
58. David, K. and Mosbatch, K., *J. Chem. Soc., Chem. Commun.*, 1989, 969-972.
59. Richard, A. L., Benkovic, S. J. and Schultz, S., *Science*, 1991, **252**, 659-666.

60. Rosatzin, T., Lars, I. A., Simon, W. and Mosbatch, K., *J. Chem. Soc., Perkin Trans.* 2, 1991, 234.

61. Nishide, H., Deguchi, J. and Tsuchida, E., *Journal of Polymer Science*, 1977, **15**, 3023- 3029.

62. Masahiro, Y., Kazuya, U., Masahiro, G, and Shintaro, F., *J. Appl. Polymer. Science*,1999, **73**(7), 1223-1230.

63. Hoo-Kyun, C., Oh-Joong, K., Chan-Kwon, C, and Chong-Su, C., *J. Appl. Polymer. Science*, 1999, **73** (13), 2749-2754.

64. Masahiro, Y., Yasuo, H., Kazuya, U., Masahiro, G, and Shintaro, F., *J. Polymer. Science*, 2000, **38,** 689-696.

65. Masahiro, Y., Kazuya, U., Masahiro, G, and Shintaro, F., *Macromolecules, 1999*, **32**, 1237-1243.

66. Fish, R., *Imprinted polymers would selectively trap metal ions*, http://www.lbl.gov/Science-Articles/Archive/imprinted-polymers.html

67. Wellington, K. W., Ph.D. Thesis, Rhodes University, 1999.

68. Hagemann, J. P., Ph.D. Thesis, Rhodes University, 1997.

69. Daubinet, A., Ph.D. Thesis, Rhodes University, 2001.

70. Reference, 15, pp. 208-249.

71. Reference, 15, pp. 56-68.

72. Ringbom, A., *Complexation in analytical chemistry*, John Wiley and Sons, London, vol.xvI, 1963, p. 5.

73. Lawrence, W. P., *Quantitative analysis theory and practice*, Harper and Row, London, 1987, p. 386.

74. Reference, 73, pp. 395-396.

75. Yanchang, S., Baozheng, Y. and Gang, Y., *J. Chem. Soc., Chem. Commun.*, 1989, 144.

76. Wayne, T. and Sondheimer, F., *J. Org. Chem.*,1981, **46** (1), 13.

77. Bestman, J. H. and Kratzer, O, (*Chem. Abstr.* 58, 13788g).

78. Furniss, B.S., Hannaford, A. J., Smith, P. W. G. and Tatchel, A. R, *Textbook of practical organic chemistry*, 5th ed, John Wiley & Sons, New York, 1989, pp. 495-498.

79. Araki, S., Hakano, M. and Butsugan, Y., *J. Org. Chem.*, 1986, **51**, 2126.
80. Allan, J., Hoozer, L. and Hoozer, J., *J. Am. Chem. Soc.*, 1967, **32**, 3387.
81. Fieser, L. F. and Fieser, M., *Reagents for Organic Synthesis*, John Wiley and Sons, New York, *vol.* 14, 1989, p. 102.
82. Cason, J. and Correia, J. S., *J. Am. Chem. Soc.*, 1961, **26**, 3545.
83. Reich, H. J. and Shah, S.K., *J. Am. Chem. Soc.*, 1975, **97**, 3252.
84. Harrison, I. T. and Harrison, S., *Compendium of Organic Synthetic Methods.*, Wiley-Interscience, New York, 1971, 486.
85. Reference, 69, p.92.
86. Goodman, J. M., *Chemical applications of molecular modelling*, Royal Society of Chemistry, UK, 1998, pp.14-23.
87. Schlecht, M. F., *Molecular modelling on the PC*, Wiley-VCH, New York, 1998, pp. 4-7.
88. Cerius^2, *Builders*, March 1997, San Diego: Molecular Simulations Inc. 1997.
89. Nakamoto, K., *Infrared and Raman Spectra of Inorganic and Coordination Compounds*, 3rd ed., John Wiley & Sons, New York, 1978, 211-215.
90. Nakamoto, K., *Infrared and Raman Spectra of Inorganic and Coordination Compounds*, 2nd ed., John Wiley & Sons, New York, 1976, pp. 212 and 229.
91. Reference, 34, pp. 611-630.
92. James, W. R., *Atomic Absorption Spectroscopy*, Edward Arnold, London, 1996, pp.140- 142.
93. Perrin, D. D. and Armarego, W. L. F., *Purification of laboratory chemicals*, Pergamon Press, Oxford, 3rd ed, 1988.
94. Still, W. C., Kahn, M. and Mitra, A., *J. Org. Chem.*, 1978, **43**, 2923.
95. Familoni, O. B., Kaye, P. T. and Klaas, P., *Chem. Commun.*, 1998, 2563-2564.
96. Fox, M. A. and Whitesell, J. K., *Organic Chemistry*, Jones and Bartlett, London, pp. 676- 680.
97. Evans, M. D. Ph.D. Thesis, Rhodes University, 1997, pp.62.
98. March, J., *Advanced Organic Chemistry: Reactions, Mechanism and Structure*, 4th ed., Wiley & Son, New York, pp. 438-440.

99. Reference, 78, p.986.

100. Reference, 67, p.114.